Second Series *October 1, 1931* *Vol. 38, No. 7*

THE

PHYSICAL REVIEW

X-RAY ABSORPTION BY A THOMAS-FERMI ATOM

By Louis C. Roess and E. H. Kennard*
Department of Physics, Cornell University

(Received August 24, 1931)

Abstract

Calculations were made on the K shell of tin, the K electron being assumed to move according to the Dirac relativistic equation in a modified Fermi-Thomas field. The ionization potential for a K electron thus found exceeds the observed energy of the K absorption edge by only 0.48 percent. Mass absorption-coefficients for the K shell for wave-lengths 1, 1.5 and 2.5 times the absorption-edge wave-length were found to be 2.42, 12.10, 37.42 respectively, as against Richtmyer's observed values of 2.36, 11.0, 37.0.

The Model and the Results

FORMULAS for the mass absorption coefficient of the K shell have been obtained[1] from both relativistic and nonrelativistic quantum mechanics on the assumption that for the heavy elements a hydrogen-like atom constitutes a sufficiently good approximation; agreement with experiment could be secured by the introduction of a screening constant of arbitrary but plausible size. A much better approximation and one involving no such arbitrary element should be obtained by employing the Thomas-Fermi field;[2] presumably the Hartree-Fock[3] field would be still better, but it would involve much more laborious calculations.

In the present paper are reported a few calculations made for tin with the Thomas-Fermi field. An atom in the middle range of atomic numbers was chosen because there the hydrogen-like model has become rather poor while at the same time the Thomas-Fermi field should give a better approximation than it does for lighter elements. In the first calculations the field for a K electron in an atom of nuclear charge Ze was taken to be that for a neutral atom of charge $(Z-1)e$ plus the Coulomb field of an extra proton

* This investigation was supported by a grant from the Heckscher Research Foundation.

[1] H. Hall and J. R. Oppenheimer, Phys. Rev. **38,** 57 (1931); L. C. Roess, Phys. Rev. **37,** 532 (1931), and references in the latter paper. The work of Hall and Oppenheimer shows that the neglect of retardation is not important for wave-lengths relatively close to the K edge.

[2] L. H. Thomas, Proc. Camb. Phil. Soc. **23,** 542 (1927); E. Fermi, Zeits. f. Physik **48,** 73 (1928).

[3] D. R. Hartree, Proc. Camb. Phil. Soc. **24,** 89, 111 (1928); V. Fock, Zeits. f. Physik **61,** 126 (1930).

in the nucleus, e being the numerical electronic charge. Such a field has been used elsewhere for a valence electron;[4] its use for an interior electron is open to question but it seems also doubtful whether any attempt at further refinement of the essentially rough Thomas-Fermi method is really worth while. However, for the last calculation such an attempt was made;† the field was taken to be: Thomas-Fermi field of atom of charge $(Z+1)e$ minus Coulomb field of proton in nucleus minus field of one valence electron minus half the field due to K electrons of atom of charge Ze. This potential may be justified by the following reasoning. The contraction of the outer electrons when one K electron is removed suggests the use of a Thomas-Fermi field corresponding to atomic number $Z+1$, corrected by subtracting the Coulomb field of one proton. A further correction must be made for the extra valence electron; this may be accomplished roughly by taking its potential to be that of a spherical shell of charge e and radius a, where a is the "atomic radius," determined, say, from x-ray measurements on crystals. To obtain the field in which the K electron moves, half the potential due to the K-shell itself was then subtracted; this potential was taken as that due to the Thomas-Fermi charges, of density $\rho(r)$, located within a sphere of such radius r_0 that $\int_{r=0}^{r=r_0}\rho(r)d\tau=-2e$.

The second field of potential thus obtained is about one percent higher than the first (at points well inside the atom). The ionization potential for a Dirac electron in this field exceeds the observed energy of the K absorption edge for tin by 0.48 percent as against a deficit of 1.6 percent when the first Thomas-Fermi field was used.

Values of the mass absorption coefficient of the K shell were obtained with the first field for $\lambda_k/\lambda=1.5$ and 2.5, and with the second field for $\lambda=\lambda_k$, λ_k being the wave-length of the absorption edge. The results are shown in Table I in comparison with the experimental values.

TABLE I. *Mass absorption coefficient* $(\tau_v/\rho)_k$ *for tin.*

λ in X.U.	λ_k/λ	Calculated		Observed	
		Thomas-Fermi	Screened Coulomb[6]	Richtmyer[5]	Allen[5]
169.58	2.5	2.421	1.9	2.365	3.16 to 3.28
282.63	1.5	12.104	9.03	11.0	13.9 to 14.6
423.94	1.0	37.42	28.5	37.0	45.9 to 47.7

[4] E. Fermi, Zeits. f. Physik **49,** 550 (1928); F. Rasetti, Zeits. f. Physik **49,** 546 (1928).

† *Note added by E. H. Kennard.*—A third possibility would be simply to subtract the assumed potential due to one K electron from the Fermi-Thomas field of the actual atom; this seemed less plausible because no allowance is then made for increased concentration of the remaining electrons. Now, classically, the work done in the reversible removal of a relatively small charge from a system in equilibrium is measured by the mean of the potentials at its location in the system before and after the removal. This consideration suggests that, as a final refinement, we might use the mean of the third field just mentioned and the second field described in the paper.

[5] F. K. Richtmyer, Phys. Rev. **27,** 1 (1927); **30,** 755 (1927). S. J. M. Allen, Phys. Rev. **28,** 907 (1926).

[6] L. C. Roess, Phys. Rev. **37,** 532 (1931).

Inspection of the table shows a much improved agreement with experiment, especially if Richtmyer's values are taken to be more nearly correct.

Theory

The mass absorption coefficient of the K shell is given by the following formula (ref. 6, Eq. (49)):

$$\left(\frac{\tau_\nu}{\rho}\right)_k = \frac{4\pi e^2 \lambda N}{3A}\left[\frac{8}{3}\left|\int_0^\infty F_0 G_1^* r^2 dr\right|^2 + 3\left|\int_0^\infty F_{-2}^* G_0 r^2 dr + \frac{1}{3}\int_0^\infty F_0 G_{-2}^* r^2 dr\right|^2\right] \tag{1}$$

in which N is the Loschmidt number, A the atomic weight, λ the wave-length of the incident radiation, and F_l and G_l are radial functions satisfying the simultaneous differential equations (ref. 6, Eq. (11)):

$$\begin{aligned} &\frac{2\pi}{h}\left(\frac{W+eV}{c}+mc\right)F_l + \frac{dG_l}{dr} - \frac{l}{r}G_l = 0, \\ &-\frac{2\pi}{h}\left(\frac{W+eV}{c}-mc\right)G_l + \frac{dF_l}{dr} + \frac{l+2}{r}F_l = 0, \end{aligned} \tag{2}$$

where W is the energy and V the potential.

For an atom of atomic number Z, the first field described above is given by

$$V_1 = \frac{e}{r}\left\{1 + (Z-1)\phi\left(\frac{r}{\mu_{z-1}}\right)\right\} \tag{3}$$

where $\phi(x)$ is the Thomas-Fermi function[2] satisfying the relations

$$\phi'' = \frac{\phi^{3/2}}{x^{1/2}}, \quad \phi(0) = 1, \quad \int_0^\infty \phi^{3/2} x^{1/2} dx = 1, \tag{4}$$

and

$$\mu_z = \left(\frac{9\pi^2}{128z}\right)^{1/3} \cdot a_0, \quad a_0 = \frac{h^2}{4\pi^2 m e^2}. \tag{5}$$

In order to obtain the second field, we must determine the potential due to the K shell. We start with a total potential $V = (Ze/r)\phi(r/\mu_Z)$ and a corresponding charge density

$$\rho(r) = -\frac{1}{4\pi r^2}\frac{d}{dr}\left(r^2\frac{dV}{dr}\right) = -\frac{Ze}{4\pi r}\frac{d^2\phi}{dr^2}, \tag{6}$$

from which we obtain for the charge inside any radius $r = \mu_Z y$

$$\int \rho(r) d\tau = -Ze\int_0^y y\phi'' dy = -Ze[y\phi'(y) + 1 - \phi(y)],$$

and as the equation defining $y_0 = r_0/\mu_Z$,

$$y_0\phi'(y_0) + 1 - \phi(y_0) = 2/Z. \tag{7}$$

Half the potential due to the distributed charge inside the radius r_0 will then be

$$\begin{aligned}
&-\frac{4\pi}{2r}\int_0^r \rho(r)r^2dr - \frac{4\pi}{2}\int_r^{r_0}\rho(r)rdr, \quad (r \leqq r_0),\\
&-\frac{e}{r} \quad (r \geqq r_0),\\
&= \begin{cases} -\dfrac{Ze}{2\mu_z y}\left[y\phi'(y_0) + 1 - \phi(y)\right] & (y \leqq y_0),\\ -\dfrac{e}{\mu_z y} & (y \geqq y_0). \end{cases}
\end{aligned} \tag{8}$$

The remainder of the derivation of the second field is elementary, and we obtain finally, putting $r=\mu_{Z+1}x$,

$$V_2 = \begin{cases} \dfrac{(Z+1)e}{\mu_{z+1}x}\phi(x) + \dfrac{Ze}{2\mu_{z+1}x}\left\{\dfrac{\mu_{z+1}x}{\mu_z}\phi'(y_0) + 1 - \phi\left(\dfrac{\mu_{z+1}}{\mu_z}\,x\right)\right\} \\ \qquad + \dfrac{e}{a} - \dfrac{e}{\mu_{z+1}x}, \quad (0 \leqq x \leqq x_0), \\ \dfrac{(Z+1)e}{\mu_{z+1}x}\phi(x) + \dfrac{e}{a} \qquad \left(x_0 \leqq x \leqq \dfrac{a}{\mu_{z+1}}\right), \\ \dfrac{(Z+1)e}{\mu_{z+1}x}\phi(x) + \dfrac{e}{\mu_{z+1}x} \qquad \left(\dfrac{a}{\mu_{z+1}} \leqq x\right). \end{cases} \tag{9}$$

If we transform Eq. (2) by putting $r=\mu_{1,2}x$, with $\mu_1=\mu_Z$, $\mu_2=\mu_{Z+1}$, and writing

$$W = mc^2 + h(\nu - \nu_k) \tag{10}$$

$$A_{1,2} = \frac{4\pi mc}{h}\mu_{1,2} \tag{11}$$

$$\epsilon_{1,2} = 2\pi\mu_{1,2}\left(\frac{1}{\lambda} - \frac{1}{\lambda_k}\right) \tag{12}$$

$$\alpha = \frac{2\pi e^2}{hc} \tag{13}$$

$$V_{1,2} = \frac{e}{\mu_{1,2}x}\phi_{1,2}(x), \tag{14}$$

we obtain

$$\begin{aligned}
&\left[A_{1,2} + \epsilon_{1,2} + \frac{\alpha\phi_{1,2}}{x}\right]F_l + \frac{dG_l}{dx} - \frac{l}{x}G_l = 0,\\
&-\left[\epsilon_{1,2} + \frac{\alpha\phi_{1,2}}{x}\right]G_l + \frac{dF_l}{dx} + \frac{l+2}{x}F_l = 0.
\end{aligned} \tag{2'}$$

In Eq. (1) the subscripts 0 refer to the discrete spectrum and the subscripts 1 and -2 to the continuous spectrum. For these values of l and these conditions on ϵ, Eqs. (2′) are to be integrated numerically, the solutions normalized to unity, and then the integrals in Eq. (1) evaluated by numerical quadrature.

Numerical Methods

For the discrete spectrum $l=0$, and F_0 and G_0 have no nodes inside the range of integration. We use this fact to obtain a single nonlinear first-order equation from Eqs. (2′). Put

$$\eta = F/G, \quad \eta'/\eta = F'/F - G'/G; \tag{15}$$

then from (2′)

$$\eta' = \epsilon + (1+\epsilon)\eta^2 - \frac{1}{x}[2\eta - \alpha\phi(1+\eta^2)], \tag{16}$$

$$G'/G = -\left[1 + \epsilon + \frac{\alpha\phi}{x}\right]\eta. \tag{17}$$

Having obtained η we can find G from (17) by numerical quadrature.

Since (16) has a singular point at the origin, a series development must be used to determine η for small values of x. Knowing[7] that $\phi(x)$ is an analytic function of $x^{1/2}$ near the origin, we write

$$\phi(x) = \sum_0^\infty a_n x^{n/2}, \quad \eta(x) = \sum_0^\infty b_n x^{n/2}, \quad \eta^2(x) = \sum_0^\infty c_n x^{n/2}, \tag{18}$$

and find

$$b_0 = \frac{\alpha Z}{1+\rho} = \frac{1-\rho}{\alpha Z}, \text{ where } \rho = (1-\alpha^2 Z^2)^{1/2}, \quad b_1 = 0,$$

$$(2\rho+1)b_2 = 1b_0^2 + (\epsilon - \alpha a_2)(1+b_0^2), \tag{19}$$

$$(2\rho + \tfrac{1}{2}n)b_n = (1+\epsilon)c_{n-2} + \alpha\left[a_0(1+b_0^2) + Z\sum_1^{n-1} b_\nu b_{n-\nu} + \sum_1^{n-1} a_\nu c_{n-\nu}\right], \quad (n>2).$$

The value of ϵ, which in the discrete case is negative, must be chosen so that η is everywhere finite. This is done by a method of trial and error, and fortunately the dependence of η on ϵ was so strong that comparatively few values of η were necessary to judge the correctness of the trial ϵ. The values of η and η' at the first four points were obtained from the series (18) and the solution was then extended by applying Milne's[8] method of numerical integration.

[7] E. B. Baker, Phys. Rev. **36**, 630 (1930).
[8] W. E. Milne, Am. Math. Monthly **33**, 455 (1926).

In the continuous spectrum l takes on the values 1 and -2, and ϵ is positive. Near the origin the solution proceeds exactly as in the discrete case, with

$$b_0 = \frac{\alpha Z}{l+1+\rho_l} = \frac{l+1-\rho_l}{\alpha Z}, \quad \text{where } \rho_l = ((l+1)^2 - \alpha^2 Z^2)^{1/2},$$

and ρ_l substituted for ρ in Eq. (19). The equation for η can be used except near a root of G, where $\xi = 1/\eta$ may sometimes be used; but to continue this solution to infinity by the usual method is naturally out of the question.

The method employed for values of x greater than the first zero of either F or G follows readily from a suggestion made by Madelung.[9] We first transform Eq. (2′) to the normal form for the second order by putting

$$g = \frac{xG}{\left(A+\epsilon+\frac{\alpha\phi}{x}\right)^{1/2}}, \quad f = \frac{xF}{\left(\epsilon+\frac{\alpha\phi}{x}\right)^{1/2}} \tag{20}$$

and obtain for g

$$\frac{d^2g}{dx^2} + J(x,\epsilon)g = 0 \tag{21}$$

in which

$$\begin{aligned} J(x,\epsilon) = {} & \epsilon(A+\epsilon) + (A+2\epsilon)\frac{\alpha\phi}{x} + \left(\frac{\alpha\phi}{x}\right)^2 - \frac{l(l+1)}{x^2} \\ & + \frac{l+1}{x\left(A+\epsilon+\frac{\alpha\phi}{x}\right)}\left(\frac{\alpha\phi}{x}\right)' + \frac{1}{2\left(A+\epsilon+\frac{\alpha\phi}{x}\right)}\left(\frac{\alpha\phi}{x}\right)'' \\ & - \frac{3}{4\left(A+\epsilon+\frac{\alpha\phi}{x}\right)^2}\left[\left(\frac{\alpha\phi}{x}\right)'\right]^2. \end{aligned} \tag{22}$$

The asymptotic form of J being $J = \epsilon(A+\epsilon) = \text{const.}$, we put

$$g = BW \sin\left\{\int_{x_0}^{x} \frac{dx}{W^2} + \beta\right\} \tag{23}$$

in which B and β are constants, and obtain from Eq. (21)

$$W'' + JW - 1/W^3 = 0. \tag{24}$$

We want to find that solution of Eq. (24) which has a known simple form at infinity and which fluctuates as little as possible over a large range of x, since such a solution will be easily computed and will moreover give at once the asymptotic form of g. As Madelung[9] has indicated, such a solution can be found by means of the following iteration process:

[9] E. Madelung, Zeits. f. Physik **67**, 516 (1931).

$$JW^4{}_{n+1} = 1 - W_n{}^3 \cdot W_n'', \; W_0 = J^{-1/4}. \tag{25}$$

For the particular form of J given by Eq. (22) one can readily show that the iteration process converges for sufficiently large x, and that $\lim_{x\to\infty} W = J(\infty, \epsilon)^{-1/4} = [\epsilon(A+\epsilon)]^{-1/4}$. It is worth mentioning that when $\epsilon \to 0$ a numerical simplification results if one puts $W = (2a)^{1/2}x^{1/4}V$, also $x = (ay)^2$ $(a = 1/2(A\alpha)^{-1/2})$ in Eq. (24), and then obtains V by means of a similar iteration process.

Having thus determined W, we choose B and β to make the solution g join smoothly onto the solution G already found near the origin. If the subscript 0 means the values of the functions at the junction point, x_0, one finds readily that

$$\tan\beta = \frac{1}{W_0[W_0 g_0'/g_0 - W_0']}, \quad B = \frac{g_0}{W_0 \sin\beta}. \tag{26}$$

By use of the first of Eqs. (2′) and Eqs. (23) and (20), we find that F and G have the asymptotic forms

$$\begin{aligned} F &\sim M_x \frac{B}{(A+\epsilon)^{1/2}W(\infty)} \frac{\cos\left[[\epsilon(A+\epsilon)]^{1/2}x + \delta(x)\right]}{x} \\ G &\sim M_x (A+\epsilon)^{1/2} B W(\infty) \frac{\sin\left[[\epsilon(A+\epsilon)]^{1/2}x + \delta(x)\right]}{x} \end{aligned} \tag{27}$$

in which $\delta(x)$ is a slowly-varying function of x, and M_x is the "radial" normalizing factor in terms of x. Comparing Eq. (27) with Eq. (36) of reference 6 shows that F and G have the same asymptotic form here as there, and that

$$C = (A+\epsilon)^{1/2} B W(\infty), \; D = 1/(A+\epsilon)W(\infty)^2. \tag{28}$$

Therefore, with the proper change of variable, the normalization can be carried out here exactly as it was done there and one obtains

$$M_x{}^2 = \frac{2\mu}{hc}\frac{1}{DC^2} = \frac{2\mu}{hc}\frac{1}{B^2}. \tag{29}$$

We now have the solutions for both the discrete and continuous spectrum properly normalized, so that the evaluation of Eq. (1) is readily accomplished. In all numerical quadratures the interval of integration was taken small enough so that Simpson's rule gave the desired accuracy.

THE PERIODIC SYSTEM OF ATOMIC NUCLEI AND THE PRINCIPLE OF REGULARITY AND CONTINUITY OF SERIES

By William D. Harkins
George Herbert Jones Laboratory
The University of Chicago

(Received August 6, 1931)

Abstract

New relations which concern the existence and stability of atomic nuclei are presented, together with a discussion of evidence for the relations given earlier as exhibited by the newer data on the existence of isotopes. It is shown that the four series, the helium, uranium, lithium and beryllium series, exhibit a considerable amount of regularity and are now almost continuous. The more abundant species of odd atomic number keep in general to a constant isotopic number as the atomic number increases, or else the isotopic number increases by the same amount as the atomic number. There is a general tendency as the atomic number increases for the isotopic number of the most abundant isotope of elements of both even and odd atomic number (a) to remain constant, (b) to increase at the same rate as the atomic number or (c) to decrease along a line of constant electronic number.

The atomic, mass, isotopic, and electronic numbers of all known isotopes are given in figures which exhibit the periodic and other relations of atomic nuclei. Many undiscovered atomic species (isotopes of each element) between atomic numbers 61 and 18, are predicted, and the general relations predict the existence of a considerable number of additional species among elements of lower number.

These relations are presented in the form of fourteen rules, several of which are new, and three are fundamental laws presented earlier. The bearing of the newer data on these rules is discussed.

The paper discusses nuclear stability and abundance as related to the pairing of nuclear electrons and the oddness and evenness of the electronic number, to the evenness and oddness of the nuclear charge (atomic number) as exhibited by the most recent work on the composition of the crust of the earth, the meteorites, and the atmosphere of the sun, and to the ratio of nuclear electrons to protons.

The neutron, or nuclear neutral particle may play a part in atom building. The figures, fundamental laws, rules, and relations presented, especially the principle of continuity and regularity of series, when taken in connection with known facts, seem to indicate that atomic nuclei are built in steps, and, except in the simplest cases, not as single events. That is the general picture revealed by all of these appears to be in discord with the theory of Millikan and Cameron.

1. Introduction

THE atomic species, often, but incorrectly, called isotopes, give a pattern which exhibits a considerable number of regularities when they are plotted in any natural way. The most important of these regularities have been expressed by the writer in the form of a set of relations or rules in a series of papers.[1,2]

[1] Harkins and Wilson, J. Am. Chem. Soc. **37,** 1367–9 (1915), Phil. Mag., (1915).

[2] Harkins, J. Am. Chem. Soc. **39,** 859, Table II (1917); Science **50,** 580–1; Phys. Rev. **15,** 85 (1920); Phil. Mag. **42,** (1921); J. Am. Chem. Soc. **42,** 1976 (1920); J. Am. Chem. Soc. **43,** 1050 (1921); J. Franklin Inst. **195,** 554 (1923); J. Am. Chem. Soc. **45,** 1426 (1923).

While the most important of these rules have thus been known for a considerable time, the present paper gives additional interesting relations whose importance is revealed by more recent work. This has been so extensive, due to the efforts of Aston and others, that every one of the first sixty elements, except only columbium, masurium, rhodium, and palladium, has been tested for isotopes. While the number of isotopes which exist for such elements as strontium and barium is much larger than the number thus far found, the attainment of the present stage of completeness makes it essential to examine the relations which exist between the species now known.

2. Periodic System of the Atomic Species (Elements 1 to 60)

The values for two experimentally determined variables which relate to atomic nuclei, are well known. These variables are the mass number (P), supposed to give the number of protons in the nucleus, and the atomic number (Z). A derived variable, $P-Z$, is supposed to give the number of nuclear electrons (N).

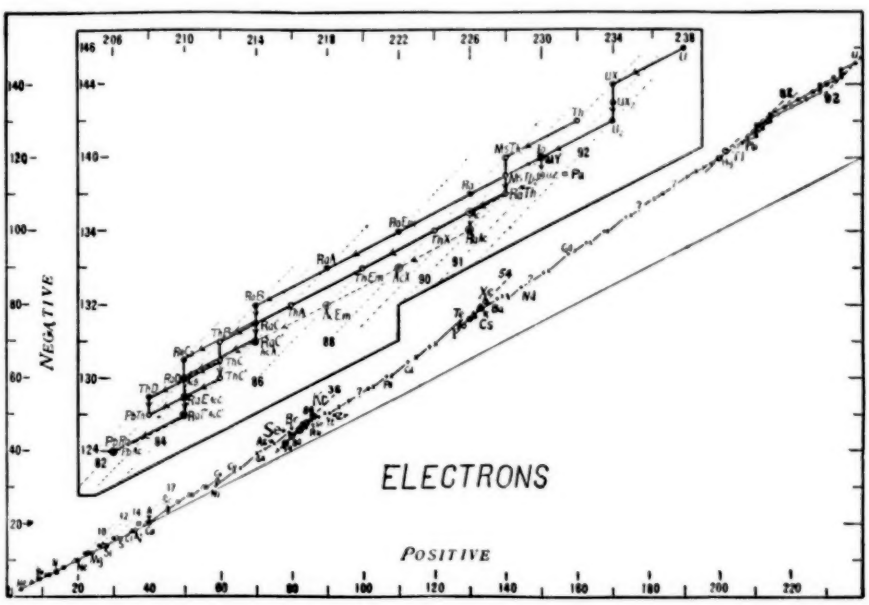

Fig. 1. The negative electron content of atomic nuclei as a function of the number of protons (positive electrons)

Fig. 1 shows the general form of the diagram which is obtained when the number of protons is plotted on the X-axis and the number of electrons on the Y-axis. The most abundant atomic species are found to lie in this plot on a line with a slope of $\frac{1}{2}$ which passes through the origin, and all of the other species are found to lie on 54 other equidistant lines above and parallel to this line. The scale of Fig. 1 is too small to show these lines except in the enlarged section in which the radioactive species are shown. These 55 parallel lines, when numbered, give the isotopic number, (n), a number as natural as, and on a par with, the atomic number.

The isotopic number has been defined by the writer[3] by the equations:

$$n = P - 2Z \tag{1}$$

$$n = 2N - P \tag{2}$$

$$n = N - Z. \tag{3}$$

If the formula of any nucleus is written as $(p_2e)_z(pe)_n$, then n is the isotopic number if p represents a proton and e, an electron.

If Fig. 1 is now rotated clockwise through the angle whose sine is $\frac{1}{2}$, and skewed so that the lines of constant atomic number are vertical, Fig. 2 results. This is the most compact and simple diagram which presents the relations between atomic nuclei. This and other forms of representation have been discussed by Harkins and Madorsky.[4]

In the figure every intersection of a vertical with a horizontal line represents a possible atomic species. The general position of the symbols which represent the atomic species shows that the band of greatest stability has somewhat the form of one limb of an hyperbola.

Species which belong to the thorium series ($P = 4M$) are designated by circles, those of the uranium series ($P = 4M + 2$) by diamond shaped symbols, those of the lithium series ($P = 4M + 3$) by triangles, and those of the beryllium series ($P = 2M + 1$) by squares. M is taken to represent any whole number. The thorium and uranium series are named for the radioactive series which they include and the other two series begin with the principal isotope of lithium and of beryllium, respectively.

The principal general pattern of Fig. 2 is that of a double network of squares, produced by the lines which give the atomic and the isotopic number. The heavier lines of this network represent even and the light lines odd numbers. It is evident that the greatest number of species occur where heavy horizontal lines meet heavy vertical lines.

The considerable regularity in the pattern exhibited is in accord with the rules listed in the next section.

It may be noted that the proton or hydrogen nucleus has an atomic number 1 and an isotopic number -1. The electron has an atomic number -1 and an isotopic number 2.

In Fig. 2, the lines of slope -1 give the number of nuclear electrons, and the dashed lines of slope -2 give the number of protons or the mass number. The double arrow-heads designate the mean atomic weight for the element. If these are not shown the mean value coincides somewhat closely with that for the principal isotope of the element.

The ratio N/P of negative electrons to protons is given by the lines which radiate from the origin.

The most abundant isotope of columbium or of rhenium has not been found by the positive ray method but the existence of both these species is indicated by the atomic weight of the element, so they are included in the figure.

[3] W. D. Harkins, Phil. Mag **42,** 305 (1921)

[4] W. D. Harkins and S. L. Madorsky, Phys. Rev. **19,** 135 (1922).

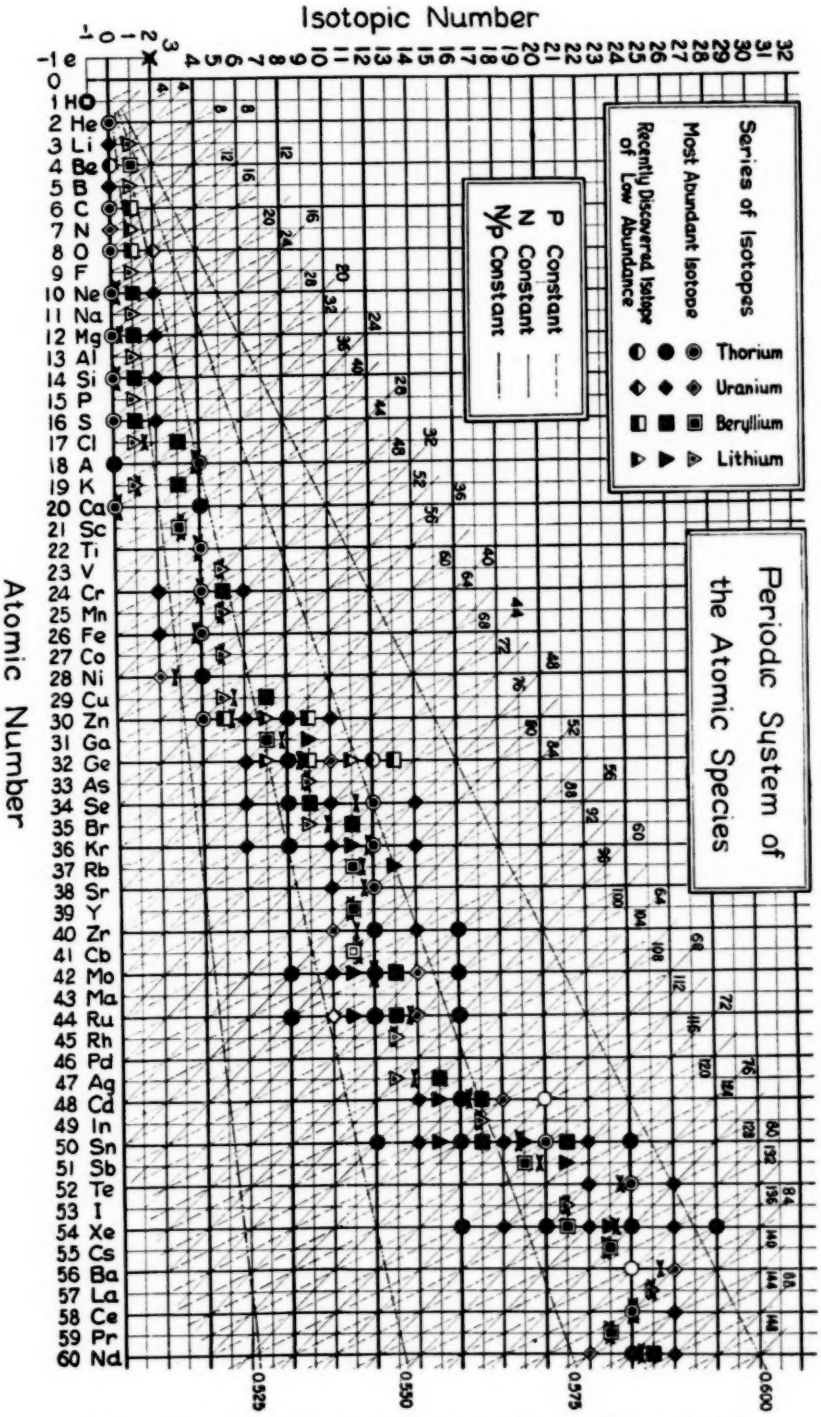

Fig. 2. Periodic system of atomic nuclei of nuclear charges −1 to 60.

3. Rules Concerning the Abundance and Stability of Atomic Nuclei

The most important rules which concern the stability and abundance of atomic nuclei are given below with special reference to Fig. 2, which emphasizes the fact that these rules are of even more general import than the limited earlier knowledge revealed.

In order to exhibit the extent to which the rules themselves apply it is necessary to consider a third dimension, to represent either abundance or stability, in connection with Fig. 2. Certain abundance relations are shown in Fig. 6.

Rule 1. Nearly all atomic nuclei contain an even number of electrons. Thus there seem to be at least 125 atoms of even to one atom of odd electronic number in the earth's crust. The extremely striking evidence for this rule is presented in Section 11, and the more detailed evidence in earlier papers by the writer. Corollary: Most atomic species have an even electronic number. Thus of the 156 known species for elements 1 to 60 inclusive, 125 have an even and 31 an odd electronic number. In Fig. 2 species of even electronic number lie on lines of slope -1, and those of odd number half way between the lines.

Rule 2. The number of electrons in the nucleus of any atom, other than hydrogen, is in no case less than half the number of protons (See Fig. 12).

Rule 3. Nearly all atomic nuclei have an even net nuclear charge, that is the atomic number is almost always even. The remarkable new evidence for this rule is presented in Section 10, and the more detailed earlier evidence in former papers of this series. Corollary: Most atomic species have an even atomic number. For example, of the 156 known species represented in Fig. 2 the atomic number is even for 116, and odd for 40.

Rule 4. Nearly all atomic nuclei contain an even number of protons. Corollary: More atomic species have an even than an odd mass number. Thus Fig. 2 shows 90 species with an even to 66 with an odd protonic number.

Rule 5. The number of protons in atomic nuclei is more often divisible by 4 than is to be expected by chance.

This relation is not so apparent in the number of species as it is in abundance especially of the light atoms. Thus 46 of the 156 species shown in Fig. 2 have mass numbers divisible by 4, and 43 divisible by 2 but not by 4. The number of species with mass numbers divisible by 3 should be 4/3 times the number divisible by 4, or 58, while the number found in Fig. 2 is 50.

However Rule 5 is of considerable significance, since all of the 5 most abundant species known in the meteorites have mass numbers divisible by 4.

Rule 6. If N is even then P is more often even than odd, and if N is odd, P is more often odd than even. Thus there is a certain matching of N and P with respect to evenness or oddness. There are almost no atoms in which the number of nuclear electrons is odd and the number of protons even. The 3 species of this type which exist are lithium 6, boron 10, and nitrogen 14, of isotopic number 0. They are the only species known which belong to Class IV according to Table I.

Rule 7. For light atoms (up to $Z = 28$) the isotopic number which represents the chemical atomic weight is in general higher for odd than for even-numbered elements. Above atomic number 28 this value is usually higher for even than for odd-numbered elements; that is, the relation is inverted.

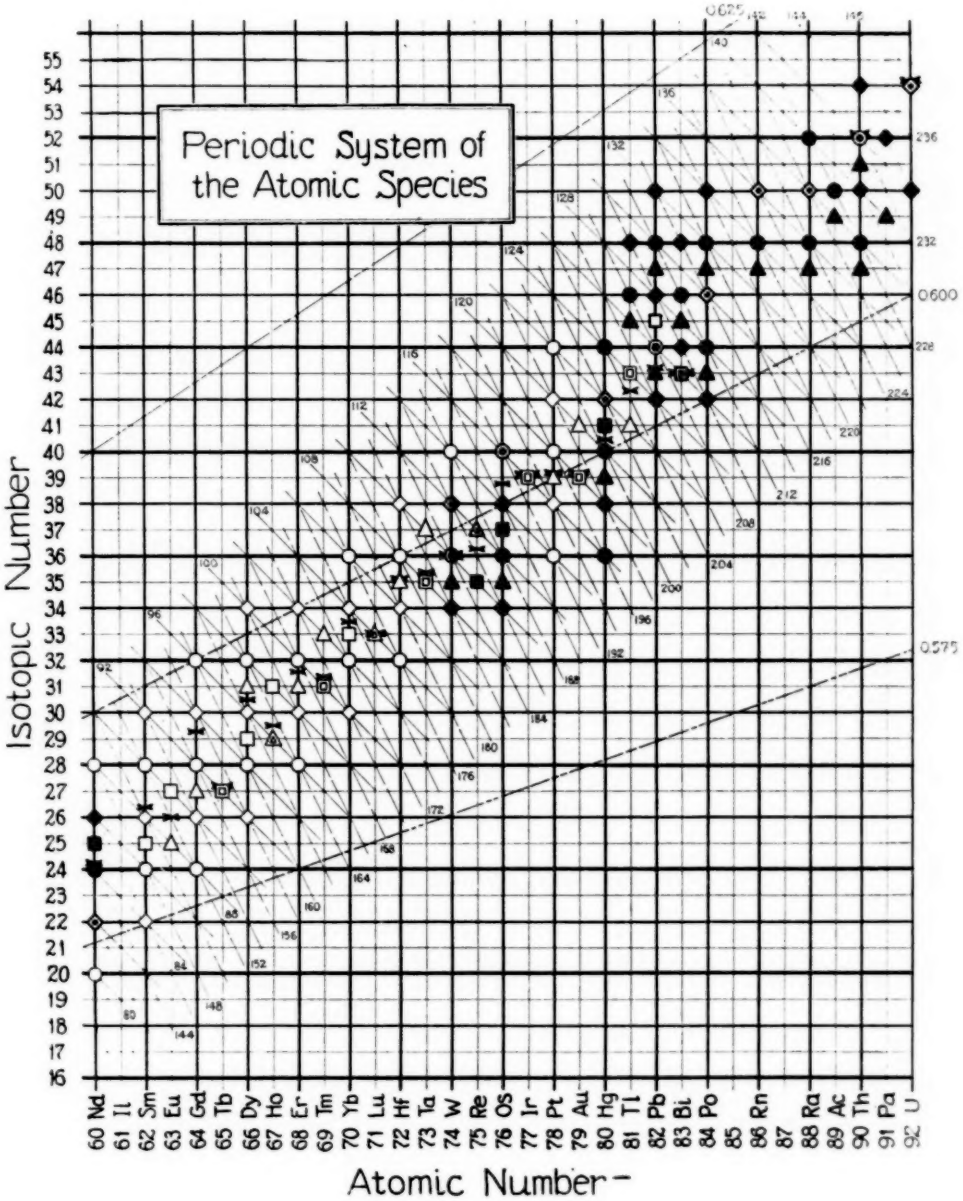
Periodic System of the Atomic Species
Isotopic Number
Atomic Number
0.625
0.600
0.575
Nd Il Sm Eu Gd Tb Dy Ho Er Tm Yb Lu Hf Ta W Re Os Ir Pt Au Hg Tl Pb Bi Po Rn Ra Ac Th Pa U

Fig. 3. Elements 60 to 92.

The above seven rules were discovered by the writer. An eighth found by Aston is as follows:

Rule 8. Not more than two isotopes are known for any element of odd atomic number, except among the radioactive elements.

TABLE I. *Classification of atomic nuclei according to even and odd number of electrons, and the corresponding abundance in the meteorites and the crust of the earth.*

Class			Abundance in Atomic Percentage	
			Earth's crust	Meteorites
Class I	N=even	P=even	87.4	95.4
Class II	N=even	P=odd	10.8	2.1
Class III	N=odd	P=odd	1.8	2.5
Class IV	N=odd	P=even	0.0007	0.0

Only 3 species of Class IV are known, and all of these have an isotopic number zero: lithium 6, boron 10, and nitrogen 14.

To the above may be added the following relation:

Rule 9. The difference of isotopic and of mass number between the two isotopes of an element of odd atomic number is always 2, except where species of Class IV of isotopic number 0 occur. (Li^6, B^{10}, N^{14}). The first two of these species have a mass number less by 1 than that of the more abundant isotopes.

4. Periodic System of the Atomic Species (Elements 60 to 92)

The general pattern for elements 60 to 92 is shown in Fig. 3, in which the symbols have the same significance as in Fig. 2.

Undiscovered species which are almost certain to be discovered later are designated by open symbols. A line around the inner part of the symbol indicates the most abundant isotope of the element.

From illinium (61) to tantalum (73) no atomic species have been found since these elements have not been investigated. It may be expected that all of the species listed in this region will be found when these elements are tested by methods with a moderate degree of sensitivity. The general pattern may be expected to be just that given. With more delicate methods the limits may be expected to extend beyond the species listed.

The more abundant isotope for each element of odd number is indicated, and the predictions may be expected to be correct in each case for which the chemical atomic weight is known.

It may be seen that rhenium and thallium are in discord with the otherwise general rule that the lighter of the two isotopes of an element of odd number is the more abundant.

Two other exceptions to this rule are found in lithium and beryllium, but this is due to the abnormal occurrence of isotopes of an entirely different class, those of Class IV according to one of the important schemes of classification introduced by the writer.

5. The Radioactive Series

The radioactive series are shown in Fig. 4. The atomic weight of members of the actinium series are unknown. The values given are those generally thought the most probable. If they are correct, the actinium series is a part

of the lithium series. On this basis, the members of this series have odd isotopic numbers and give odd isotopes to the elements of even number. The atomic weights or number of protons, and the number of electrons are given in the figure. Thus for radium the atomic weight is 226 and the number of electrons 138.

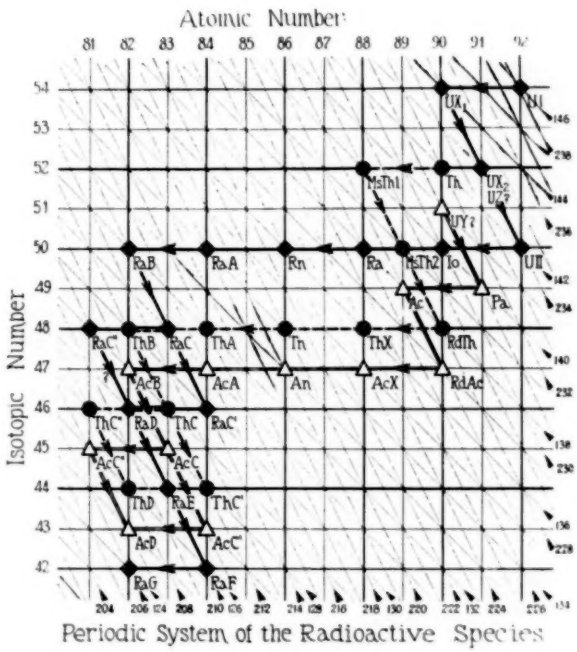

Fig. 4. The radioactive elements.

6. Variation in Abundance of Isotopes

Rule 10. For light elements of even number the most abundant isotopic species in an element of even number has an isotopic number of zero, or one divisible by 4, that is the most abundant isotope belongs to the helium-thorium ($4M$) series.

Up to element 38 there are only three exceptions: beryllium, nickel, and germanium.

Rule 11. For light elements of odd number the most abundant isotope has first an isotopic number 1, which increases (by 4) to 5 for elements 23 to 29.

Thus for either even or odd elements the most abundant isotopes tend to lie on lines of constant isotopic number, which, when varied increase by 4 as the atomic number rises.

Rule 12. (a) For light elements (up to 30) the most abundant isotope of an element of even number has the same electronic number as the next preceding element of odd number. For elements of higher number this relation is commonly reversed.

Rule 12. (b) Thus successive most abundant isotopes often lie on a line of constant electronic number. For example, the electronic number is 82 for the principal isotope of Ba (56), La (57), Ce (58), Pr (59), and Nb (60), and it is 50 for the principal isotope of Sr (38), Yr (39), and Zr (40).

An interesting relation is revealed by Fig. 3. The principal isotope of each element of odd number from Tb (65) to Ir (77) lies on a straight line of slope 1. On this same straight line lie the principal isotopes of the even-numbered elements Nd (60), Hg (80), Ra (88), Th (90), and U (92), and one of the two most abundant isotopes of W (74).

The increment along such a line is p_3e_2 between adjacent elements and p_6e_4 between odd (or even) elements. That this relation is not fortuitous, at least for the elements of odd number, is shown by the fact that the principal isotopes of Rh (45), In (49), Sb (51), I (53), Cs(55), and La (57) also lie on another line of slope 1. The same is true of Cu (29), Ga (31), and As (33), and also of K (19), Sc (21), and V (23).

Rule 13. In general for elements of odd number, with increase of atomic number:

(a) the isotopic number of the principal isotope remains constant, so the mass number increases by 4, and the electronic number by 2—that is the increment has the composition of an alpha-particle, or

(b) the isotopic number increases at the same rate as the atomic number, —that is the increase in mass number is 6, and in number of electrons is 4.

In one case, from lanthanum to praeseodymium, Rule 12 becomes more prominent and the isotopic number decreases along a line of constant electronic number.

The relations expressed by Rule 13 are expressed in Fig. 5.

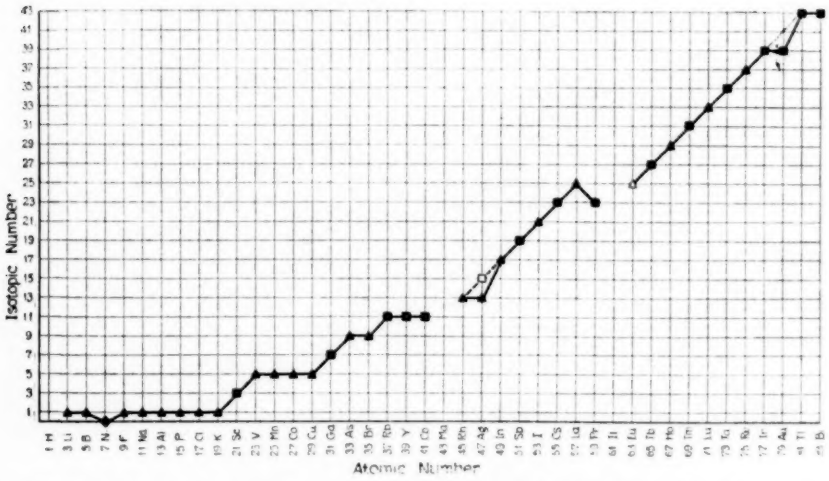

Fig. 5. The variation of the isotopic number for the most abundant isotopes of the elements of odd number. The two isotopes of silver have almost the same abundance.

7. Distribution of Abundance among Isotopes

The distribution of abundance among isotopes is very simple for elements of odd number.

Rule 14. The more abundant of the two isotopes of an element of odd number has in general the lower isotopic and the lower mass number.

This is not true for two elements, lithium and boron, which have isotopes

of the exceptional Class IV, but is true for nitrogen. As with certain other rules, some exceptions are found in elements of high atomic number. Thus in rhenium (75) and thallium (81) the higher isotope is the more abundant. In silver the two isotopes have almost the same abundance as judged from the chemical atomic weight and the packing fraction (See Fig. 5).

The variation in abundance of the isotopes of 9 well distributed elements is shown in Fig. 6. The vertical distance between two adjacent horizontal lines represents 50 percent, except for oxygen, at the top where the distance is twice as great, or 100 percent. The values for small percentages are printed in the figure. Thus oxygen consists of 99.9 percent isotopic number 0, 0.01

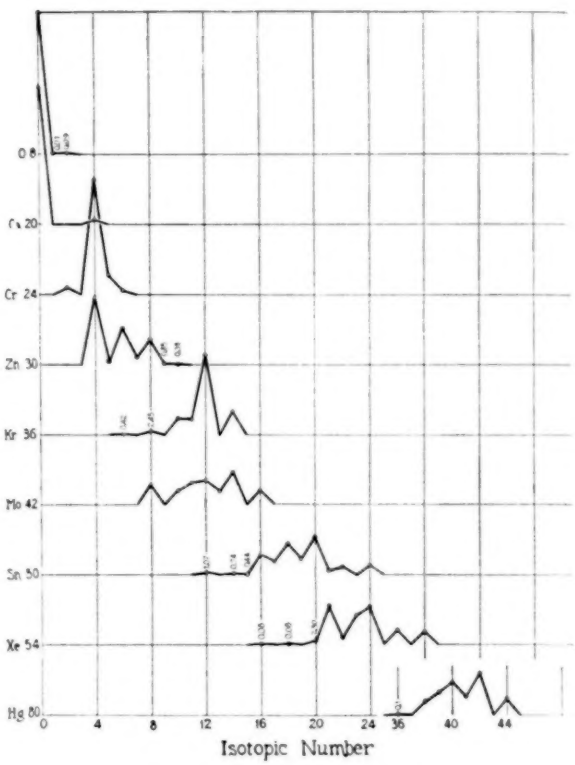

Fig. 6. Abundance of isotopes.

percent number 1, and 0.09 percent number 2. The pattern for neon, magnesium, silicon and sulphur, is in each case the same as for oxygen, except that isotopes 1 and 2 are relatively more abundant, especially for magnesium. The patterns for calcium and argon are the inverse of each other, with isotopes of number 0 and 4, with almost the whole material concentrated in the 0 isotope of calcium, and in isotope 4 of argon. Fig. 2 indicates the probability that both argon and calcium have undiscovered species of number 2, and probably 3, and that argon and possibly calcium probably contain species of isotopic number 1.

As the atomic number increases several peaks of abundance become prom-

inent instead of the single high peak found for oxygen, neon, magnesium, silicon, sulphur, argon, calcium, chromium, and krypton. Also, Rule 15, the abundance is much higher on the whole for even than for odd isotopic numbers. In xenon isotopes 21 and 24 are the most abundant, which represents an exceptional case in so far as 21 is concerned.

The distribution of abundance for two other elements is as follows; as found by Aston:

Ruthenium, atomic number = 44		
Isotopic number	Mass number	Percent
8	96	5
10	98	?
11	99	12
12	100	14
13	101	22
14	102	30
16	104	17

Ruthenium, like molybdenum (42) has the maximum of abundance at isotopic number 14, and the two patterns are much alike.

Osmium, atomic number = 76		
Isotopic number	Mass number	Percent
34	186	1.0
35	187	0.6
36	188	13.5
37	189	17.3
38	190	25.1
40	192	42.6

Here is an exceptional case, in that the highest isotope (thus far found) is the most abundant.

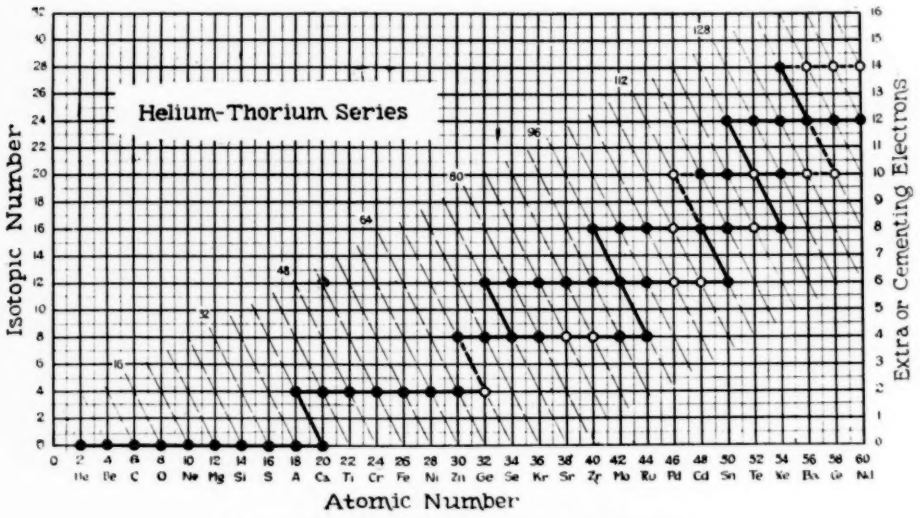

Fig. 7. Continuity in the helium-thorium series.

8. The Principle of Continuity and Regularity of Series of Atomic Nuclei (Atomic Species)

Certain regularities in the system of atomic nuclei are made more apparent by a separation of the atomic species into the four following series:

A. Even Series
   1. Helium-Thorium ($4M$) Series
   2. (Lithium 6) -Uranium ($4M+2$) Series

B. Odd Series
   3. Lithium 7 or lithium ($4M+3$) Series
   4. Beryllium 9 or beryllium ($4M+1$) Series

Thus the helium-thorium series (Fig. 7) exhibits a regular pattern as shown: the isotopic number increases by 4 at each step, and between calcium

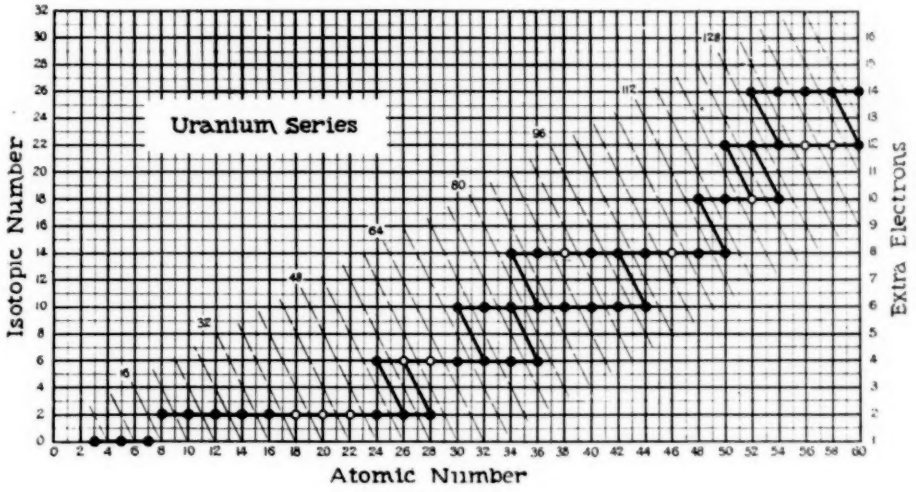

Fig. 8.

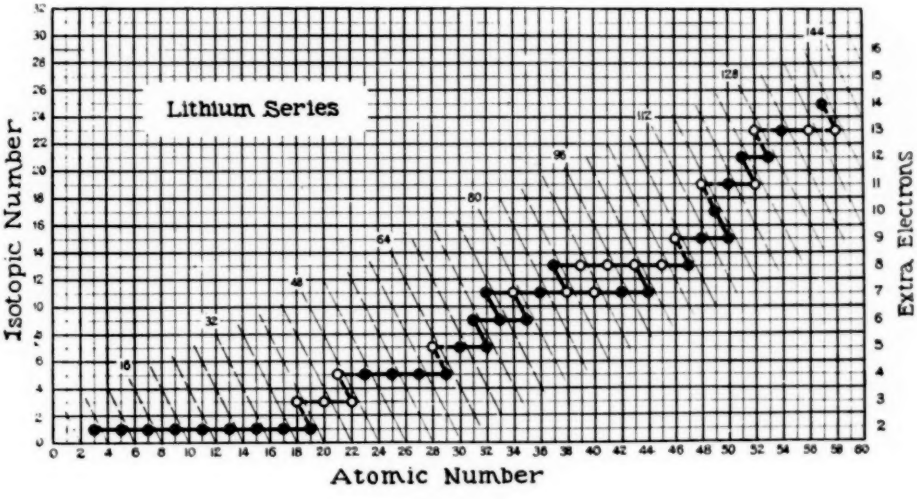

Fig. 9.

($P=40$, $n=0$) and argon ($P=40$, $n=4$) the atomic number decreases by two as the isotopic number makes its first step above zero. According to the principle of continuity all species which belong to the series and which lie on a line of constant isotopic number between the limits of known species are in general supposed to exist.

Thus the principle of continuity definitely predicts the following species: strontium ($n=8$, $P=84$), zirconium ($n=8$, $P=88$), palladium, two unknown species ($n=12$, $P=104$, and $n=16$, $P=108$), cadmium ($n=12$, $P=108$), tellurium, two unknown species ($n=12$, $P=120$ and $n=16$, $P=126$), or seven species in all, while 47 of the 54 species are now known.

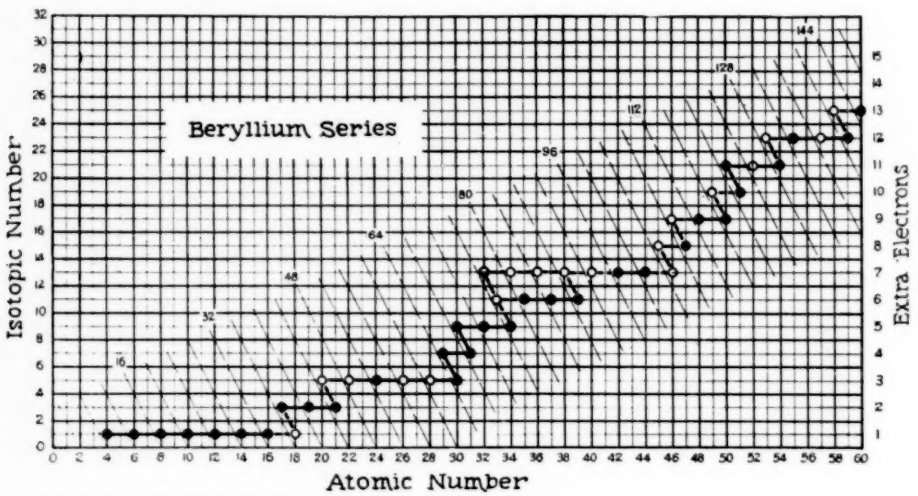

Fig. 10.

Species such as germanium ($n=4$, $P=68$) are not so definitely predicted, for here the existence of nickel ($n=8$, $P=64$) would meet the condition of regularity as well. It is also not so certain that the particular type of regularity which would be preserved by the existence of either of these two species is so persistent as the general form of the pattern otherwise.

There are undoubtedly great differences in the stability of species along any line of constant isotopic number, just as in the radioactive series, It, therefore, need not be surprising if a small number of species predicted by this principle remain undiscovered until much more delicate means of detection are discovered.

What is more apparent, however, is that the isotopic composition now given for such elements as strontium and barium is entirely inadequate, that zirconium contains a lower isotope than is now known, etc. The principle indicates that masurium ($Z=43$) has either an isotope of mass number 97 or of 99, and that probably both are present. The following table gives the length of each level as at present known:

This agrees with Latimer's nuclear model which is based on a part of the above relation expressed by Fig. 7, as given by the writer[5] in 1921.

[5] Harkins, Phil. Mag. **42**, 306, Pl. XII (1921).

Level	Isotopic Number	Number of Species Between Known Limits	In Table
1	0	10	10
2	4	7	8
3	8	8	8
4	12	10	10
5	16	8	8

The helium-thorium series is shown in another form in Fig. 11 in which lines of constant atomic number have a slope of 2, and the atomic number at the X-axis is twice the number of α-particles, and the number of electrons 2 times the number of α-particles plus the number of cementing or extra

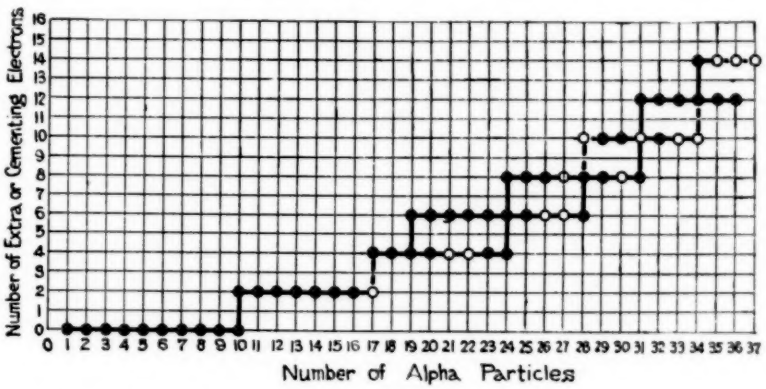

Fig. 11. The helium-thorium series. The atomic number is twice the number of alpha particles minus the number of cementing or extra electrons.

electrons. This form of representation was used early by the writer and has been adopted by Gamow and others.

The uranium series is much like the thorium series, but shifted two isotopic numbers higher.

A marked difference occurs in that the two lowest levels are only two isotopic numbers apart, but this is due to the presence of the three abnormal species of Class IV.

Level	Isotopic Number	Number of Species in Known Series
0	0	(3)
1	2	11
2	6	7
3	10	8
4	14	9

Here as in the thorium series levels 1 and 4 are the longest.

Odd Series. The odd series exhibit extremely interesting relations. Thus the two series would become almost coincident if the atomic number of every species in the beryllium series were increased by one. Unlike the even series, which occupy even isotopic levels but not in common (exception Class IV), each of the two odd series occupies every odd isotopic level. Like the even series the first level is especially long.

The lithium and the beryllium series together constitute what may be considered as a single combined or odd series.

9. The Ratio of Nuclear Electrons to Protons and the Isotopic Number

The isotopic number, defined in Section 1, has not come into general use, because, although it is an entirely natural and necessary number, it does not seem to be related to a sufficiently simple characteristic of atom nuclei to make it easily comprehensible to physicists or chemists in general. If, as in Fig. 12, the ratio of nuclear electrons to protons is plotted on one axis, and the atomic number (or the number of protons) on the other, it is found that every point which represents an atomic species lies on one of 55 lines. These

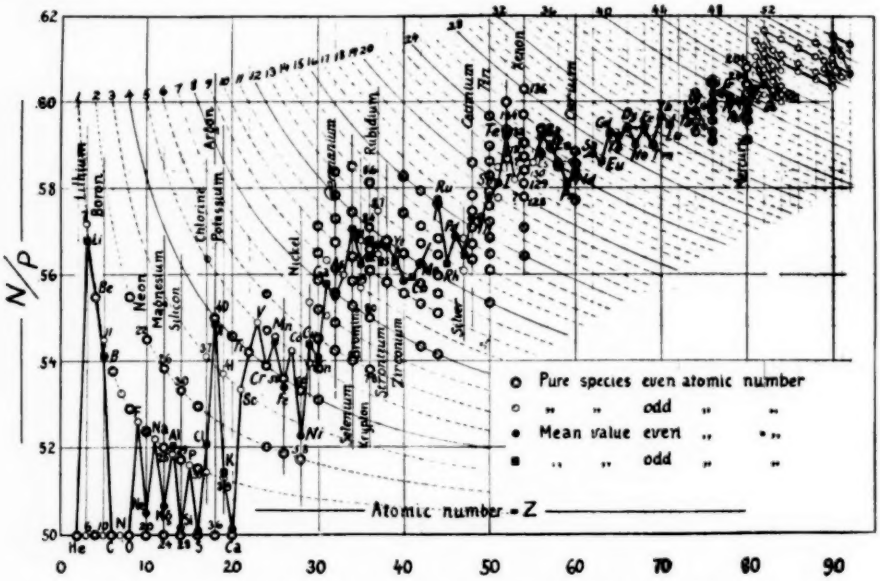

Fig. 12. Variation of the relative negativeness (N/P) of atomic nuclei with their net positive charge (ε).

lines give the isotopic number. In Fig. 12 one of these lines is straight, while each of the others has nearly the form of one branch of an equilateral hyperbola. The straight line, which is thus different from all the rest, is given the isotopic number zero, and the curved lines are numbered from 1 to 54.

As has already been shown by the writer the stability of an atomic nucleus is highly dependent upon the values of N/P and Z. Thus as the net positive nuclear charge (Z) grows larger the relative negativeness (N/P) of the nucleus must also increase if the nuclei formed are to be stable. For any value of Z stable nuclei have a certain range of values of N/P.

The present known range for N/P is largest for lithium (0.071), is 0.055 for beryllium and oxygen, 0.045 for selenium, and almost this last value for tin and germanium. The range of N/P decreases in general as the nuclear positive charge (Z) increases. It is appreciably less than 0.02 for mercury or any radioactive element.

The range in the known isotopes of sulphur ($Z=16$) is 0.029, which is abnormally low for a light element. According to the early theory of the writer, adopted in Latimer's recent nuclear model, this is due to the fact that in the sulphur nucleus the first pair of cementing elections, which are present in argon 40 ($Z=18$), have not as yet entered the nucleus. Thus in addition to a matching of N/P and Z in the nucleus, certain specific constituitive influences affect the stability.

No atomic species is known in which the ratio N/P is greater than 0.62.

10. The High Abundance of the Chemical Elements of Even Number (Rule 3)

The theory of nuclear structure and stability developed by the writer[1] in 1915 indicated that the elements of even number should be much more stable and abundant than those which are odd. It is very surprising that such an important and striking fact should have remained so long unrecognized.

The data which supported this rule were considered comprehensively in the 1917 paper.[2] However the great progress made since that time in the investigation of the abundance of the elements in the rare earths by Goldschmidt, in the meteorites and in the earth's crust by Ida and Walter Noddack, in the atmosphere of the sun by Russell, and in the stars by Payne, as carried out by x-ray and ordinary spectroscopic methods,[6] makes it essential to consider the relationship between the rule and the newer data. This is particularly important, since, as was predicted when the rule was discovered, its application in connection with cosmic composition is now found to be of fundamental importance.

Thus the newest data indicate that the atomic nuclei of the elements of even number are 50 times more abundant in the meteorites, 10 times more abundant in the surface of the earth, 10 times more abundant in the atmosphere of the sun, and more abundant, by an unknown factor, in the stars than the elements of odd number.

The meteorites give the best idea of the composition of material in general, since they are more available for analysis than the stars, and come from much more widely distributed regions than the crust of the earth. The six most abundant elements in the meteorites are all even in atomic number, and these six alone contain 97 percent of all of the atoms in the meteorites. Their relative abundance in terms of number of atoms is as follows:

Oxygen	1
Iron	0.59
Silicon	0.30
Magnesium	0.25
Nickel	0.42
Sulphur	0.04

[6] V. Goldschmidt and Thomassen, Videnskaps. Skrift. I. Mat.-naturw. Kl. 1924, No. 5. I. and W. Noddack, Naturwissenschaften **18**, 757 (1930); H. N. Russell, Astrophys. J. **70**, 11 (1929); Miss Payne ,Stellar Atmospheres (Harvard Observatory Monographs, No. 1), Cambridge, Mass., p. 184 (1925).

The recent data of Ida and Walter Noddack are represented in Fig. 13. All of the high peaks are for elements of even number. Of all of the 31 peaks only one, for arsenic, represents an element of odd number. This element

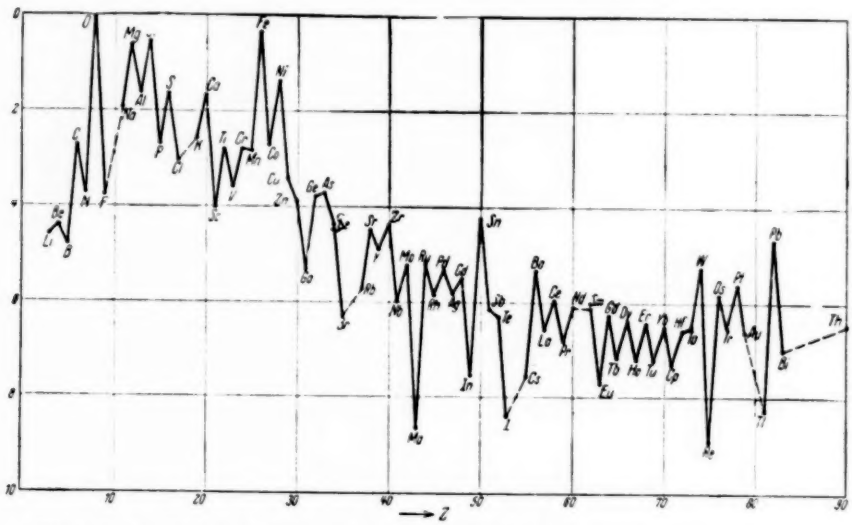

Fig. 13. Logarithm of the atomic abundance of the elements in the meteorites (Noddack). (Abundance of oxygen taken as unity).

seems anomalous in the earth's crust also, with an abnormally high abundance (only 5.5×10^{-6} parts by weight, however) and is found to have an abnormally

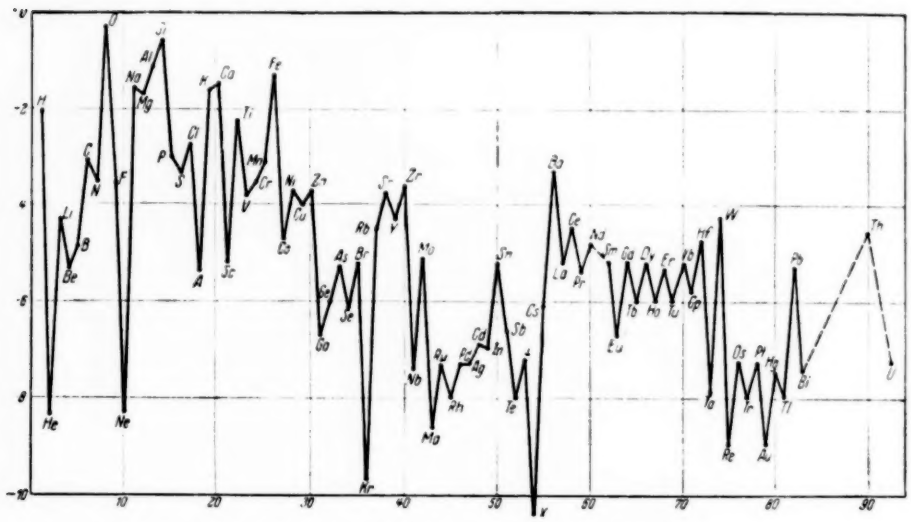

Fig. 14. Logarithm of the atomic abundance of the elements in the earth's crust. (Noddack). (Fraction of the total number of atoms.)

low abundance in the atmosphere of the sun. Fig. 14 represents the crust of the earth, in which 32 of the 34 peaks (hydrogen excluded) represent elements of even number.

The fact that the lowest troughs occur for the rare gases indicates that here the chemical and physical characteristics rule, and not the stability of the nuclei. Otherwise masurium, rhenium, and gold are the rarest in the earth's crust, and masurium and rhenium in the meteorites.

In general in both the meteorites and the earth's crust, each element of even number is much more abundant than either of the two adjacent elements of odd number. In individual cases where this is not true the element of even number is more abundant than the arithmetic mean of the two that of the two adjacent elements of odd number.

Concerning the atmosphere of the sun Russell states "Every element of even number except beryllium, is more abundant than the mean of the adjacent elements, and every odd element less abundant, with the exception of europium, for which the data are uncertain. Among the rare earths only those with even atomic numbers have been conclusively identified in the sun". He adopts the early idea of the writer that the low abundance of lithium and beryllium may be due to the small number of the component parts of which their nuclei are built: too few to give high stability. It should be remembered that there are several types of stability.

11. The Pairing of Nuclear Electrons and the High Abundance of Atomic Nuclei of Even Electronic Number (Rule 1)

The theory that the electrons in the nucleus are almost always associated in pairs was developed on the basis of the "hydrogen-helium" theory[1] according to which the nucleus of the atom is built up of groups of the composition of alpha particles, and other groups, almost all of which contain a pair of electrons. In addition it was noticed that cementing electrons occur in general in pairs. Thus in the 26 light species listed in 1917[7] the formulae give 209 pairs of electrons to 2 unpaired electrons. The pairs seem to be more prominent still in the heavier atoms.[8]

The theory that the electrons are associated in pairs suggested Rule 1, according to which nuclei in which the electronic number is even are extremely more abundant than those in which it is odd.

Only two species of odd electronic number for which the atomic fraction in the earth's crust is greater than 1×10^{-5} are known;—magnesium 24 and silicon 29. Of the 214 atomic species listed in Figs. 2 and 3 as discovered by radioactive means, by positive rays, or by band spectra, 52 or nearly one-fourth have an odd electronic number. However, the species of odd electronic number have an extremely small abundance. Thus there seem to be at least 125 atoms of even to one of odd electronic number in the earth's crust. The most important experiment in this connection would be to determine accurately the quantitative isotopic composition of silicon and magnesium.

Although recent theory attributes nuclear spin entirely to the protons of the nucleus, and although there seems to be some connection between nuclear spin and stability, the above considerations seem to indicate that the

[7] W. D. Harkins, J. Am. Chem. Soc. **39**, Table II, 859 (1917).
[8] W. D. Harkins, Phys. Rev. **15**, Tables II and III, pages 85 and 86 (1920).

pairing of nuclear electrons is a more fundamental phenomenon in relation to stability than spin. Up to the present time the new quantum mechanics has not been successful in bringing this most fundamental pairing into the theory. This type of pairing seems in some way to be associated with the presence of protons. The pairing of electrons in the nucleus, as discovered by the writer, is more general, and represents a much more intimate association, than their pairing in molecules as found by Stark and G. N. Lewis.

12. Atom Building in Steps

The general relations presented in this paper, especially those concerned with the principle of continuity and regularity of series, and with the relations of the most abundant isotopes, suggest strongly that atom nuclei are built in steps, and not in single events. That is they seem to be in entire disagreement with the idea that atomic nuclei are all formed almost instantaneously (say 10^{-12} seconds) as is assumed in the theory of Millikan and Cameron.[9]

That atoms are actually built in steps under some conditions is demonstrated by the well known synthesis of oxygen 17 from nitrogen 14.

13. Atom Building by Neutrons

There is no evidence whatever that neutrons, or electrically neutral nuclear particles, play any part in atom building, or even that they exist. However the difficulty which a positively charged particle would in general have in penetrating the potential barrier around a nucleus of high charge, suggests that some other process may be utilized in the formation of atomic nuclei. Proceeding from this point of view both Rutherford and Harkins suggested independently in 1920 that such neutral nuclear particles (neutrons) may add themselves to atomic nuclei.[10] The same idea has been revived by Langer and Rosen[11] who seem to consider it to be an entirely new suggestion. Neutrons could not be detected by chemical means, and their percentage in the earth's crust would be very minute, provided they exist.

Rule 2, according to which the ratio of electrons to protons in any nucleus which contains both, is in no case less than $\frac{1}{2}$, is not in discord with this idea, but the fact, shown so plainly in Fig. 12, that there is no known nucleus in which this ratio is more than 0.62, shows that the existence of neutrons would give an entirely different order of magnitude for this ratio. This seems to indicate that neutrons may not exist, but the simple neutron (*pe*) represents a limiting case, which might well be an exception to the rule.

If, as is now supposed, nuclear spin is associated entirely with electrons, the simple neutron would be expected to exhibit a spin of $h/2\pi$. The general properties of neutrons and neutronal material as assumed by Langer and Rosen are the same as those given earlier.

[9] R. A. Millikan and Cameron, Phys. Rev. **31,** 921 (1928).

[10] W. D. Harkins, J. Am. Chem. Soc. **42,** 1965 (1920), Chemical Reviews, **5,** 431 (1928). Ernest Rutherford, Proc. Roy. Soc., London, **42,** 1964 (1920).

[11] R. M. Langer and N. Rosen, Phys. Rev. **37,** 1579 (1931).

MULTIPLET STRUCTURE AND ZEEMAN EFFECT

By J. B. Green* and R. A. Loring
Mendenhall Laboratory of Physics, Ohio State University

(Received August 4, 1931)

Abstract

Houston's method as applied to triplets and singlets cannot account for any inversions in the triplet terms. This is probably due to the fact that spin-spin and mutual spin-orbit interactions are neglected. The results of Houston's and Goudsmit's work are applied to the Zeeman effects of the spectra of Sn III and Sb I, and the agreement is found to be very satisfactory.

THE relation of multiplet structure to Zeeman effect has been discussed in detail by Houston[1] for the case of one *s*-electron and one other electron. The arguments used by Houston and the formulas he derives have been shown by Laporte[2] and by Condon[3] to apply equally well to the case of one *s*-electron and a shell of other electrons lacking one for completion. Houston's results depend on the previous work of Heisenberg[4] on the spectrum of helium, which has since been done more rigorously by Gaunt,[5] using Dirac's method.

Briefly, the method consists in setting up the Hamiltonian function as an operator in three parts, (1) the ordinary kinetic and potential energy, (2) the electrostatic interaction of the two electrons, (3) the other perturbations, such as the interaction of each electron spin with its orbital momentum, the magnetic interaction of the two electrons, and the interactions between each electron spin and the orbit of the other. Of the last named perturbations, only the individual spin-orbit interaction involves the atomic number Z, so that for high effective atomic numbers, the others may be neglected as being of order $1/Z$ compared with it.

This is the case that Houston has considered in his work. As a consequence, his results can apply only to cases for which the effective atomic number is large, and should not be expected to fit the cases where either the real atomic number is small, or where we are dealing with a "nonpenetrating orbit." A comparison of Heisenberg's results with Houston's shows this very clearly. Both Heisenberg and Gaunt get an inversion for the triplet spectra of He I and Li II, as is really the case, while Houston's results do not yield the possibility of accounting for any such inversions. On the other hand, both Heisenberg's and Gaunt's calculations depend on the assumption of a large

* John Simon Guggenheim Memorial Fellow.
[1] Houston, Phys. Rev. **33,** 297 (1929).
[2] Laporte and Inglis, Phys. Rev. **35,** 1337 (1930).
[3] Condon and Shortley, Phys. Rev. **35,** 1342 (1930).
[4] Heisenberg, Zeits. f. Physik. **38,** 411 (1926).
[5] Gaunt, Phil. Trans. Roy. Soc. **A228,** 151 (1929).

spin-orbit interaction, i.e., a large energy difference between the triplet and singlet terms of the same electron configuration, so that they are of no use in considering several of the cases covered by Houston's work.

These partial inversions also occur in the two-electron spectra of high atomic number elements, such as the ^3F terms of Tl II and Pb III.[6] Here, the cause of the inversion is possibly attributable to the nonpenetrating character of the orbits, so that the terms are nearly hydrogenic and the effective Z is small, and the neglect of the higher order terms in the perturbations is not permissible. It seems, therefore, that the theory should be extended to cover these cases too, by the calculation of these spin-spin and mutual spin-orbit interactions. However, the mathematical tedium is probably too great and so it has not yet been done.

In spite of these drawbacks, Houston's results do give us one good clue as a help in spectral classification where the triplet terms are in their normal order. The positions for Russell-Saunders coupling measured from the center of gravity of the triplet are $L-1$, and $-L-1$. If the center triplet level is lower than -1, then we should look for the related singlet level higher than L. If the center triplet level is higher than -1, then we should look for the related singlet level lower than $-L-1$. An application of this method to the spectrum of Pb III indicates that Smith's choice of 7^1D_2 is probably incorrect, and that the term he has called pp^1D_2 is the proper choice for 7^1D_2.

The method also gives us an excellent comparison of interval ratios and Zeeman effects, as Houston has already shown. But there has been no very careful check on the g-values of highly-ionized atoms. With a view toward supplying this deficiency, we have carefully remeasured our plates for Sn III.[7] These had previously been measured for qualitative purposes, principally for use in spectral classification. Even so, certain anomalies in the Zeeman patterns of the lines were noticed. The new measurements appear in Table I.

TABLE I. *Zeeman patterns of Sn III lines.*

Wave-length	Classification	Zeeman pattern			
4585	$^3S_1{}^3P_2$	(0) (0.502)	(1.002)	1.508	1.984
4856	$^3S_1{}^3P_1$	(0.535)	1.442	1.983	
5291	$^3P_1{}^3D_1$	0.479	(0.926)	1.445	
5369	$^3P_0{}^3D_1$	(0) 0.512			
4330	$^1P_1{}^3S_1$	(0.95)	1.06	2.01	

The weighted g-values based on the intensities of the components and the ease of the setting of the microscope, together with the Landé g-values and those calculated with the aid of Houston's formulas are as follows. The agreement between Houston's formulas and experiment is seen to be quite good, probably well within the limits of experimental error. For the last two levels, belonging to the same electron configuration, Pauli's g-sum rule is satisfied.

[6] Smith, Phys. Rev. **34,** 393 (1929).

[7] Green and Loring, Phys. Rev. **30,** 574 (1927).

TABLE II. *Observed and calculated g-values for Sn III.*

Level	Observed	Landé	Houston
$^3S_1$	2.001	2	2
$^3P_2$	1.505	3/2	3/2
$^3D_1$	.503	1/2	1/2
$^3P_1$	1.447	3/2	1.456
$^1P_1$	1.055	1	1.044

Goudsmit's[8] extension of Houston's and Slater's methods also gives us a method of comparing Zeeman effect data with the theory of interval ratios. As examples, the p^2 configuration of Sn I and Pb I serve excellently. The formula for the g-value in this case becomes

$$g = \frac{(5/2)E - 3X - (7/2)A}{2E - 2X - 3A}$$

TABLE III. *Observed and calculated g-values in the spectra of Sn I and Pb I.*

Element	Level	Landé	Observed	Calculated
Sn I	$^3P_2$	3/2	1.45	1.46
	$^1D_2$	1	1.05	1.04
Pb I	$^3P_2$	3/2	1.27	1.29
	$^1D_2$	1	1.23	1.21

whence we find the values of g given in Table III. For the configuration ^3P+s the g-formula is

$$g = \frac{(10/3)E - (8/3)X + 8A}{2E - X + 5A}$$

and we find in the spectrum of Sb I the g-values given in Table IV. It is not

TABLE IV. *Observed and calculated g-values in the spectrum of Sb I.*

Level	Landé	Observed	Calculated
$^4P_{1/2}$	8/3	2.333	2.370
$^2P_{1/2}$	2/3	1.004	0.963

possible to carry out the same sort of calculation for the $^4P_{3/2}$ and $^2P_{3/2}$ levels of the same configuration, for the partial g-sum is not constant as in the above examples, where $j=\frac{1}{2}$, for all types of coupling, but is influenced by the proximity of the $(^1D_2+s)^2D_{3/2}$ term.

[8] Goudsmit, Phys. Rev. **35**, 1327 (1930).

THE ROTATIONAL ANALYSIS OF THE FIRST NEGATIVE GROUP OF OXYGEN (O_2^+) BANDS

By Daniel S. Stevens
Ryerson Physical Laboratory, University of Chicago

(Received August 24, 1931)

Abstract

The ultraviolet O_2^+ bands have been produced by a hollow cathode discharge, or with greater intensity from a mixture of helium with a small amount of oxygen in a large discharge tube. Photographs were taken in the second order of a 21 foot Rowland grating (dispersion = 1.32A/mm). The following bands were used for a rotational analysis: 1-8; 0-8; 1-9; 0-9. As was expected, since NO and O_2^+ have the same number of electrons, these bands correspond to a $^2\Pi \rightarrow {}^2\Pi$ transition like the double headed β bands of NO. The lower $^2\Pi$ is case a as in NO. Unlike the case of NO, however, the upper $^2\Pi$ is case b. The lower $^2\Pi$ is regular, with a doublet separation A'' (corresponding to zero rotation) of 195 cm^{-1}. In the upper $^2\Pi$ the value of the spin-orbital coupling coefficient A' is +8.2. Each band consists of eight branches (four P and four R), the Q branches apparently being too weak to appear on the plates. This is in agreement with theory. Λ-type doubling is negligible in the upper $^2\Pi$ but is present in the lower $^2\Pi$ state. Alternate levels in each successive Λ-type doublet are missing. This is as predicted by the quantum theory of homopolar molecules, since it is known that the nuclear spin of the oxygen atom is zero. The probable electronic configuration of the upper $^2\Pi$ state is given as $\cdots 2p\pi^3\, 3d\pi^2$, and that of the lower $^2\Pi$ state as $\cdots 2p\pi^4\, 3d\pi$. The constants of the molecule in the two electronic states are given by: $B' = 1.048 - 0.014\, v'$; $B'' = 1.610 - 0.009\, v''$; $r_e' = 1.41 \times 10^{-8}$ cm, $r_e'' = 1.14 \times 10^{-8}$ cm; $A' = +8.2$ cm^{-1}; $A'' = +195$ cm^{-1}.

Introduction

A SYSTEM of double headed bands lying in the region λλ4400–2000 can be obtained[1] by passing a discharge through pure oxygen. These bands are called the first negative group of oxygen and are attributed to O_2^+. From the type of transition and the molecular constants determined by the present rotational analysis there can be no doubt that O_2^+ is actually the emitter.

The vibrational analysis of these bands has been recently investigated by Ellsworth and Hopfield.[2] It seems probable that the v'' numbering as given by these investigators should be increased by two units. This was pointed out by Mulliken[3] from the intensity distribution in the band system. Stueckelberg[4] has shown that such a revised v'' numbering is the most probable from the Franck-Condon principle of transition probabilities. Ellsworth and Hopfield also found evidence on their plates of band progressions to lower final vibrational states than the level they called $v'' = 0$. For these reasons the bands which were used in the present rotational analysis have been called 1–8;

[1] J. Stark, Ann. d. Physik **43**, 319 (1914); R. C. Johnson, Proc. Roy. Soc. **A105**, 683 (1924).
[2] V. Ellsworth and J. Hopfield, Phys. Rev. **29**, 79 (1927).
[3] R. S. Mulliken, Phys. Rev. **32**, 213 (1928).
[4] E. C. G. Stueckelberg, Phys. Rev. **34**, 66 (1929).

0–8; 1–9; 0–9; although they were designated by Ellsworth and Hopfield as 1–6; 0–6; 1–7; 0–7.

Since NO and O_2^+ have the same number of electrons it would be expected that their band systems would be similar. The beta bands of NO and the first

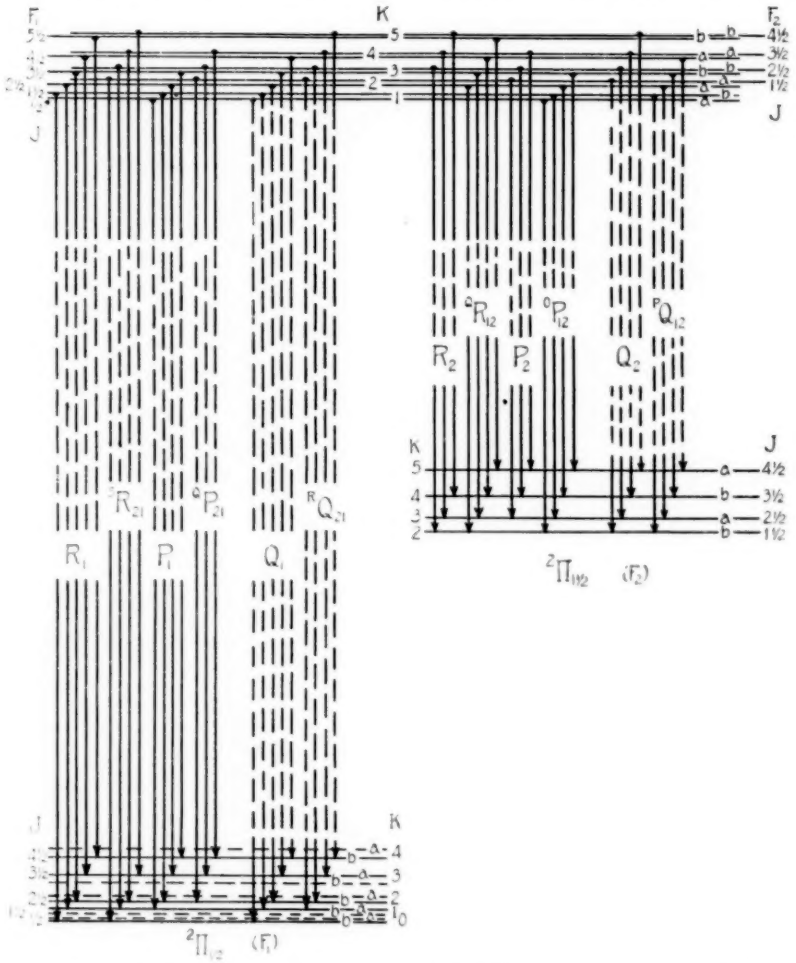

Fig. 1. First few rotational terms for the initial state $v'=0$ and final state $v''=9$ of the first negative group of oxygen (O_2^+) bands. The possible transitions are grouped into branches. The Q branches (shown dashed) were not found in the bands. The other branches were all definitely located and established the case b $^2\Pi \rightarrow$ case a $^2\Pi$ nature of transition. All the rotational levels are drawn to the same scale except that the Λ-type doubling is magnified 50X. Even then, it shows only in the lower $^2\Pi_{\frac{1}{2}}$ state. The levels shown dashed do not exist physically (cf. section on Λ-type doubling). The a and b classification on the levels shown in full is in all cases for the level actually present.

negative group of O_2^+ bands lie in the same spectral region and are similar in appearance, (both are double headed and degrade toward the red). The NO beta bands have been analyzed[5] and found to be $^2\Pi \rightarrow {}^2\Pi$, both states being

[5] F. A. Jenkins, H. A. Barton and R. S. Mulliken, Phys. Rev. **30**, 150–174 (1927); **30**, 175–188 (1927).

case *a*. For each of the two heads there is a strong *R* and a strong *P* branch, also a very weak *Q* branch. It was expected that the first negative group of O_2^+ bands would have a similar structure. But four strong branches were found in each head of each band. This situation can be accounted for[6] if the transition is from a case *b* state to a case *a* state rather than between two case *a* states.

In transitions between two case *a* states, there are the selection rules $\Delta\Sigma = 0$ and $\Delta J = 0, \pm 1$. In case *b*, Σ is no longer a quantum number,[7] and the selection rule $\Delta\Sigma = 0$ no longer holds in case *b*→case *a* transitions but the selection rule $\Delta J = 0, \pm 1$ still holds. The various branches[8] which can appear in a $^2\Pi$ case *b*→ $^2\Pi$ case *a* transition are shown by Fig. 1.

The *Q* branches, which are shown with broken lines in the figure, were too weak to be found in the bands. The other branches, however, have all been definitely located and establish the case *b*→case *a* type of transition. The "main" *R* and *P* branches (R_1 and P_1; R_2 and P_2) are of about equal intensity and have their maximum at about $J = 20\frac{1}{2}$. The "satellite" branches ($^SR_{21}$ and $^QP_{21}$; $^QR_{12}$ and $^OP_{12}$) are somewhat weaker than the main branches.

Experimental Procedure

The bands were produced in a hollow cathode discharge. The tube was similar to that described by Frerichs.[9] It was, however, found advantageous to construct the cathode with a block of tin instead of the aluminum used by Frerichs. Cooling coils were embedded in the tin so that a large current (1.5 amp.) could be passed through the cathode for many hours (50–100). Some bands due to the cathode material appeared on the high frequency side of the 1–8 and 0–8 O_2^+ bands, but those foreign bands did not interfere with the analysis. The bands were photographed in the second order of a 21 foot Rowland grating giving a dispersion of 1.32 A/mm.

Recently Drs. S. M. Naudé and W. Weizel, while photographing the visible O_2^+ bands in this laboratory, have found a more intense source of O_2^+ spectra by using helium with a small amount of oxygen in a discharge tube similar to that described by Naudé and Christy.[10] They have kindly furnished me with a plate taken in the same region as mine. By means of this plate it was possible to show that there were no errors due to the presence of the tin bands. Only a few faint lines of the tin bands had appeared inside the heads of the 1–8 and 0–8 bands of O_2^+.

Data and Results

Due to the presence of many branches the appearance of the bands was rather complex and many of the lines were blends. This was especially true

[6] Cf. R. S. Mulliken, Reviews of Modern Physics **3,** 128–146 (1931).

[7] For a discussion of cases *a* and *b* cf. R. S. Mulliken, Reviews of Modern Physics **2,** 105–108 (1930).

[8] For the nomenclature of the branches, cf. R. S. Mulliken, Reviews of Modern Physics **3.** 119 (1931).

[9] R. Frerichs, Zeits. f. Physik **35,** 683 (1926).

[10] S. M. Naudé, and A. Christy, Phys. Rev. **37,** 492 (1931).

TABLE I. *Wave number and intensity data for the 0—8; 1—8; 0—9; 1—9 bands of the first negative group of oxygen* (O_2^+) *bands. The first six numbers represent the wave number of a given line, the next figure in bold-face type gives the number of times the line was used in the scheme of analysis and the last figure is an estimate of the relative intensity of the line. The letter d means that the line appeared diffuse and A means atomic line.*

1—8 Band, First head

$J''+\frac{1}{2}$	$^SR_{21}$	$^QP_{21}$	R_1	P_1
1	28620.644		28613.733*d*	
2	21.344		13.033*d*	28605.921
3	21.244	28607.311	11.311	00.411
4	20.744	02.436	09.122	28594.111
5	19.222	28597.236	05.821	87.212
6	16.712*d*	89.9310	01.136	78.412*d*
7	13.533*d*	82.625	28596.336	69.211
8	09.222	73.824	89.1310	58.512
9	03.736	64.624	82.625	47.513
10	28597.036	53.925	73.624	34.313
11	89.9310	42.827	64.524	21.614
12	81.012	29.826	53.525	06.414
13	72.111	16.728	42.727	28491.215*d*
14	61.314	01.928	29.826	74.215
15	50.114	28486.725*d*	16.828	57.215
16	37.515	69.827	02.128	38.316
17	24.513	52.6210	28487.125*d*	19.324
18	09.613	33.728	70.227	28398.326
19	28494.814	14.744	53.6210	77.315
20	77.614	28393.514	34.428	54.115
21	61.014	72.412	15.444	31.315
22	41.913	49.212	28394.436	06.015
23	23.422*d*	26.112	73.612	28280.915
24	02.048*d*	01.212	50.512	53.926*d*
25	28381.124*d*	28276.124	27.712	27.015
26	58.025	49.011	02.512	28197.725*d*
27	35.711	22.311	28277.724	68.937*d*
28	10.612	28193.311	49.912	37.715
29	28285.311	64.211		06.915
30	57.623	33.711		28073.114*d*
31	30.511			40.825*d*
32	01.412			05.415
33	28173.712			27970.715
34				33.115
35				27896.514

1—8 Band, Second head

$J''+\frac{1}{2}$	R_2	P_2	$^QR_{12}$	$^OP_{12}$
2	28429.421		28420.622	28413.222
3	29.521	28415.344	19.324	08.424
4	28.211	10.921	17.511	02.348*d*
5	26.511	04.911	13.222	28394.436
6	24.122*d*	28398.326	08.424	85.526*d*
7	20.622	90.311	02.348*d*	75.824
8	15.344	81.124	28396.111	64.726*d*
9	09.721	69.726	88.413*d*	53.124
10	02.348*d*	59.313	79.414	39.912
11	28394.436	47.012	69.626	26.122
12	85.526*d*	34.112	58.125	10.622
13	75.824	20.012	46.412	28294.812
14	64.726*d*	04.512	33.112	77.424
15	52.724	28288.613	19.112	59.213
16	38.912	71.214	03.813	39.913
17	25.212	53.126	28287.713	19.614
18	09.613	33.515	70.212	28198.125
19	28293.513	13.415	52.112	76.012*d*
20	76.124	28191.012	32.412	52.514
21	57.613	69.537*d*	12.312	28.214
22	37.914	45.715	28190.712	02.314*d*
23	17.814	21.715	68.137*d*	28076.015
24	28195.914	28095.516	44.613	48.328*d*
25	73.724	69.025*d*	20.312	19.814
26	49.915	41.125*d*	28094.212	27989.815
27	25.615	12.926	67.712	59.714
28	28099.215	27982.227	39.712	27.214
29	74.228*d*	52.326	13.026	
30	45.915		27982.727	
31	18.012		52.326	
32	27987.611		19.812	
33	57.111			
34	24.111			
35	27892.112*d*			

TABLE I. (*Cont.*)

0−8 Band, First head

$J''+\frac{1}{2}$	$^{S}R_{21}$	$^{Q}P_{21}$	R_1	P_1
1	27747.311		27740.121	
2	48.725		40.121	27732.712
3	49.825	27735.411	39.224	28.124
4	49.925	31.028*d*	37.411	22.423*d*
5	48.825	25.923	34.225	14.815
6	46.214*d*	19.225*d*	30.828*d*	07.315
7	43.616*d*	12.211	25.823	27698.212
8	39.224	03.511	19.125*d*	87.412
9	34.525	27694.624	13.026*d*	76.914
10	28.124	84.224	04.726	64.612
11	21.723*d*	73.413	27696.013	51.812
12	13.026*d*	61.013*d*	85.413	37.312
13	04.726	48.313	74.914	22.5210
14	27694.624	34.014	62.714	06.228
15	84.224	19.114	50.217	27589.426
16	72.014	03.015	35.917	71.025
17	59.814	27586.713	21.7210	52.637
18	45.814	68.213	05.928	32.1510*d*
19	31.717	50.024	27589.426	11.715
20	15.514	29.713	71.025	27489.635
21	27599.314	09.636	52.937	67.114
22	81.515*d*	27487.111	32.8510*d*	42.813
23	63.514	65.124	12.814	18.613
24	43.511	41.422	27490.713	27392.513
25	23.525	16.911	68.715	66.515
26	01.418	27390.711	44.712	38.112
27	27479.324	64.912	20.714	10.524
28	55.813	37.524	27394.813	27280.113
29	32.012	09.122	68.825	50.422
30	05.724*d*	27278.711	40.911	18.122
31	27380.212	49.022	13.411	27186.635
32	52.011	18.022	27283.424	52.422
33	25.014	27186.635	53.413	
34	27294.711	52.422	21.712	
35	65.011	18.713	27190.212	
36	33.311		56.511	
37	02.011		23.111	

0−8 Band, Second head

$J''+\frac{1}{2}$	R_2	P_2	$^{Q}R_{12}$	$^{O}P_{12}$
2	27557.921		27549.434	27542.311
3	58.211	27543.711	47.911	36.911
4	57.421	38.923*d*	45.522	30.313
5	55.811	33.1410*d*	42.321	23.225
6	53.037	26.135	37.711	14.513
7	49.734	18.623	32.8410*d*	05.113
8	45.122	09.836	26.135	27494.213
9	40.323*d*	00.325	18.623	82.714
10	33.1410*d*	27489.635	09.436	69.914
11	26.135	78.117	00.325	56.414
12	17.413	65.124	27489.635	41.422
13	08.312	51.711	78.724	25.915*d*
14	27497.612	37.027	65.712	09.116*d*
15	86.712	21.525	52.512	27391.613
16	73.712	04.514	37.527	72.714
17	60.413	27387.213	22.125	53.213
18	45.713	68.313	05.724*d*	32.315
19	30.415*d*	48.813	27388.216	10.524
20	13.614	27.913	69.325	27287.816
21	27396.412	06.413	50.112	64.116
22	77.713	27283.424	29.311	39.114
23	58.413	60.123	08.012	13.714
24	37.524	35.113	27285.012	27186.635
25	16.313	10.014	61.823	59.313
26	27293.414	27182.714	36.614*d*	30.214
27	70.311	55.514	11.512	01.214
28	45.214	26.314	27184.211	
29	20.015	27097.214	57.412	
30	27193.012		27.912	
31	65.912		27099.013	
32	36.813			
33	07.714			

TABLE I. (*Cont.*)
1−9 Band, First head

$J''+\frac{1}{2}$	${}^{S}R_{21}$	${}^{Q}P_{21}$	R_1	P_1
1	26972.326		26965.721	
2	74.224		65.721	26959.111
3	75.911	26961.611	64.628	53.926
4	74.811	57.316	63.114	49.211
5	73.924	52.128	60.426	41.712
6	72.126	45.928*d*	56.012	33.713
7	69.612*d*	38.9310	51.928	25.31*A*
8	64.728	30.3310	45.928*d*	14.813
9	60.426	21.214	38.9310	04.013
10	53.826	10.714	30.3310	26891.413
11	47.315	00.014	22.014	78.713
12	38.9310	26887.514	11.713	64.413
13	30.3310	74.914	01.313	49.613
14	20.114	60.516	26888.914	33.311
15	09.615	46.114	76.515	16.715
16	26897.715	29.514	62.216	26798.416
17	85.314	12.913	48.015	79.738
18	71.015	26795.014	31.615	59.4410
19	56.815	76.736	15.415	38.938
20	40.315	56.314	26796.915	16.6410
21	24.815	36.312	78.938	26694.926
22	06.513	14.113*d*	49.4410	70.524
23	26788.513*d*	26692.112	39.038	46.415
24	68.024	67.512	16.6410	20.3310
25	48.413	43.812	26694.926	26594.225
26	26.114	17.514	70.524	66.224
27	04.314*d*	26591.812	46.415	38.323
28	26680.318	63.525	20.2310	08.125
29	56.726*d*	35.536*d*	26594.225	78.425
30	30.113	05.711	66.824	
31	04.327*d*		38.323	
32	26576.3310		08.125	
33	49.215*d*		26478.425	
34	19.227			
35	26489.415			

1−9 Band, Second head

$J''+\frac{1}{2}$	R_2	P_2	${}^{Q}R_{12}$	${}^{O}P_{12}$
2	26785.035		26776.736	26769.711
3	85.335	26771.639	75.711	65.025
4	84.435	66.523*d*	72.839	58.211
5	82.612	60.7110	69.424	50.813*d*
6	79.938	53.7310	65.125	42.513
7	76.836	46.411	59.6410	33.01*A*
8	71.639	37.126	52.7310	22.214
9	66.723*d*	27.826	45.613*d*	10.715
10	60.4410	17.0410	37.126	26697.814
11	53.0310	05.727	27.626	84.316
12	44.212	26692.928	17.3410	69.614
13	34.838	79.628	05.827	54.114
14	24.314	64.62*A*	26693.128	37.517
15	13.014	49.126	79.628	20.1310
16	00.113	32.424*d*	64.72*A*	01.115
17	26687.015	15.028	49.626	26581.515
18	72.015	26596.025	32.624*d*	60.616
19	56.726	76.6310	15.128	39.218
20	39.917	55.613	26596.725	16.217
21	22.617	34.236	77.1310	26492.617
22	04.127*d*	11.218	56.912	68.015
23	26584.417	26488.115	35.236	
24	63.515	63.113		
25	42.216			
26	19.227			
27	26495.917			
28	71.117			

TABLE I. (*Cont.*)

0−9 Band, Second head

$J''+\frac{1}{2}$	R_2	P_2	$^QR_{12}$	$^OP_{12}$
2	25913.538		25905.012	25898.523
3	14.238	25899.611	03.912	93.325
4	13.738	95.122	01.712	86.612
5	12.327	89.224	25898.523	79.313
6	09.525*d*	82.824	94.122	71.113
7	06.712	75.83*A*	89.224	61.515*d*
8	02.412	67.037	82.824	51.517
9	25897.3210	57.537	75.83*A*	40.016
10	91.314	46.925	67.637	27.616
11	84.614	36.125	58.614	14.516
12	76.63*A*	23.815	48.528*d*	00.316
13	67.637	11.015	37.714	25785.115
14	57.537	25796.616	25.628	68.716
15	46.925	81.816	12.928	51.72*A*
16	34.716	65.328*d*	25798.616	33.548*d*
17	22.116	48.716*d*	84.037	14.727
18	08.018	30.518*d*	67.814	25694.627
19	25793.517	11.818	51.32*A*	73.712
20	77.517	25691.718	33.548*d*	51.425
21	61.117	71.017	14.727	28.716
22	43.218	48.917	25694.627	04.716
23	24.918	26.6110	74.312	25580.116
24	04.818	02.519	52.311	53.62*A*
25	25684.618	25578.117	30.228	
26	62.718	52.118	06.213	
27	40.718*d*		25582.013	
28	16.718		56.02*A*	
29	25592.718			
30	66.818			
31	40.918			

0−9 Band, First head

$J''+\frac{1}{2}$	$^SR_{21}$	$^QP_{21}$	R_1	P_1
1	26102.426		26095.048	
2	04.326		95.548	26088.411*d*
3	05.228	26091.137	95.148	84.226
4	05.528	86.624	93.411*d*	78.427
5	04.526	81.9210*d*	90.837	71.126
6	02.326	75.113	86.624	63.228*d*
7	26099.814	68.115*d*	81.9210*d*	54.312
8	95.548	59.918	76.014	44.411
9	91.237	51.517*d*	69.515	33.424
10	85.226	41.115	61.416	21.525
11	79.127	30.716	53.427*d*	09.112
12	71.126	18.716	43.326	25995.012
13	63.228*d*	06.728	33.424	80.715
14	53.227*d*	25992.615	21.525	64.716
15	43.626	78.528*d*	09.716	48.715
16	31.914	62.926	25996.016	30.717
17	20.413	47.015	82.317	13.028
18	06.928	29.315	66.718	25893.325
19	25993.515	11.827	51.218	73.713
20	78.128*d*	25892.213	33.918	52.213
21	62.926	73.013	16.518	30.628*d*
22	45.613	51.526	25897.3310	07.226
23	28.613	30.228*d*	78.115	25784.037
24	09.525*d*	07.026	56.937	58.728*d*
25	25890.612	25784.237	35.725	33.548*d*
26	69.612	59.128*d*	12.929	06.314
27	48.828*d*	34.348*d*	25790.316	25679.514
28	25.628	07.011	65.328	50.313
29	03.512	25680.411	40.813	21.913
30	25778.612	51.425	13.613	25590.814
31	54.211	23.111	25687.316	60.314
32	27.413	25592.2210	58.517	
33	01.111	62.011	30.228	
34	25672.512		25599.513	
35	44.415		69.614	
36	13.711		36.913	

near the heads, where the assignment of lines was difficult. In the second head of each band the branches were better separated. The structure of the bands was determined by locating first the branches in the second head and from them calculating the positions of the rotational levels of the upper electronic state. Knowing these levels and one or two branches in the first head, the remaining branches in the first head could be calculated. The wave numbers of the lines which form the various branches are given in Table I.

Determination of the Δ_2F's

By reference to Fig. 1, it will be seen that various internal combinations can be obtained in each band. For the first heads of the bands, the relations for the lower $^2\Pi$ are:

$$^{S}R_{21}(J-1) - {}^{Q}P_{21}(J+1) = R_1(J-1) - P_1(J+1)$$
$$= F_1''(J+1) - F_1''(J-1) \equiv \Delta_2F_1''(J) \quad (1)$$

and for the second heads:

$$^{Q}R_{12}(J-1) - {}^{O}P_{12}(J+1) = R_2(J-1) - P_2(J+1)$$
$$= F_2''(J+1) - F_2''(J-1) \equiv \Delta_2F_2''(J). \quad (2)$$

Similar relations that give the Δ_2F's of the upper electronic state are:

$$^{S}R_{21}(J) - {}^{Q}P_{21}(J) = R_2(J) - P_2(J) = \Delta_2F_2'(J) \quad (3)$$
$$R_1(J) - P_1(J) = {}^{Q}R_{12}(J) - {}^{O}P_{12}(J) = \Delta_2F_1'(J). \quad (4)$$

All of these Δ_2F's are listed in Tables II and III. The vibrational quantum numbers of the four bands used in the analysis were such that the rotational levels associated with two adjacent vibrational levels ($v'=0, 1$; $v''=8, 9$) of both the upper and lower electronic states were obtained. Furthermore every Δ_2F in both the upper and lower states is determined independently four times by the differences of four pairs of lines. In the following tables data are given only for the vibrational states $v'=0$ and $v''=9$. Similar data for the vibrational states $v'=1$ and $v''=8$ may readily be obtained from the wave numbers of Table I.

After a series of lines had been located in a band it was not possible to tell immediately what branch it corresponded to. The combination relations just given were used to determine the proper designations of the series. The combinations between the series were first obtained. Then by reference to Fig. 1 it will be seen that for a given J value any member of the $^{S}R_{21}$ branch would have a larger wave number than the corresponding member of the R_1 branch. Exactly the same relation held between the $^{Q}P_{21}$ branch and the P_1 branch.

Values of the Constants B, D and A

The terms of the upper $^2\Pi$ state can be represented accurately by Hill and Van Vleck's equation (see Eq. (9) following). This state, however, is so close to Hund's case b that the terms, except for the lowest K values, can also be represented by the following equation:[7]

TABLE II. *The first set of data gives the values of $\Delta_2F_1''(J)$ for the 9 vibrational state obtained from Eq. (1). The second set of data gives the values of $\Delta_2F_2''(J)$ for the 9 vibrational state obtained from Eq. (2). The J values have been omitted from the column headings so that R_1-P_1 really stands for $R_1(J-1)-P_1(J-1)$. Other column headings are exactly similar.*

$\Delta_2F_1''(J)$						$\Delta_2F_2''(J)$					
	0−9 Band		1−9 Band				0−9 Band		1−9 Band		
$J+\frac{1}{2}$	${}^sR_{21}-{}^QP_{21}$	R_1-P_1	${}^sR_{21}-{}^QP_{21}$	R_1-P_1	av.	$J+\frac{1}{2}$	R_2-P_2	${}^QR_{12}-{}^OP_{12}$	R_2-P_2	${}^QR_{12}-{}^OP_{12}$	av.
2	11.3	10.8	10.7	13.4	11.6	3	18.4	18.4	18.5	18.5	18.5
3	17.7	17.1	16.9	16.5	17.1	4	25.0	24.6	24.6	24.9	24.8
4	23.3	24.0	23.8	22.9	23.5	5	30.9	30.6	30.7	30.3	30.8
5	30.4	30.2	28.9	29.4	29.7	6	36.5	37.0	36.2	36.4	36.5
6	36.4	36.5	35.0	35.1	35.8	7	42.5	42.6	42.8	42.9	42.7
7	42.4	42.2	41.8	41.2	41.4	8	49.2	49.2	49.0	48.9	49.0
8	48.3	48.5	48.4	47.9	48.3	9	55.5	55.2	54.6	54.9	55.1
9	54.4	54.5	54.0	54.5	54.4	10	61.2	61.3	61.0	61.3	61.2
10	60.5	60.4	60.4	60.2	60.4	11	67.5	67.3	67.5	67.5	67.5
11	66.5	66.4	66.3	65.9	66.3	12	73.6	73.5	73.4	73.5	73.5
12	72.4	72.7	72.4	72.4	72.5	13	80.0	79.8	79.6	79.8	79.8
13	78.5	78.6	78.4	78.4	78.5	14	85.8	86.0	85.7	85.7	85.8
14	84.7	84.7	84.2	84.6	84.6	15	92.2	92.1	91.9	92.0	92.2
15	90.3	90.8	90.6	90.5	90.6	16	98.2	98.2	98.0	98.1	98.1
16	96.6	96.7	96.7	96.8	96.7	17	104.2	104.6	104.1	104.1	104.3
17	102.6	102.7	102.7	102.8	102.7	18	110.3	110.3	110.4	110.4	110.4
18	108.6	108.6	108.6	109.1	108.7	19	116.3	116.4	116.4	116.4	116.4
19	114.7	114.5	114.7	115.0	114.7	20	122.5	122.6	122.5	122.5	122.5
20	120.5	120.6	120.5	120.5	120.5	21	128.6	128.8	128.7	128.7	128.7
21	126.6	126.7	126.2	126.4	126.6	22	134.5	134.6	134.5		134.5
22	132.7	132.5	132.7	132.5	132.6	23	140.7	141.0	141.0		140.9
23	138.6	138.6	139.0	139.1	138.8	24	146.8				146.8
24	144.4	144.6	144.7	144.8	144.6	25	152.7				152.7
25	150.4	150.6	150.5	150.4	150.6						
26	156.3	156.2	156.6	156.6	156.4						
27	162.7	162.6	162.6	162.4	162.6						
28	168.4	168.4	168.8	168.0	168.4						
29	174.2	174.5	174.6		174.3						
30	180.4	180.5			180.5						
31	186.4				186.4						
32	192.2				192.2						

TABLE III. *The first set of data gives the values of $\Delta_2F_1'(K=J-\frac{1}{2})$ for the 0 vibrational state obtained from Eq. (4). The second set of data gives the values of $\Delta_2F_2'(K=J+\frac{1}{2})$ for the 0 vibrational state obtained from Eq. (3). The J values have been omitted from the column headings so that R_1-P_1 really stands for $R_1(J)-P_1(J)$. Other column headings are exactly similar.*

$\Delta_2F_1'(K=J-\frac{1}{2})$						$\Delta_2F_2'(K=J+\frac{1}{2})$					
	0−8 Band		0−9 Band				0−8 Band		0−9 Band		
$J+\frac{1}{2}$	R_1-P_1	${}^{Q}R_{12}-{}^{O}P_{12}$	R_1-P_1	${}^{Q}R_{12}-{}^{O}P_{12}$	*av.*	$J+\frac{1}{2}$	${}^{S}R_{21}-{}^{Q}P_{21}$	R_2-P_2	${}^{S}R_{21}-{}^{Q}P_{21}$	R_2-P_2	*av.*
2	7.4	7.1	7.1	6.5	7.0	3	14.4	14.5	14.1	14.6	14.4
3	11.1	11.0	10.9	10.6	10.9	4	18.9	18.5	18.9	18.6	18.7
4	15.0	15.2	15.0	15.1	15.1	5	22.9	22.7	22.6	23.1	22.8
5	19.7	19.1	19.7	19.2	19.4	6	27.0	26.9	27.2	26.7	26.9
6	23.5	23.2	23.4	23.0	23.3	7	31.4	31.1	31.7	30.9	31.1
7	27.7	27.7	27.6	27.7	27.7	8	35.4	35.3	35.6	35.4	35.4
8	31.7	31.9	31.6	31.3	31.8	9	39.1	40.0	39.7	39.8	39.6
9	36.1	35.9	36.1	35.8	36.0	10	43.9	43.5	44.1	44.4	44.0
10	40.1	39.5	39.9	40.0	39.9	11	48.3	48.0	48.4	48.5	48.4
11	44.2	43.9	44.3	44.1	44.1	12	52.0	52.3	52.4	52.8	52.4
12	48.1	48.2	48.3	48.2	48.2	13	56.4	56.6	56.5	56.6	56.5
13	52.4	52.8	52.7	52.6	52.6	14	60.6	60.6	60.6	60.9	60.7
14	56.5	56.6	56.8	56.9	56.7	15	65.1	65.2	65.1	65.1	65.1
15	60.8	60.9	61.0	61.2	61.0	16	69.0	69.2	69.0	69.4	69.2
16	64.9	64.8	65.3	65.1	65.0	17	73.1	73.2	73.4	73.4	73.3
17	69.1	68.9	69.3	69.3	69.2	18	77.6	77.4	77.6	77.5	77.5
18	73.8	73.4	73.4	73.2	73.4	19	81.7	81.6	81.7	81.7	81.7
19	77.7	77.7	77.5	77.6	77.6	20	85.8	85.7	85.9	85.8	85.8
20	81.4	81.5	81.7	82.1	81.9	21	89.7	90.0	89.9	90.1	90.0
21	85.8	86.0	85.9	86.0	85.9	22	94.4	94.3	94.1	94.3	94.3
22	90.0	90.2	90.1	89.9	90.0	23	98.4	98.3	98.4	98.3	98.3
23	94.2	94.3	94.1	94.2	94.2	24	102.1	102.4	102.5	102.3	102.3
24	98.2	98.4	98.2	98.7	98.4	25	106.6	106.3	106.4	106.5	106.4
25	102.2	102.5	102.2		102.3	26	110.7	110.7	110.5	110.6	110.6
26	106.6	106.4	106.6		106.5	27	114.4	114.8	114.5		114.6
27	110.2	110.3	110.8		110.4	28	118.3	118.9	118.6		118.6
28	114.7		115.0		114.8	29	122.9	122.8	123.1		122.9
29	118.4		118.9		118.7	30	127.0		127.2		127.1
30	122.8		122.8		122.8	31	131.2		131.1		131.2
31	126.8		127.0		126.9	32	134.0		135.2		135.2
32	131.0				131.0	33	138.4		139.1		139.1
						34	142.3				142.3
						35	146.3				146.3

$$T = T_0^e + G(v) + B_v[K(K+1) - \Lambda^2 + \overline{G^2}] + f(K, J-K) + \phi_i(K, J) + D_v K^2(K+1)^2 + \cdots \quad (5)$$

The lower $^2\Pi$ state is co close to Hund's case a that the terms can be represented by the following equation:[7]

$$T = T_0^e + G(v) + A\Lambda\Sigma + B_v^*[J(J+1) - \Omega^2 + \overline{G^2} + S_{perp}{}^2] + \phi_i(\Sigma, J) + D_v J^2(J+1)^2 + \cdots \quad (6)$$

By use of Eq. (5), the $\Delta_2 F$'s of the upper $^2\Pi$ state should be given very closely by the relation:

$$\Delta_2 F'(K) = 2B_v(2K+1) \quad (7)$$

From Eq. (6), the $\Delta_2 F$'s of the lower $^2\Pi$ state should be given by:

$$\Delta_2 F''(J) = 2B_v^*(2J+1). \quad (8)$$

The use of these simplified expressions for the $\Delta_2 F$'s can be justified except for the lowest values of K of the upper $^2\Pi$ state and for the highest values of the rotational quantum number in either electronic state. In both Eqs. (5) and (6), the ϕ function represents the Λ-type doubling. In the upper electronic state the Λ-type doubling is experimentally found to be negligible. There is Λ-type doubling in the lower electronic state, but the rate of change of the ϕ function with J is so small that it does not affect the $\Delta_2 F$'s. The same argument can be applied to the other neglected terms which are either constant or change very slowly with respect to J. The last statement holds for the term

TABLE IV. *B values.*

	upper $^2\Pi$	
	$v'=0$	$v'=1$
$B(F_1)$	1.050	1.030
$B(F_2)$	1.047	1.037
$B(av)$	1.048	1.034
	lower $^2\Pi$	
	$v''=8$	$v''=9$
$B^*(F_1)$	1.525	1.520
$B^*(F_2)$	1.550	1.538
$B(av)$	1.538	1.529

involving D for rotational quantum numbers less than 15. For values above this number, the $\Delta_2 F$'s are increasingly less than those given by Eqs. (7) and (8), since D is inherently negative. $[D = -4B_e^3/\omega_e^2]$. From this relation, for the upper electronic state $D' = 5.6 \times 10^{-6}$ and for the lower electronic state $D'' = 4.6 \times 10^{-6}$. D values calculated from the departure of the $\Delta_2 F$'s from a straight line agree with these fairly well. This would be expected for the upper electronic state which is case b but not necessarily for the lower case a electronic state.

Considering Eqs. (7) and (8), it is seen that they predict a linear relation between the $\Delta_2 F$'s and the rotational quantum numbers; the slope of the line in each case being $4B$. The plot of the actual $\Delta_2 F$'s in each case lay on a straight line for moderate values of the rotational quantum number, and the slope of the line was used to obtain the B values listed in Table IV. Since K has integral values and J half-integral values for these states, it would be expected that the intercept of the line on the axis of rotational quantum numbers would be close to a whole number for the upper $^2\Pi$ state and close to a half-number for the lower $^2\Pi$ state. This was found to be the case.

Since the upper $^2\Pi$ in case b, B_v should have practically the same value for the F_1 and F_2 sets of rotational levels. This was observed. For the lower $^2\Pi$ state, which is case a, the observed B_v's are called B_v^* since they are not true B_v values. The values of B_v^* differ for the F_1 and F_2 sets of levels as follows:[11]

$$B_v^* = B_v(1 \pm B_v/A\Lambda)$$

with $\pm B_v/A$ according as $\Sigma = \pm\frac{1}{2}$

From the above equation the difference between the B_v^* values for the F_2 and F_1 sets of levels of the lower $^2\Pi$ state should be ≈ 0.023. This is close to the observed values. The true B_v is obtained by taking the average of $B_v^*(F_1)$ and $B_v^*(F_2)$.

B_v is related to other molecular constants[12] by the equations:

$$B_v = B_e - \alpha(v + \tfrac{1}{2}) = B_0 - \alpha v,$$

$$B_e = h/8\pi^2\mu c r_e^2 = 27.70 \times 10^{-40}/\mu r_e^2.$$

Values of some of these constants are given in Table VII.

The value of A'', the parameter governing the doublet separation of the lower $^2\Pi$ state, can be calculated from Eq. (6). This is done by taking the difference between a line in the first head and a line in the second head which come from the same upper level and end on lower levels of the same J value. An expression for this term difference involving A'' may be obtained from Eq. (6). The smallest J values, for which the data were considered most reliable, were chosen to calculate A''. The result was $A'' = 195$ cm^{-1}.

The value of A' for the upper $^2\Pi$ state can be determined by the use of Hill and Van Vleck's formula:[13]

$$T = T_0^e + G(v) + B_v\{(J + \tfrac{1}{2})^2 - \Lambda^2 \pm \tfrac{1}{2}[4(J + \tfrac{1}{2})^2 - 4A\Lambda^2/B_v + A^2\Lambda^2/B_v^2]^{1/2} + \overline{G^2}\} + \phi_i(J) + \cdots \quad (9)$$

This equation is quadratic in A and gives two possible values, i.e., for the upper electronic state $A' = +8.2$ or -4.0. One can decide between these

[11] For a discussion of B^* cf. R. S. Mulliken, Reviews of Modern Physics **2**, 113 (1930); **3**, 110 (1931).

[12] Cf. R. S. Mulliken, Reviews of Modern Physics **2**, 65–67 (1930).

[13] E. L. Hill and J. H. Van Vleck, Phys. Rev. **32**, 261–2 (1928).

two values in the following way. Either A' value will give the same term value for all rotational levels except the lowest ($J=\frac{1}{2}$). Also for every J value except the lowest, there are two rotational levels, one of which can be classified as an F_1 level and the other level as belonging to the F_2 set. There is only one level for $J=\frac{1}{2}$.[14] According as A' is positive or negative the position of this level should from the theory be such that it would be naturally classified with the F_1 set or with the F_2 set of levels.

By reference to Fig. 1 it will be seen that one more line near the origin would be added to the P_1 and ${}^{O}P_{12}$ branches than to the ${}^{Q}P_{21}$ and P_2 branches if the level $J=\frac{1}{2}$ belongs to the F_1 set of levels. The converse will be true if this level belongs to the F_2 group of levels. In most of the bands it was not possible to decide definitely between the two possible positions of the level $J=\frac{1}{2}$. In four instances, however, it appeared that this level belonged to the F_1 set of levels rather than to the F_2 set, thus indicating that $A'=+8.2$. [The first line of each of the following branches appears to come from the level $J=\frac{1}{2}$: P_1 of the 0–9 and 1–9 bands, ${}^{O}P_{12}$ of the 1–9 band. On the other hand a line from this level appeared to be definitely absent in the case of P_2 branch of the 1–8 band.]

Calculation of the $\Delta_1 F$'s of the Upper $^2\Pi$ State

Since there were no Q branches present, it was impossible to obtain the $\Delta_1 F$'s directly by combinations between the lines. In the upper electronic state for each value of K there is an F_2 level with $J=K-\frac{1}{2}$, slightly above an F_1 level with $J=K+\frac{1}{2}$. The relative position of the F_2 and F_1 levels is a function of A/B_v.[15] The separation of these two levels for a given value of K will be called the spin-doubling distance (ϵ_K) since it is due to the two orientations of the spin vector with respect to K.

For moderate and large values of K the spin-doubling distance changes very slowly with K, so it can be obtained with sufficient accuracy from the lines in the following way. By reference to Fig. 1 it is seen that:

$$\begin{aligned} {}^{S}R_{21}(J-1) - R_1(J-1) &= {}^{Q}P_{21}(J+1) - P_1(J+1) \\ &= R_2(J-1) - {}^{Q}R_{12}(J-1) \\ &= P_2(J+1) - {}^{O}P_{12}(J+1) \\ &= \Delta_1 F_1'(J+\tfrac{1}{2}) + \epsilon_{K=J+1/2}. \end{aligned} \tag{10}$$

[For definition of $\Delta_1 F$ cf. end of next section on p. 1309] From Eq. (10):

$$\Delta_1 F_1'(J+\tfrac{1}{2}) + \epsilon_{K=J+1/2} + \Delta_1 F_1'(J-\tfrac{1}{2}) + \epsilon_{K=J-1/2} = \Delta_2 F_1'(J) + 2\epsilon_{K=J}. \tag{11}$$

In the right hand member of Eq. (11) the sum of the two ϵ terms corresponding to $K=J-\frac{1}{2}$ and $K=J+\frac{1}{2}$ is practically the same as twice the value which ϵ_K would have for a hypothetical intermediate level with $K=J$.

Values of ϵ are readily calculated from Eq. (11) since the $\Delta_2 F'_1(J)$ terms can be obtained directly from the line differences according to Eq. (4), or by

[14] Cf. R. S. Mulliken, Reviews of Modern Physics **2**, 109 (1930).
[15] Cf. R. S. Mulliken, Reviews of Modern Physics **2**, 114 (1930).

reference to Table III. Fig. 2 is a plot of ϵ against K. The solid line shows the values obtained by Hill and Van Vleck's formula and the circles are the values obtained from the lines by the method outlined. For the lowest K values many of the lines were not resolved. The lowest term differences, that were considered most reliable, were used to determine the constants in Hill and Van Vleck's equation, and then the position of the lowest rotational levels was calculated. The first members of the branches could then be located. The first values of ϵ in Fig. 2 are from these blended lines.

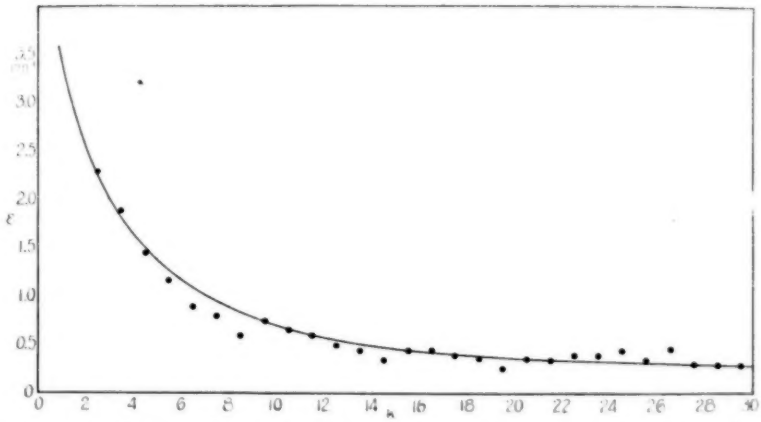

Fig. 2. A graph of ϵ_K (the spin-doubling distance) for the upper $^2\Pi$ state against K. The solid line is drawn from values obtained from Hill and Van Vleck's equation. The circles are values obtained from the lines according to Eq. (11).

The quantities given by Eq. (10) are listed in columns 2 through 10 of Table V. By subtracting the ϵ's from these quantities the $\Delta_1 F$'s of the upper $^2\Pi$ state are obtained. These are listed in columns 11 and 12 of Table V.

Calculation of the $\Delta_1 F^*$'s of the Lower $^2\Pi$ State

The $\Delta_1 F^*$'s of this state were obtained in a similar manner. The $\Delta_1 F^*$'s of the vibrational state $v''=9$ as listed in Table VI will be taken as an example. In columns 2 and 6 is listed the difference:

$$^sR_{21}(J) - R_1(J+1)$$

and in columns 4 and 8

$$^qP_{21}(J) - P_1(J+1)$$

These columns are labelled uncorrected since they must be corrected by subtracting the proper ϵ_K (already obtained, cf. Fig. 2) from each difference to obtain the $\Delta_1 F_1^*$ of the lower state. This will be seen by reference to Fig. 1. It will be noted that the ϵ_K to be subtracted from any one member of columns 2 and 6 is for a K value two units greater than the ϵ_K to be subtracted from the corresponding member of columns 4 and 8. These two values of ϵ are practically the same for moderate and high values of K but not so for low values of K (cf. Fig. 2). The columns labelled uncorrected have the appear-

TABLE V. *Values of* $\Delta_1F_1'(K=J)$ *and* $\Delta_1F_2'(K=J)$ *for the 0 vibrational state obtained from Eqs. (10) and (11). The J values have been omitted from the column headings, so that:* (1) $^{S}R_{21}-R_1$ *stands for* $^{S}R_{21}(J-1)-R_1(J-1)$; $R_2-{}^{Q}R_{12}$ *stands for* $R_2(J-1)-{}^{Q}R_{12}(J-1)$; *and* (2) $^{Q}P_{21}-P_1$ *stands for* $^{Q}P_{21}(J+1)-P_1(J+1)$; $P_2-{}^{O}P_{12}$ *stands for* $P_2(J+1)-{}^{O}P_{12}(J+1)$.

	0−8 Band				0−9 Band						
$J+\frac{1}{2}$	$^{S}R_{21}-R_1$	$^{Q}P_{21}-P_1$	$R_2-{}^{Q}R_{12}$	$P_2-{}^{O}P_{12}$	$^{S}R_{21}-R_1$	$^{Q}P_{21}-P_1$	$R_2-{}^{Q}R_{12}$	$P_2-{}^{O}P_{12}$	*av.*	$\Delta_1F_2'(K\equiv J)$ $=av-\epsilon_{K=J-\frac{1}{2}}$	$\Delta_1F_1'(K\equiv J)$ $=av-\epsilon_{K=J+\frac{1}{2}}$
1	7.2	7.3		6.8	7.4	6.9		6.3	7.0	3.6	4.5
2	8.6	8.6	8.5	8.6	8.8	8.2	8.5	8.5	8.5	6.0	6.5
3	10.6	11.1	10.3	9.9	10.1	10.8	10.3	9.9	10.4	8.4	8.7
4	12.5	11.9	11.9	11.6	12.1	11.9	12.0	11.7	11.9	10.2	10.4
5	14.6	14.0	13.5	13.5	13.7	13.8	13.8	14.3	13.9	12.4	12.7
6	15.4	16.1	15.3	15.6	15.7	15.5	15.4	15.5	15.6	14.4	14.6
7	17.8	17.7	16.9	17.6	17.9	18.1	17.5	17.5	17.6	16.6	16.6
8	20.1	19.6	19.0	19.7	19.5	19.6	19.6	19.3	19.6	18.6	18.8
9	21.5	21.6	21.7	21.7	21.7	21.6	21.5	21.6	21.8	21.0	21.1
10	23.4	23.7	23.7	23.7	23.8	23.7	23.7	23.5	23.6	22.9	22.9
11	25.7	25.8	25.8	25.8	25.7	26.0	26.0	25.9	25.8	25.1	25.2
12	27.6	27.8	27.8	27.9	27.8	27.9	28.1	27.9	27.8	27.2	27.2
13	29.8	29.7	29.6	29.9	29.8	29.8	29.9	30.1	29.8	29.2	29.3
14	31.9	32.0	31.9	31.8	31.7	32.2	31.9	31.8	31.9	31.4	31.4
15	34.0	34.1	34.2	34.0	33.9	34.0	34.0	34.0	34.0	33.5	33.6
16	36.1	36.1	36.2	36.0	35.9	36.0	36.1	35.9	36.0	35.6	35.6
17	38.1	38.3	38.3	38.2	38.1	38.1	38.1	38.1	38.2	37.8	37.8
18	39.9	40.1	40.0	40.1	40.2	40.0	40.2	40.3	40.1	39.7	39.7
19	42.3	42.5	42.2	42.3	42.3	42.4	42.2	42.3	42.3	41.9	41.9
20	44.5	44.3	44.3	44.3	44.2	44.3	44.0	44.2	44.3	43.9	43.9
21	46.4	46.5	46.3	46.4	46.4	46.2	46.4	46.5	46.4	46.2	46.0
22	48.7	48.9	48.4	48.5	48.3	48.3	48.6	48.9	48.6	48.2	48.2
23	50.7	50.4	50.4	50.7	50.5	50.7	50.6		50.6	50.2	50.2
24	52.8	52.6	52.5	52.5	52.6	52.8	52.5		52.6	52.2	52.3
25	54.8	54.4	54.5	54.3	54.9	54.8	54.4		54.6	54.3	54.3
26	56.7	57.4	56.8		56.7	56.7	56.5		56.8	56.5	56.5
27	58.6	58.7	58.8		58.5	58.5	58.7		58.6	58.3	58.3
28	61.0	60.6	61.0		60.3	60.6	60.7		60.7	60.4	60.5
29	63.2	62.4	62.6		62.7	62.8			62.7	62.5	62.5
30	64.8	65.6	65.1		65.0				65.1	64.9	64.9
31	66.8		66.9		66.9				66.9	66.7	66.7
32	68.6				68.9				68.8	68.6	68.6
33	71.6				70.9				71.2	71.0	71.0
34	73.0				73.0				73.0	72.8	72.8

TABLE VI. *The values of* $\Delta_1 F_1''^*(J+\frac{1}{2})$ *for the 9 vibrational state.*

$J+\frac{1}{2}$	0−9 Band $R_{21}(J)-R_1(J+1)-\epsilon_{K=J+1\frac{1}{2}}$ uncorr.	corr.	${}^QP_{21}(J)-P_1(J+1)-\epsilon_{K=J-\frac{1}{2}}$ uncorr.	corr.	1−9 Band $R_{21}(J)-R_1(J+1)-\epsilon_{K=J+1\frac{1}{2}}$ uncorr.	corr.	${}^QP_{21}(J)-P_1(J+1)-\epsilon_{K=J-\frac{1}{2}}$ uncorr.	corr.	$\Delta_1 F_1''^*(J+\frac{1}{2})$ av. of corr.
1	6.9	4.4			6.6	4.1			4.3
2	9.2	7.2			9.6	7.6			7.4
3	11.8	10.1	12.7	10.2	12.8	11.1	12.4	9.9	10.3
4	14.7	13.2	15.5	13.5	14.4	12.9	15.6	13.6	13.3
5	17.9	16.7	18.7	17.0	17.9	16.7	18.4	16.7	16.7
6	20.4	19.4	20.8	19.3	20.2	19.2	20.6	19.1	19.3
7	23.8	22.8	23.7	22.5	23.7	22.7	24.1	22.9	22.7
8	26.0	25.2	26.5	25.5	25.8	25.0	26.3	25.3	25.2
9	29.8	29.1	30.0	29.0	30.1	29.4	29.8	28.8	29.1
10	31.8	31.1	32.0	31.2	31.8	31.1	32.0	31.2	31.1
11	35.8	35.2	35.7	35.0	35.6	35.0	35.6	34.9	35.0
12	37.7	37.1	38.0	37.3	37.6	37.0	37.9	37.2	37.1
13	41.7	41.2	42.0	41.4	41.4	40.9	41.6	41.0	41.2
14	43.5	43.0	43.9	43.3	43.6	43.1	43.8	43.2	43.1
15	47.6	47.2	47.8	47.3	47.4	47.0	47.7	47.2	47.2
16	49.6	49.1	49.9	49.4	49.7	49.3	49.8	49.3	49.3
17	53.7	53.3	53.7	53.3	53.7	53.3	53.5	53.1	53.3
18	55.7	55.3	55.6	55.2	55.6	55.1	56.1	55.7	55.3
19	59.6	59.2	59.6	59.2	59.9	59.5	60.1	59.7	59.5
20	61.6	61.4	61.6	61.2	61.4	61.0	61.4	61.0	61.2
21	65.6	65.2	65.8	65.4	65.4	65.0	65.8	65.4	65.3
22	67.5	67.1	67.5	67.1	67.5	67.1	67.7	67.3	67.1
23	71.7	71.3	71.5	71.1	71.9	71.5	71.8	71.4	71.3
24	73.8	73.5	73.5	73.1	73.1	72.8	73.3	72.9	73.1
25	77.7	77.4	77.9	77.5	77.9	77.7	77.6	77.2	77.4
26	79.3	79.0	79.6	79.3	79.7	79.4	79.2	78.9	79.2
27	83.5	83.2	84.0	83.7	84.1	83.8	83.7	83.4	83.4
28	84.8	84.6	85.1	84.8	86.1	85.9	85.1	84.8	84.8
29	89.9	89.7	89.6	89.3	89.9	89.7			89.6
30	91.3	91.1	91.1	90.8	91.8	91.6			91.1
31	95.7	95.5			96.2	96.0			95.7
32	97.2	97.0			97.9	97.7			97.3
33	101.6	101.4							101.4
34	102.9	102.7							102.7
35	107.5	107.3							107.3

TABLE VI (*Continued*). *The values of* $\Delta_1 F_2''^*(J+\frac{1}{2})$ *for the 9 vibrational state*

$J+\frac{1}{2}$	0–9 Band $R_2(J)-{}^QR_{12}(J+1)-\epsilon_{K=J+1\frac{1}{2}}$ uncorr.	corr.	$P_2(J)-P_{12}(J+1)-\epsilon_{K=J-\frac{1}{2}}$ uncorr.	corr.	1–9 Band $R_2(J)-{}^QR_{12}(J+1)-\epsilon_{K=J+1\frac{1}{2}}$ uncorr.	corr.	$P_2(J)-{}^QP_{12}(J+1)-\epsilon_{K=J-\frac{1}{2}}$ uncorr.	corr.	$\Delta_1 F_2''^*(J+\frac{1}{2})$ av. of corr.
2	9.6	7.6			9.3	7.3			7.5
3	12.5	10.8	13.0	10.5	12.5	11.8	13.4	10.9	11.0
4	15.2	13.7	15.8	13.8	15.0	13.5	15.7	13.7	13.7
5	18.2	17.0	18.1	16.4	17.5	16.3	18.2	16.5	16.4
6	20.3	19.3	21.3	19.8	20.3	19.3	20.7	19.2	19.4
7	23.9	22.9	24.3	23.1	24.1	23.1	24.2	23.0	23.0
8	26.6	25.8	27.0	26.0	26.0	25.2	26.4	25.4	25.6
9	29.7	29.0	29.9	28.9	29.6	28.9	30.0	29.0	29.0
10	32.7	32.0	32.4	31.6	32.8	32.1	32.7	31.9	31.9
11	36.1	35.5	35.8	35.1	35.7	35.1	36.1	35.4	35.3
12	38.9	38.3	38.7	38.0	38.4	37.8	38.8	38.1	38.0
13	42.0	41.5	42.3	41.7	41.7	41.2	42.1	41.5	41.5
14	44.6	44.1	44.9	44.3	44.7	44.2	44.5	43.9	44.1
15	48.3	47.9	48.3	47.8	48.3	47.9	48.0	47.5	47.8
16	50.7	50.3	50.6	50.1	50.5	50.1	50.9	50.4	50.3
17	54.3	53.9	54.1	53.7	54.4	54.0	54.4	54.0	53.9
18	56.7	56.3	56.8	56.4	56.9	56.5	56.8	56.4	56.4
19	60.0	59.6	60.4	60.0	60.0	59.6	60.4	60.4	60.0
20	62.8	62.4	63.0	62.6	62.8	62.4	63.0	62.6	62.5
21	66.5	66.1	66.3	65.9	65.7	65.3	66.2	65.8	65.8
22	68.9	68.5	68.8	68.4	68.9	68.5			68.5
23	72.6	72.2	73.0	72.6	74.3	73.9			72.6
24	74.6	74.3							74.3
25	78.4	78.1							78.1
26	80.7	80.4							80.4
27	84.7	84.4							84.4

ance of giving combination agreements except near the origin and this caused considerable confusion before the branches had been classified.

It should be noted that the quantities above called $\Delta_1 F$ or $\Delta_1 F^*$ are not "true" $\Delta_1 F$'s, because of the existence of Λ-type doubling. As explained in the following section on Λ-type doubling, each rotational level has an a and b component. A "true" $\Delta_1 F(J+\frac{1}{2})$ would be the distance from the a or b component of the J level to the a or b component respectively of the $J+1$ levels. In the case of O_2^+, however, alternate levels in the successive Λ-type doublets are missing. Because of this the quantity which has physical existence is the distance from the a level of J to the b level of $J+1$ (cf. Fig. 3), or from the b level of J to the a level of $J+1$. This quantity, for the lower

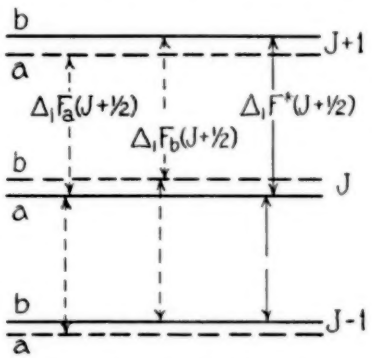

Fig. 3. The relation of the $\Delta_1 F^*$'s to the $\Delta_1 F$'s.

$^2\Pi$ state, will be denoted as $\Delta_1 F''^*$. In the upper $^2\Pi$ state this distinction will not be made since the Λ-type doubling in this state cannot be detected experimentally. This means that a $\Delta_1 F_1'^*$ is identical within experimental error with a "true" $\Delta_1 F'$.

Λ-type Doubling

For an electronic state with $\Lambda > 0$, the rotational levels are double, one level of the doublet being classified as an a level and the other as a b level.[16] However O_2^+ is a homonuclear molecule and the angular momentum (I) of the oxygen atom is zero,[17] as is known from the atmospheric oxygen bands. This means that alternate levels in the successive Λ-type doublets should be missing (cf. Fig. 3).

Alternate levels were actually observed to be missing. This is shown by the fact that the number of lines in any one series was the same as though there were no Λ-type doubling. But the lines were staggered since each rotational level was in effect slightly displaced, i.e., every other line was of slightly greater or smaller wave number than if there had been no Λ-type doubling. The staggering was made evident by plotting successive differences

[16] For a discussion of the nomenclature of these levels cf. R. S. Mulliken, Reviews of Modern Physics **3**, 93 (1931).

[17] For a discussion of homonuclear molecules cf. R. S. Mulliken, Reviews of Modern Physics **3**, 146 (1931).

of the lines of a branch against an arbitrary number. A straight line could be drawn between the points such that alternate points lay on opposite sides of this line. If there had been no Λ-type doubling the points would all have been on this line.

The Λ-type doubling should also appear in a plot of the $\Delta_1 F^*$'s. This causes the $\Delta_1 F^*$'s to stagger similarly to the series discussed above. The amount of this staggering is equal to the width of the Λ-type doublet, i.e., the distance which there would be between an a and b level of the same J value if both levels physically existed in the case of O_2^+.

When the $\Delta_1 F^*$'s were plotted it was found that there was Λ-type doubling in the lower $^2\Pi$ state, but not an appreciable amount in the upper $^2\Pi$

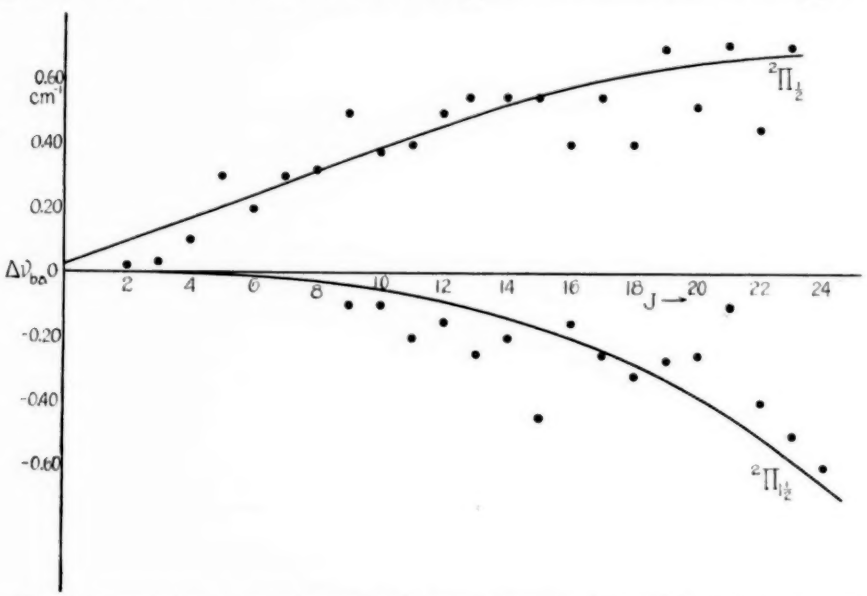

Fig. 4. Comparison of experimentally observed Λ-type doublet widths with the theoretical curves of Eqs. (12) and (13). The value of p was obtained from the slope of the initial portion of the curve through the points of the lower $^2\Pi_{\frac{1}{2}}$ state.

state. The Λ-type doublet widths are shown by Fig. 4. The following theoretical relations are expected:[18]

For a case a $^2\Pi_{\frac{1}{2}}$ state

$$\Delta\nu_{ba} = p(J + \tfrac{1}{2}). \tag{12}$$

For a case a $^2\Pi_{1\frac{1}{2}}$ state

$$\Delta\nu_{ba} = [p/Y^2 + 2q/Y](J - \tfrac{1}{2})(J + \tfrac{1}{2})(J + 3/2). \tag{13}$$

These relations represent the data fairly well and give $p = 0.036$, $q = 0.0027$.

There are reasons for believing that the upper electronic state of O_2^+ is $^2\Pi_u$ and the lower state $^2\Pi_g$. If this is true, then since for oxygen the complete ψ is Sy and for an atom with $I = 0$ ψ_{nu} is s, only−rotational levels can

[18] R. S. Mulliken and A. Christy, Phys. Rev. **38**, 94 (1931).

exist in the upper $^2\Pi$ state and + rotational levels in the lower $^2\Pi$ state.[17] If these conditions are correct, then the designations *a* and *b* as assigned here correspond respectively to the *c* and *d* classes of rotational levels.[16]

From an examination of the staggering of the $\Delta_1 F''^*$'s in the lower $^2\Pi_{\frac{1}{2}}$ state, it is found that those $\Delta_1 F''^*$ (N)'s, where $N = J + \frac{1}{2}$, for which N is an odd integer have slightly larger values than they would have if there were no Λ-type doubling. Also those $\Delta_1 F''^*(N)$'s, for which N is an even integer have slightly smaller values than they would have if there were no Λ-type doubling. This means that for the lower $^2\Pi_{\frac{1}{2}}$ state the *a* levels are above the *b* levels in each Λ-type doublet. For the lower $^2\Pi_{1\frac{1}{2}}$ state the reverse is true, i.e., the *b* levels are above the *a* levels. This difference is in agreement with theory.[18]

Conclusion

A possible explanation why the upper $^2\Pi$ is case *b* can be found by considering the probable electron configuration[19] of this state. The electronic configuration of normal O_2^+ has been designated as $1s\sigma^2\ 2p\sigma^2\ 2s\sigma^2\ 3p\sigma^2\ 3d\sigma^2\ 2p\pi^4\ 3d\pi^2$. The removal of a $3d\pi$ electron probably gives the lower $^2\Pi$ state of O_2^+ with the electronic configuration $\cdots\ 3d\sigma^2\ 2p\pi^4\ 3d\pi$. The removal of a $2p\pi$ electron would give the electronic configuration $\cdots\ 3d\sigma^2\ 2p\pi^3\ 3d\pi^2$. Such a configuration would give several electronic states one of which is a $^2\Pi$ state that would be expected to have a small coupling of the spin with the electric axis, corresponding to the upper $^2\Pi$ case *b* state.

Table VII. *Values of the molecular constants.*

upper $^2\Pi$	lower $^2\Pi$
$A' = +8.2\ \text{cm}^{-1}$	$A'' = +195\ \text{cm}^{-1}$
$B' = 1.048 - 0.014v'$	$B'' = 1.610 - 0.009v''$
(observed $v' = 0, 1$)	(observed $v'' = 8, 9$)
D' (cal.) $= 5.6 \times 10^{-6}$	D'' (cal.) $= 4.6 \times 10^{-6}$
D' (obs.) $\approx 5 \times 10^{-6}$	$r_e'' = 1.14 \times 10^{-8}$ cm
$r_e' = 1.41 \times 10^{-8}$ cm	$p = 0.036$
	$q = 0.0027$

In conclusion I wish to thank Professor R. S. Mulliken for proposing the problem and for his many valuable suggestions; also Dr. A. Christy for his interest and advice during the investigation.

[19] Cf. R. S. Mulliken, Phys. Rev. **37**, 1711 A (1931).

SECONDARY EMISSION FROM NICKEL BY IMPACT OF METASTABLE ATOMS AND POSITIVE IONS OF HELIUM

By Marshall C. Harrington
Palmer Physical Laboratory, Princeton University, Princeton, N. J.

(Received August 24, 1931)

Abstract

Experiments on the secondary electron emission from Ni electrodes due to bombardment by positive ions and metastable atoms in a helium discharge under conditions similar to those obtaining in a glow discharge are reported. The method of measurement is similar to that of Uyterhoeven and Harrington.[1] The proportion of the measured current at the cathode which is carried by electrons is found to be 15 to 50 percent depending on experimental conditions. Similarly the number of electrons per slow positive ion is found to range between about 8 and 20 percent. The secondary electrons originate at the surface of the collector with about 15 volts maximum initial energy.

THE experiments of W. Uyterhoeven and the author[1] on the secondary electron emission from nickel by impact of metastable atoms and positive ions of neon under conditions similar to those in a glow discharge have been extended to helium with a similar apparatus. As was to be expected from the similarity of the two gases, the data indicate that helium behaves in an analogous manner. Here, as in neon, the condition for emission by impact of slow positive ions is fulfilled, namely $V_i \geqq 2\phi$, where V_i is the ionization potential and ϕ is Richardson's work functions.[2] ($V_i = 24$ and ϕ = about 4.5 or 5).

Apparatus

The experimental arrangement was similar to that of the previous experiments in neon.[1] The discharge tube (see Fig. 1) was spherical in shape (20 cm diameter) with four side arms. The anode and cathode occupied two of these; a third at the bottom housed the main experimental electrode; the fourth at the top contained the movable electrode C. The cathode K was of a standard type of the General Electric Company consisting of an oxide coated nickel cylinder heated by a tungsten filament within. The anode A was a nickel cylinder. The main experimental electrode P (see Fig. 2) was a circular nickel disk (diameter 18.2 mm) with a coplanar concentric guard ring G (outer diameter 29.2 mm). The former was supported by the cylinder M and the latter by the outer cylinder L. The joints were made by electric spot welding. The cylinder L was protected by the cylindrical glass cover H in order to avoid drawing larger currents than necessary from the main dis-

[1] Uyterhoeven and Harrington, Science **70,** 586 (1929); Phys. Rev. **35,** 124 (1930); **35,** 438 (1930); **35,** 1421 (1930); **36,** 709 (1930).

[2] Holst and Oosterhuis, Physica **4,** 375 (1924).

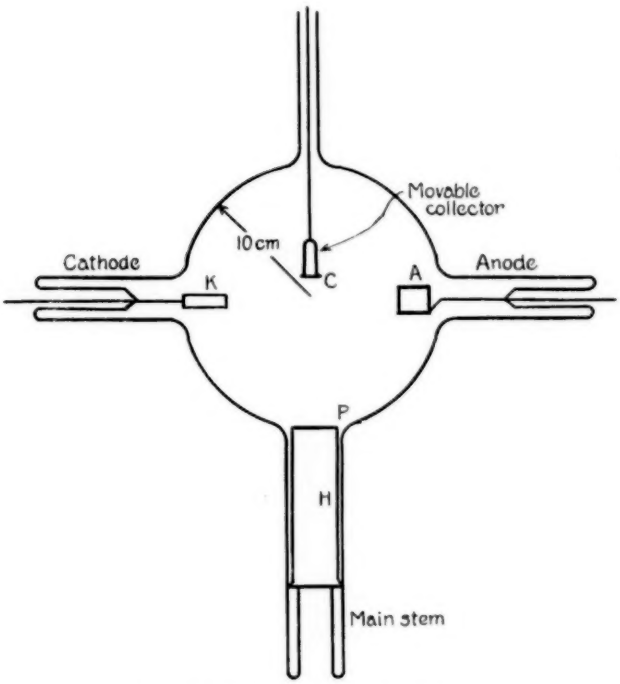

Fig. 1. The experimental tube.

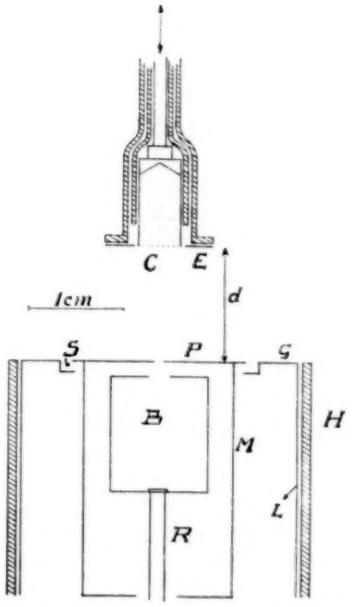

Fig. 2. Detail of collecting electrodes.

charge. The cylinder M protected the Faraday box B, which was at its center, from whatever charged or uncharged particles may have come through the annular slit S between the plate P and its guard ring G. The Faraday box B itself was a nickel cylinder closed at its top and bottom and supported by the rod R. In the center of the upper cover of B there was a circular hole (diameter 2 mm) which was immediately below a small hole (diameter 0.74 mm) in the center of the plate P.

The collector C was a small cylinder of nickel with one open end exposed to the discharge. This open end was covered with nickel gauze in order to allow the electrons which came to it to be trapped without much reflection. The sides and back were protected by glass. This was fitted with a plane annular guard ring E concentric and coplanar with the exposed end of C. The collector C was movable along its axis, that is, in a direction perpendicular to the plane of the plate P, opposite to which it was placed.

The metal used in the construction of the electrodes was outgassed by the induction furnace in the usual manner.

The discharge was run at about 0.5 to 1 ampere, and a more or less uniform luminosity filled the whole sphere. The helium gas used was constantly circulated and purified by a misch-metal arc, and liquid air traps were used to avoid condensible vapors. The tube was baked out before being used for about five hours at approximately 425° C with the pumps running until the pressure was no longer readable on a McLeod gauge.

Experimental Methods and Results

Two of the methods described in the paper[3] reporting the experiments in neon were used here. The first method[4] gave a measurement of the proportion of measured current carried by electrons at the plate P. The cylinder C was placed at a fixed distance d from the plate P and given a definite negative potential $(V_C)_A$ measured with respect to the anode so that it drew a positive current i_C. The potential of the plate $(V_P)_A$ measured with respect to the anode was lowered from about $(V_C)_A+50$ to $(V_C)_A-100$. The currents to the plate i_P and to the cylinder i_C were measured. The latter current was also put through a mirror galvanometer compensated with an opposing current in order to make a sensitive measurement of the variations in i_C from an arbitrary zero point. Some difficulty was encountered in making this steady due to fluctuations in the discharge. A typical curve of i_C *vs.* $(V_P)_A$ is given in Fig. 3.

Secondary electrons emitted from the plate P were accelerated by the drop across the sheath on the plate P, and a certain proportion of them arrived at the outer edge of the sheath on the collector C. The rest were scattered on the way. When the drop across the sheath on the plate P was greater than that on C, the electrons were received at C, giving a decrease (Fig. 3) in the measured current i_C. Actually since secondary electrons had some initial velocity, they started to come in when the negative potential $(V_P)_A$

[3] Uyterhoeven and Harrington, Phys. Rev. **36**, 709 (1930).

[4] See reference 3, pp. 712 ff.

was somewhat less than $(V_C)_A$, say about 15 volts. Table I gives some illustrative material.

TABLE I.

$(V_C)_A$	I	V	Δi_C	$i_{\bar{P}}$	i_P	γ
−100	0.520	29	18.3	30	250	12
−125	0.525	30	20.5	34.2	255	13
−150	0.520	31	20.9	34.9	260	13.5
−175	0.520	31	22.2	36.9	264	14
−200	0.520	31	24.0	40	269	15

I = total current in tube in amperes. V = drop across the tube in volts. Δi_C = electron current received at C in $\mu A/cm^2$. $i_{\bar{P}}$ = electron current originating at plate calculated from Δi_C using measured distance $d = 4.3$ cm and mean free path. $\gamma = i_{\bar{P}}/i_P$ in percent. Pressure = 1.5×10^{-2} mm of Hg.

The electron current originating from the plate P was calculated from Δi_C by assuming an exponential decrease. The gas kinetic mean free path was taken as 0.1259 cm at 1 mm.[5] The value of the proportion γ of the current i_P carried by electrons is given in the table. This is about the same as that found in neon, and varied with the discharge conditions.

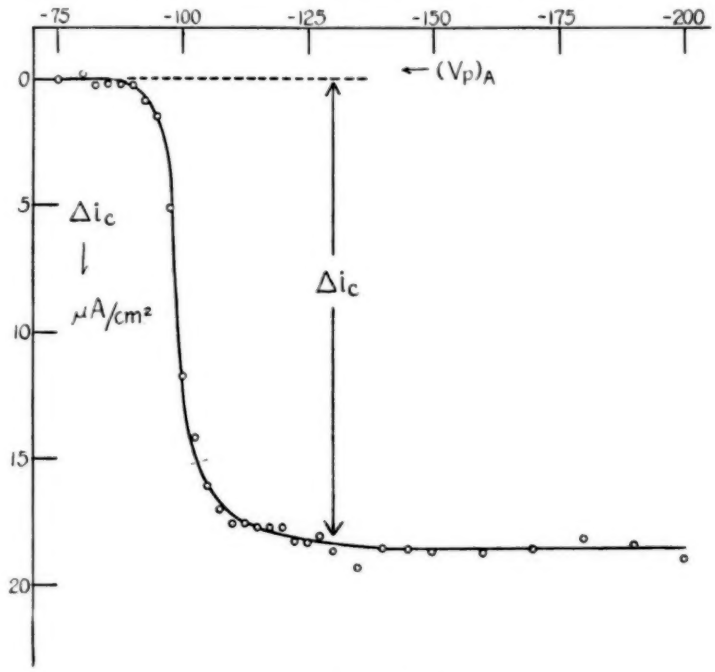

Fig. 3. i_C vs. $(V_P)_A$.

It is to be noted that electron reflection or secondary electron emission[6] due to impact of electrons at the collector C would introduce an error in

[5] Compton and Van Voorhis, Phys. Rev. **26,** 450 (1925).

[6] Compton and Langmuir, Revs. Mod. Phys. **2,** 171 (1930). See section 7 and references cited there.

Δi_C, which would make the calculated electron current i_P, and consequently γ, too small. In view of the fact that the electrode C was constructed especially to minimize reflection, and that the percentage reflection is only 3 or 4 in any case, the error thus introduced is not large.

Another method[7] enabled the secondary electron current to be separated into two parts, one part due to the bombardment of positive ions and the other due to the impact of neutral particles. This gave data on the number α of electrons emitted per impinging positive ion. The movable collector C was withdrawn into its side tube, as it was not used. The plate P and its guard ring G were put at some definite negative potential $(V_P)_A$ (say -100 v) measured with respect to the anode. The plate P and guard ring G thus drew

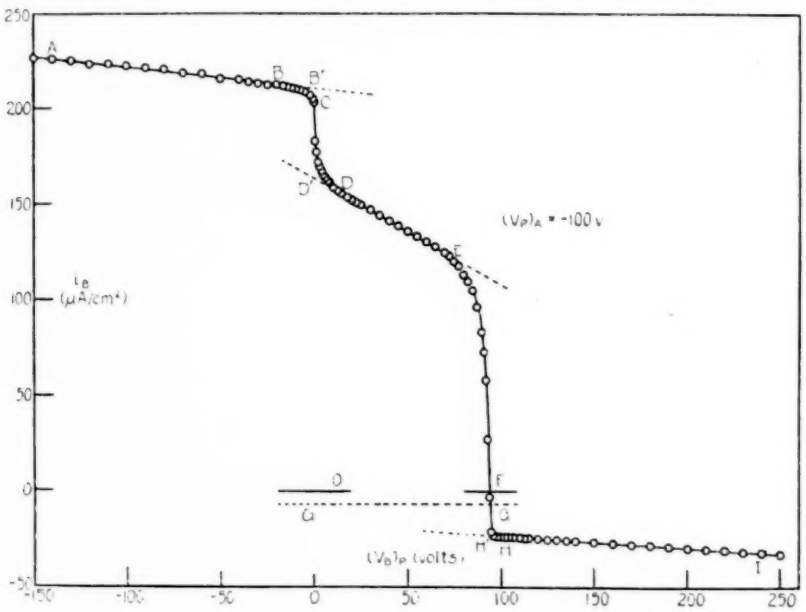

Fig. 4. Box currents i_B *vs.* box potential $(V_B)_P$ for plate potential $(V_P)_A = -100$ v.

a definite positive current i_P which was composed in part of a positive ion current i^+ coming in and in part of an electron current i^- going out. The ions received at P were accelerated by the potential drop across the sheath which existed above P, and hit the latter with the corresponding energy. Some ions went through the hole in the plate P and on into the box B beneath whenever the potential $(V_B)_P$ of the box (measured with respect to the plate P) permitted them. Fig. 4 gives a typical plot of the current i_B received at the box B as a function of the box potential $(V_B)_P$.

The general behavior of the currents in helium was the same as that in neon in the experiment previously described[3] and the interpretation given to the data is the same. The box B was first made negative and its potential $(V_B)_P$ raised from -250 to $+250$. The positive ions which came through the hole in the plate were received at the box until the potential of the box

[7] See reference 3, pp. 720 ff.

became equal to that of the space outside the sheath above the plate P from which the ions came. (Points *ABCDEFII* of Fig. 4). As can be seen in Fig. 4, the potential $(V_B)_P$ at which this occurred was very nearly equal to $-(V_P)_A$, indicating that the space from which the ions came had a potential almost equal to that of the anode. This gave a very good method of measuring the space potential, and was in all cases more definite than the method used by Langmuir and others.[8] It is to be noted, however, that in this case the information needed was the actual potential drop across the sheath when the plate was receiving considerable current. This was in all likelihood somewhat different from the space potential existing when the plate was floating, for the semilog plots according to Langmuir's method[8] indicated a somewhat lower potential. The positive ions thus received when $(V_B)_P$ equalled $-(V_P)_A$ went into the box B through the hole in its upper cover, and any electrons emitted because of them had a very small chance of escape. This offered opportunity to measure the actual positive ion current.

Uncharged particles, however, came through the hole in the plate P in a more or less random direction. Of these some, such as metastable atoms, had sufficient potential energy for the ejection of electrons from surfaces at which they lost their potential energies. This process does not necessarily occur at the surface first struck, for according to Oliphant[9] metastable atoms can be reflected from metal surfaces. Kenty[10] has pointed out that there should be included with the metastable atoms, the photons of the resonance radiation which have very nearly the same energy. The photoelectric efficiency of visible light is too small to account for the magnitudes of the currents found previously in neon[3] or here in helium. So far as is known to the author, there are aside from Kenty's work[10] no estimates of the photoelectric efficiency of the resonance light of the noble gases. Obviously, however, the experimental method used here does not distinguish between the photoelectric effect and the metastable atom effect. In order, however, to simplify the wording of the explanation of the data here presented, the phrase "metastable atoms" is to be understood as "metastable atoms and photons of resonance radiation."

A portion of the metastable atoms (see Fig. 2) went into the interior of the box B along with the positive ions, and any secondary electrons arising therefrom were trapped within and were not recorded. The rest, however, hit either the box B on its outer surfaces, or the under side of the plate P or cylinder M, and electrons ejected flowed to or from B as the potential $(V_B)_P$ permitted. As in neon,[3] it was found that the electrons had certain initial velocities of which the maximum was about 15 volts, corresponding to the difference between the potential energy of the metastable atoms and the work function of nickel ($V_m = 19$ and $\phi =$ about 5). This checks the value found by the other method described above. The dip $B\ C\ D$ in the curve i_B vs. $(V_B)_P$ (see Fig. 4) is due to these currents, which flowed first one way and then the

[8] Langmuir and Mott-Smith, Gen. Elec. Rev. **27,** 810 (1924) and other papers referred to therein.

[9] Oliphant, Roy. Soc. Proc. **A124,** 228 (1929).

[10] Kenty, Phys. Rev. **38,** 377 (1931) and private communication.

other as the potential $(V_B)_P$ was raised. The negative current i_1 from the box B, for instance, flowed when $(V_B)_P$ was less than $+15$ volts, and was proportional to CD' where D' is the point where ED extended backward cuts the axis of zero potential. The other current i_2, which flowed to the box, was received when $(V_B)_P$ was more than -15 volts, and was proportional to CB' where B' is the intersection of AB extended and the zero axis.

The exact position of the point C where the curve (Fig. 4) crosses the axis of zero voltage was somewhat in doubt, since the curve had a vertical inflection there and varied rapidly with the voltage. However, the total of these two currents i_1 and i_2 was $B'D'$, and this was divided in the same ratio as the areas $BB'C$ and $CD'D$ between the curve and the extrapolated lines which respectively determine B' and D'.

The real positive ion current i^+ received by the box at $(V_B)_P=0$ was thus the apparent positive ion current OD' plus the current i_2, which was received when $(V_B)_P>-15$ volts. As the potential of the box was raised, the ion current received gradually decreased (points D to E of Fig. 4). This may have been due to the presence of slow ions which were repelled from the box in increasing numbers as the potential was raised or to distortion of the fields around the hole in the plate as the potential of the box was changed. At $(V_B)_P=-(V_P)_A$ the ion current was entirely cut off, and the residual current FII' (points II to I, Fig. 4) was negative partly because of the current i_2 mentioned above and partly because of secondary electrons liberated by the impact on the underside of the plate of ions repelled by the box and subsequently received by the box. FII' was then composed of two parts $FG=B'C=i_2$ and $GII'=i_3$ which was ascribable to the effect of the ions. This latter current was divided by i^+ to give the number α of electrons per positive ion. All currents were reduced to amperes per cm² in order that they might be compared directly. The current received by the plate was thus divided by the area of the plate, and the currents received at the box were divided by the area of the hole in the plate. Here, as in the first method described above, an estimate of the proportion γ of measured current which was carried by electrons could be made. Illustrative material is presented in Table II.

TABLE II.

p	I	V	$(V_P)_A$	i_P	i^+	i_3	α	i^-	γ
4 $\times10^{-2}$	0.483	32	−100	358	171	15	9	187	52
	0.481	34	−120	376	167	14	9	209	55
	0.479	37	−140	388	169	14	9	219	56
	0.478	37	−160	413	173	15	9	240	57
	0.480	36	−180	440	181	17	9	259	59
	0.480	35	−200	454	173	19	8	286	62
2 $\times10^{-2}$	0.730	37	−160	413	329	26	8	84	21
2 $\times10^{-2}$	0.493	32	−160	275	230	21	9	45	20
4.5$\times10^{-2}$	0.415	56	−150	315	96	19	20	219	69

p = pressure in mm of Hg. I = total current through tube in amperes. V = drop across tube in volts. $(V_P)_A$ = potential of plate. i_P = apparent current at plate in $\mu A/cm^2$. i^+ = positive ion current in $\mu A/cm^2$. i_3 = secondary electron current due to positive ions in $\mu A/cm^2$. $\alpha=100i_3/i^+$. $i^-=i_P-i^+$. $\gamma=100i^-/i_P$.

Discussion

The measurements offer some inherent difficulties which unfortunately affect adversely the accuracy of the results. In general, the curves for helium were not as smooth or as consistent as those reported for neon.[3] The runs given in Table II are typical of results obtained during several months. The variations must be due to undetected changes in gas purity or in the surface condition of the electrodes caused by sputtering or by surface layers. This gives an indication as to the variations which may be anticipated under conditions which appear to be excellent as regards the present best technique of gas and electrode purification.

The values of α (8 to 20) found in helium (Table II) were about the same as those reported for neon[3] (14 to 20).

The values of γ (Table II) found by the second method were in general considerably higher than those found by the first method (Table I). However, the electrostatic field which existed between the edge of the sheath and the plate P was such that the effective size of the hole in P was less than its measured size, as can be seen from the following argument.[11] Consider the edge of the sheath S above P as a plane at zero potential emitting positive ions of zero velocity at a definite uniform rate. The points of plate P (at, say, -100 volts) are therefore the termini of the lines of force beginning on S. These lines of force will be parallel, running perpendicular both to S and to P except at P in the neighborhood of the hole where the lines will spread as they approach P. The locus of the termini on S of the lines of force which touch the edge of the hole in P is then a circle of area A_1 smaller than that of the hole A_2. Charged particles of zero mass liberated at S would follow these lines, but since the positive ions have considerable mass, they will go along lines of less curvature. The area A_3 on S from which the positive ions will go through the hole A_2 in the plate is thus larger than A_1, but not as large as A_2. The error in i^+ introduced in this manner is obviously not inconsiderable, but unfortunately difficult to calculate exactly. The value of $i^- = i_P - i^+$ is thus larger than it should be and consequently γ also. The errors in the two methods are such that, if allowance be made, the values of γ would be more nearly the same.

The values of γ reported here for helium are of the same order as those found in neon.[3]

Since the work on neon[3],[12] was reported a number of papers on related problems have appeared. Massey[13] presented a theoretical paper on the extraction of electrons from metals by positive ions and metastable atoms. The theory of the effect is presented from the point of view of the Sommerfeld theory of metals and the analytic method of wave mechanics, and the conclusion is drawn that the mechanism assumed is adequate to account for the neutralization of positive ions and the emission of electrons by metastable

[11] Semenoff and Walther, *Die physikalischen Grundlagen der electrischen Festigkeitslehre*, Springer, p. 23, and Mott-Smith and Langmuir, Phys. Rev. **27**, 760 (1926).

[12] For references to older work see Langmuir and Compton, Revs. Mod. Phys. **2**, 175–181 (1930), Sections 8 and 9.

[13] Massey, Camb. Phil. Soc. Proc. **26**, 386–401 (1930).

atoms. Langmuir and Found[14] report some interesting experiments on the production by resonance radiation in neon of metastable atoms which in turn eject electrons. An arc was run in a small portion of the total length of a long tube. Metastable atoms were produced considerably beyond the end of the arc as shown by secondary electron emission from electrodes. Similar emission from the walls left them positively charged. The metastable atoms from the discharge fall off $1/e$th for each 0.4 radius of the tube along the tube, so that metastable atoms from the discharge did not produce the effect. A shutter in the tube also showed that metastable atoms were produced at the end of the tube by something which traveled in straight lines, i.e., light. Kenty,[15] on the other hand, is of the opinion that in neon under conditions similar to those obtaining in Langmuir and Found's experiment,[14] the preponderance of the emission is attributable to the direct photoelectric action of the resonance radiation (about 700A) on the electrodes. His electrodes consisted of a nickel disk which could be turned about an axis perpendicular to the axis of the tube so that its plane could be placed either parallel or perpendicular to the axis of the tube, and a gauze cylinder surrounding it. The main discharge was maintained at another part of the tube some centimeters away. The disk was made negative, and the current collected was several times greater when the disk was perpendicular to the axis of the tube than when it was parallel, indicating direct photoelectric action rather than the effect of metastable atoms produced near the electrodes by the resonance radiation. In each of these experiments, since the electrodes were at a considerable distance from the discharge, the effect of positive ions was small. As has been mentioned above, the method used in the experiments reported here and previously in neon[3] does not permit a distinction between the photoelectric effect and that of metastable atoms.

Penning[16] has continued his experiments on the liberation of electrons from metal surfaces by positive ions. In neon he finds $\alpha = 3$ to 5 for ions of zero velocity on degassed tungsten. This is somewhat lower than that (about 7) found last year in this laboratory for neon on nickel.[3] Penning has also used ions of velocity (500 volts) much higher than those used here, and reports $\alpha = 20$ for tungsten in neon and $\alpha = 32$ for tungsten in the presence of mercury.

Güntherschulze[17] in some work on the liberation of electrons from copper by positive ions at low gas pressure has used a method which involves the measurement of the heat delivered at the electrode. However, there was no possibility of distinction between secondary electron emission due to positive ion bombardment and that due to the impact of metastable atoms or to the photoelectric effect. His results, as far as they go, coincide with those presented here.

In conclusion the author wishes to thank Professor Karl T. Compton of the Massachusetts Institute of Technology, Professor Louis A. Turner of Princeton University and Dr. W. Uyterhoeven of N. V. Phillips Lamp Works, Eindhoven, Holland, for their assistance and advice.

[14] Langmuir and Found, Phys. Rev. **36**, 604 (1930).
[15] Kenty, Phys. Rev. **38**, 377 (1931).
[16] Penning, K. Akad. v. Wet. Amst. Proc. **33**, 841–857 (1930).
[17] Güntherschulze, Zeits. f. Physik **62**, 600–606 (1930).

SCATTERING OF HIGH VELOCITY ELECTRONS BY THIN FOILS

By H. V. Neher
Norman Bridge Laboratory, California Institute of Technology

(Received August 25, 1931)

Abstract

With a narrow, homogeneous beam of electrons, scattering by thin foils of aluminum, silver and gold has been investigated. Voltages up to 145 kv ($\beta=0.63$) were used. Under conditions where single scattering was predominate and secondary electrons were absent, the amount of scattering was studied as a function of the primary energy, atomic number and angle. Absolute values were also obtained. The above investigations have lead to the following results: (1) Secondary electrons are defined and a means of eliminating them is proposed and used. (2) Wentzel's criterion for single scattering is tested over a wide range of energies. The value of $\theta/4\omega_{\min}$ for aluminum is found to increase from 3.3 at 45 kv to 6.1 at 145 kv. (3) A more critical criterion for single scattering by thin foils is obtained which depends on the shape of the curve connecting ρ, the amount of scattering, with angle. (4) Dependence of scattering on energy of primary beam is found to agree well with either Mott's equation or with the relation k/V^2, but is at variance with the classical relativistic theory. (5) Comparison of values of scattering for aluminum, silver and gold shows that ρ increases faster than Z^2. (6) Scattering is obtained as a function of angle from 95° to 173°. For aluminum the dependence found experimentally agrees well with either Mott's or Rutherford's equation. The latter also gives the correct dependence on angle for silver and gold. Mott's equation is not applicable for these heavy elements. (7) Absolute values of scattering for aluminum compared with theory give $\rho=1.32$ of the value given by Mott's equation. This relation is valid within the ranges $\theta=95°$–$173°$, $V=56$–145 kv. (8) Secondary electrons coming from the foil are distributed according to the simple cosine law. (9) No evidence of loss of energy due to radiation is found up to one-half the energy of the primary beam.

Introduction

THE experimental study of scattering of high velocity electrons by atomic nuclei is far more difficult than the corresponding problem using α-particles. At least three fundamental complications are encountered when electrons are used for the bombarding particles. First, the relativity change of mass of the electron becomes increasingly important at energies above 40,000 volts. Second, secondary electrons emitted by the scatterer are indistinguishable from the primary electrons scattered by the nuclei. Third, effects due to loss of energy of the primary electron through radiation may be important for the light elements and large angles.

Investigations on scattering of high velocity electrons have been made with both β-rays and cathode rays. Chadwick and Mercier[1] using radium E as a source of β-rays obtained approximate agreement with the classical,

[1] Chadwick and Mercier, Phil. Mag. **50**, 208 (1925).

theoretical prediction that the amount of scattering should increase with the square of the atomic number. Comparison of absolute values with Darwin's classical relativistic equation showed the experimental results to be 25 percent too large. However, a lack of homogeniety of the β-rays together with the difficulties encountered from the γ-rays make scattering experiments with radioactive sources unreliable. Schonland,[2] using cathode rays with energies up to 79 kv obtained agreement with Darwin's theory for absolute magnitude of the scattering as well as a correct dependence upon energy and atomic number.

Because of the lack of sufficient and accurate data and the increased theoretical interest in the problem, the following more extended investigations were undertaken.

Theories of Nuclear Scattering

Rutherford's equation giving the probability of an α-particle of mass m and charge $2e$ being scattered within the solid angle $d\omega$ at an angle θ to the original direction of motion by a nucleus of atomic number Z may be written as follows:

$$d\rho = \frac{ntZ^2e^4}{m^2v^4} \operatorname{cosec}^4 \frac{\theta}{2} d\omega, \tag{1}$$

where n is the number of nuclei per cm^3, t is the thickness of matter traversed and v is the velocity of the particle. This equation does not include a relativity correction and is not applicable in the case of high velocity electrons where β is large.

Darwin[3] has calculated the orbit of a high velocity electron in the field of a heavy positive nucleus, taking into account change of mass as the electron passes the nucleus. He arrived at the result that if the electron comes within a certain critical distance p_0 it will spiral in and be absorbed by the nucleus. This can have no physical meaning since no transmutation of the elements is observed. Using Darwin's result, Crowther and Schonland[4] deduced the angular distribution of the electrons scattered by nuclei, neglecting those which spiraled into the nucleus. The value for the scattering between 90° and160° for Al, Cu and Ag found experimentally by Schonland[5] agreed well with that deduced from Darwin's orbits. Later Schonland[6] showed that these spiralling electrons could not be neglected in his case and in order to get a solution to the problem he assumed that they emerged uniformly in all directions. This gave a result at variance with his experimental work.

The equation of Crowther and Schonland, both in the original and in the latter form given by Schonland, gives a dependence on β and θ as well as an absolute magnitude not found in this work. There is also some confusion as

[2] B. F. J. Schonland, Proc. Roy. Soc. **A113,** 87 (1926–27).
[3] C. J. Darwin, Phil. Mag. **25,** 201 (1913).
[4] J. A. Crowther and B. F. J. Schonland, Proc. Roy. Soc. **A100,** 526 (1921–22).
[5] Reference 2.
[6] B. F. J. Schonland, Proc. Roy. Soc. **A119,** 673 (1928).

to the form of the correction to be applied.[7] In addition, from considerations of wave mechanics, it appears quite clear that we can no longer regard the electron as a point when the distances of approach become of the order of h/mv, the wave-length to be associated with the electron. Comparison of Darwin's relativistic scattering equation with experiment is given in Table IV. It will be noticed that the relative as well as the absolute magnitudes do not agree over a wide range of energies. Consequently we shall not consider this theory further.

Perhaps the best treatment of the problem has been given by Mott[8] who uses Dirac's wave equation which includes corrections for both relativity and spin. The result arrived at may be expressed as

$$d\rho = \frac{ntZ^2e^4}{4m_0^2c^4}\left(\frac{1-\beta^2}{\beta^4}\right)\left[\operatorname{cosec}^4\frac{\theta}{2} - \beta^2\operatorname{cosec}^2\frac{\theta}{2} + \beta\pi\frac{2\pi e^2}{hc}Z\frac{\cos^2\theta/2}{\sin^2\theta/2} + \text{terms in}\left(\frac{2\pi e^2}{hc}Z\right)^2\right].$$

For the angles θ_1 and θ_2 this becomes,

$$\rho = \frac{\pi ntZ^2e^4}{m_0^2c^4}\left(\frac{1-\beta^2}{\beta^4}\right)\left[\cot^2\frac{\theta_1}{2} - \cot^2\frac{\theta_2}{2} - 2\beta^2\log\frac{\sin\theta_2/2}{\sin\theta_1/2} + \frac{2\pi\beta Z}{137}\left(\sin\frac{\theta_1}{2} + \operatorname{cosec}\frac{\theta_1}{2} - \sin\frac{\theta_2}{2} - \operatorname{cosec}\frac{\theta_2}{2}\right) + \cdots\right]. \quad (2)$$

The quantity ρ in this equation gives the ratio of the number of electrons scattered between the angles θ_1 and θ_2 to the total number of electrons incident on the scatterer.

Description of Apparatus

The apparatus in general is similar to that used by Schonland[9] for studying the same problem. A general view of the apparatus is shown in Fig. 1.

The electron "gun".

All metal parts were turned from copper. This metal has the advantages of being nonmagnetic as well as having a low vapor pressure. To eliminate the possibility of cold emission all metal parts were given two coats of nickel, then plated with chronium and finally given a very high polish. Metal to glass seals were used throughout. This eliminated entirely waxes and greases and made possible the attaining of a high vacuum in a minimum time. The metal shield extending back over the cathode was designed to protect the glass. No difficulty was experienced when working at 145 kv after the tube had been outgassed by continuous operation at lower voltages.

The filament was of the concentrated type wound with 10 mil tungsten

[7] E. E. Rutherford, Radiation from Radioactive Sources, 225 (1930).
[8] N. F. Mott, Proc. Roy. Soc. **A124,** 425 (1929).
[9] See reference 2 and B. F. J. Schonland, Proc. Roy. Soc. **108,** 187 (1925).

wire in the form of a helix and bent back on itself. This type was found to give a more intense beam finally emerging into the scattering chambers than that given by a number of other designs constructed. The position of the filament in relation to the end of the metal tube in which it was situated had to be adjusted very accurately to secure a maximum of current. It was also found that

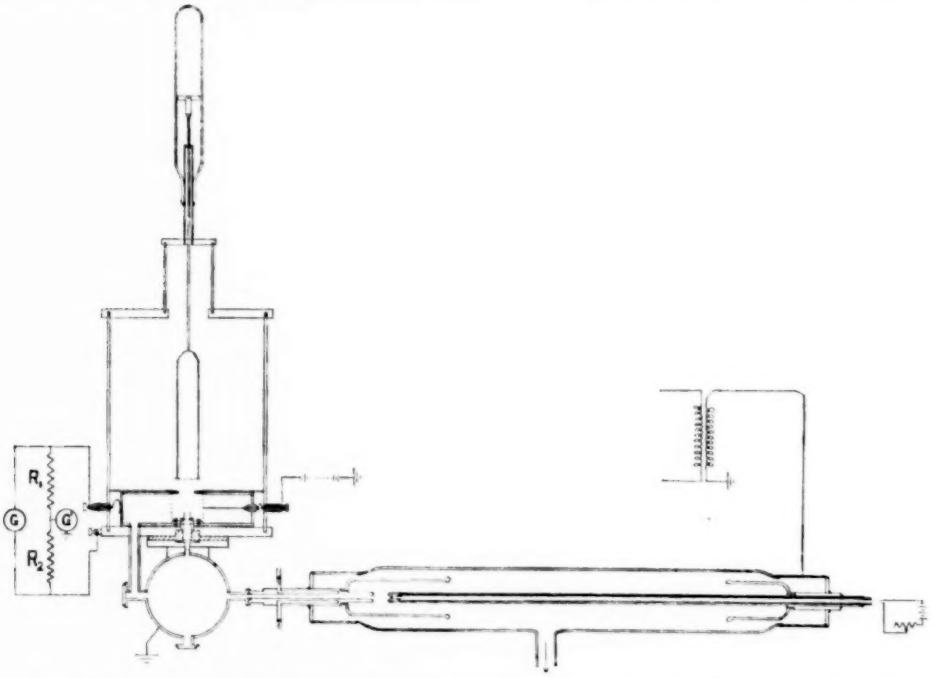

Fig. 1. Cross-section of apparatus showing electron-gun, solenoid, scattering chambers, method of varying angle and electrical connections.

a resistance of several hundred thousand ohms, placed between the filament and the metal tube surrounding it, increased the focusing action of the electric field between the cathode and anode and very materially strengthened the current received into the scattering chambers for a given total emission.

The solenoid.

This consisted of a brass cylinder 13 cm in diameter and 50 cm long wound with two layers of copper wire 1.63 mm in diameter. A section 10 cm long in the middle of the cylinder was partitioned from the remaining and could be evacuated with the rest of the apparatus. Each end of the solenoid was water cooled. Special precautions were taken to eliminate all magnetic substances in the neighborhood of the solenoid, since the maximum field was only 250 gauss.

As the solenoid was used not only as a means of obtaining a homogeneous beam but also for measuring the voltage of the electrons, it was necessary to know its constant. For an electron bent in a magnetic field,

$$(H\rho) = \frac{m_0 v}{e(1 - \beta^2)^{1/2}},$$

while the energy of the electron after falling through a potential V is,

$$Ve = m_0c^2\left(\frac{1}{(1-\beta^2)^{1/2}} - 1\right).$$

Eliminating β between these two equations,

$$(H\rho)^2 = \frac{1}{c^2}\cdot\frac{2m_0c^2}{e}\left(V + \frac{e}{2m_0c^2}V^2\right).$$

At low voltages,

$$(H\rho)^2 = kI^2 = k'V.$$

The relation between high and low voltages can then be written in terms of the respective currents in the solenoid as,

$$I^2 = \frac{1}{K}(V + 0.982 \times 10^{-6}V^2) \tag{3}$$

where $K = V/I^2$ for low voltages. V has been expressed in volts, I in amperes and the values of the constants inserted. The quantity K will be defined as the constant of the solenoid. Calibrations were made at high voltages with a standard sphere gap and by an electrical deflection method. The two methods gave results agreeing to within 1/2 percent. The constant obtained was,

$$K = 737 \pm 3 \text{ volt amp.}^{-2}.$$

Scattering chambers.

The arrangement of the scattering chambers can best be described by referring to Fig. 2. The purpose of using chambers of such large diameter

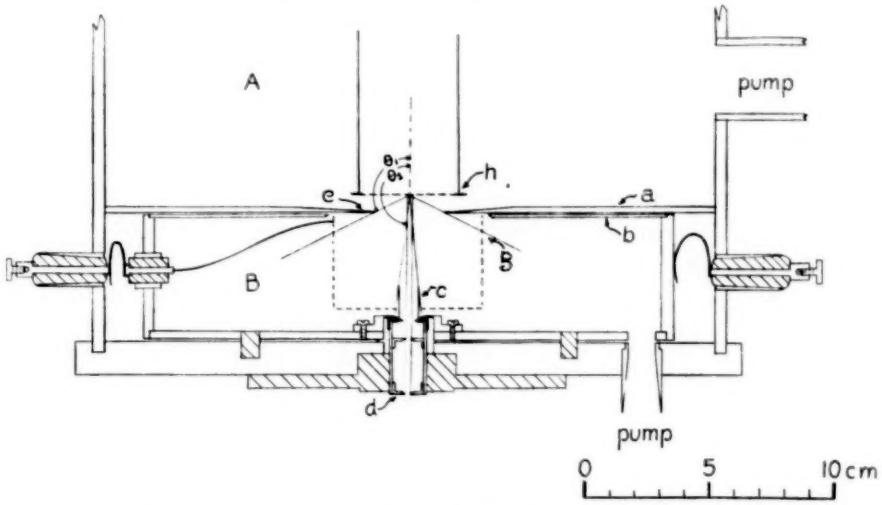

Fig. 2. Enlarged view of lower scattering chamber showing the relations of scatterer, grid and collector. The angles between which the scattered electrons were collected are also shown.

(20 and 25 cm) was to eliminate as far as practical the effect of reflected electrons going from one into the other. When the inside was brass the reflection

from the upper into the lower chamber amounted to 0.0003–0.0009 of the main beam. When the whole inside was lined with aluminum this value was reduced to 0.0001–0.0003.

The electrons were admitted from the solenoid into the scattering chambers through four collimating openings made of aluminum which were all grounded. The first three openings were 2.8 mm in diameter and the last was 4 mm. The purpose of this last opening was to stop scattered electrons from the openings below entering the lower chamber. The small, thin aluminum cylinder c was fastened to d and extended up into B a distance of 1.8 cm. It performed two functions: (1) it further prevented stray electrons from the openings below reaching B, and (2) it definitely fixed the larger angle of scattering.

Chamber B was insulated from A by thin (0.05 mm) mica disks. The metal disks a and b were fastened to A and B respectively. A thin aluminum ring 0.015 cm thick, 0.8 cm wide, with a 2.83 cm opening in its center formed the final separation between A and B. The disk b had an opening in it slightly larger than the grid g. This was found necessary since many electrons collect in the space within the grid and part of them would be collected by B if b extended beyond the edge of g.

Grids to stop secondary electrons.

For investigating secondary electrons up to 2000 volts, a wire grid was constructed. It consisted of a 4 mm mesh cylindrical framework made of 2

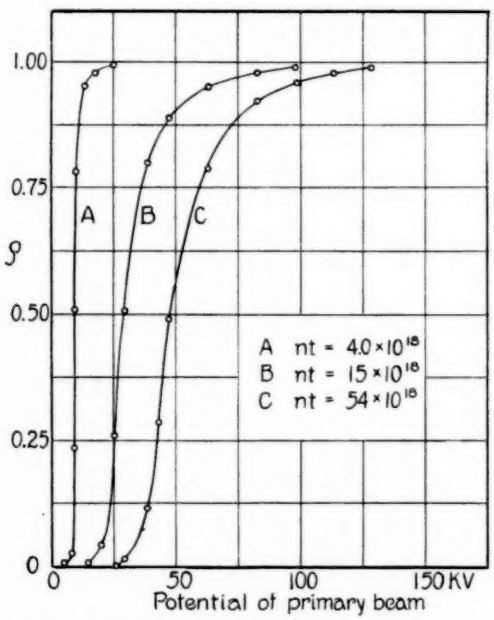

Fig. 3. The stopping power of aluminum foils of different thicknesses. The "range" may be obtained approximately from the lower knee of the curve.

mil nickel wire. The ratio of wire to total space was 0.025. The reflection coefficient of nickel is 0.30, hence a correction of 1.6 percent was applied to the readings when this grid was used.

When secondary electrons with energies greater than 2000 volts were investigated, because of the ionization currents produced and the attendant insulation difficulties, other means were resorted to than that of using actual potentials. Such a means was furnished by thin foils. Referring to Fig. 3 it will be noticed from the curve for aluminum connecting ρ (the ratio of transmitted electrons to the total number incident) with the voltage of the primary beam, that no electrons are transmitted up to a certain voltage after which there is a sudden increase. At voltages ordinarily used, from 90 to 145 kv, even a piece of aluminum 0.01 mm thick is very transparent and at the same time acts as an equivalent stopping potential of 50 to 55 kv. A small correction for voltages below 120 kv can be applied to account for those electrons scattered elastically which are stopped by this foil if it is used as a grid to stop secondary electrons. Although such foils do not form a barrier as perfect as would be furnished by an actual stopping potential, they do afford a means

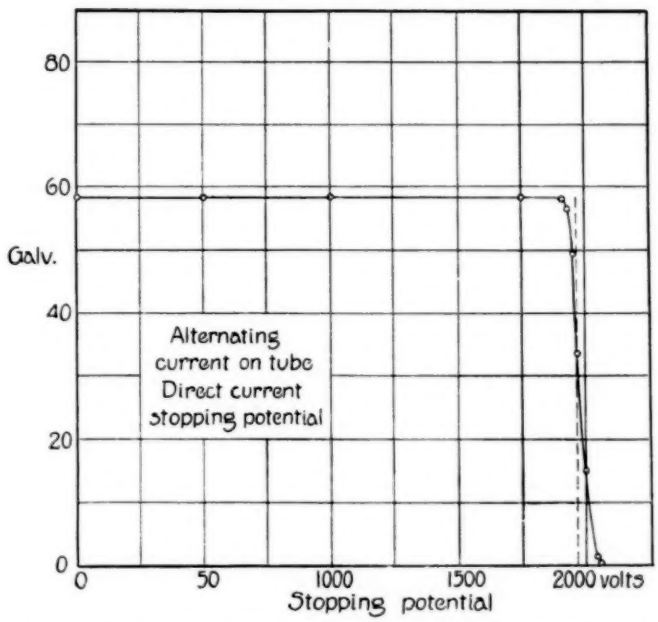

Fig. 4. Homogeniety of electron beam shown by applying D. C. stopping potentials. Dotted line represents computed voltage from known constant of solenoid.

of obtaining equivalent stopping potentials with an accuracy sufficient for the problem under consideration. This will appear more clearly in what follows.

Secondary electrons will also be set free from the foil grid on the collector side by the electrons which go through. To investigate this point a fine wire grid was placed around the foil grid and a stopping potential of 2000 volts applied. A decrease in the current received in B of 1 to 2 percent was found if the primary voltage was of the order of 50 kv, but for 100 kv the effect decreased to 0.3 to 0.4 percent. When necessary this correction was applied to the readings.

A means is thus provided by which secondary electron velocities up to

one-half the energy of the initial beam can be investigated. Reasons will be given later why one-half the energy of the initial beam is the upper limit to the energies of the secondary electrons.

Method of varying angle.

The foil acting as the scatterer was mounted on a thin metal ring, h, 3 cm in diameter, supported by a nickel wire 0.6 mm in diameter. The whole could be raised and lowered by means of a magnetic control as shown in Fig. 1. The height of the foil above the opening e could be measured to within 0.008 cm. The screw on the control mechanism was calibrated with a traveling microscope. The angles between which the electrons were collected were determined by the size of the openings c and e and by the height of the foil.

Homogeniety of beam.

The homogeniety of the beam for the case of alternating current applied to the tube was tested with d.c. stopping potentials. The result is shown in Fig. 4. Such a test was desirable since an alternating current transformer was used as a source of high voltage. The dotted line in the figure represents the voltage of the electrons computed from the constant of the solenoid. It will be noticed that the distribution of energies is almost symmetrical about the computed value. If $\pm\Delta V$ represents the heterogeneity of the beam, then if each side of the true value is considered, (cf. Eq. (1))

$$\rho' = \frac{k}{(V+\Delta V)^2} = \frac{k}{V^2}\left(1 - \frac{2\Delta V}{V} + \cdots\right)$$

$$\rho'' = \frac{k}{(V-\Delta V)^2} = \frac{k}{V^2}\left(1 + \frac{2V}{V} + \cdots\right)$$

$$\frac{\rho' + \rho''}{2} \doteq \frac{k}{V^2} = \rho.$$

If the beam of electrons is symmetrical about a mean voltage given by the constant of the solenoid, this same reasoning will apply to all $\pm\Delta V$'s and if the spread of voltage is not more than 5 percent on either side, the error introduced into the experimental results due to the lack of homogeniety will be negligible.

Determination of nt.

It was soon found that the variations in the thickness of the foils were too great to permit weighing a large sheet of the material and computing the average value of nt. Consequently a quartz torsion balance which had a constant of 0.1214×10^{-6} gm/div. was constructed. The constant was determined by weighing small sections of very fine wire a long piece of which had been previously weighed on an analytical balance. Aluminum foils 5×10^{-5} cm thick and 3 mm square could be weighed to 1 percent.

If m is the mass of a piece of foil of area A, then the product nt is given by: $nt = 6.06\times10^{23}\, m/MA$, where M is the atomic weight of the element compos-

ing the foil. The value of nt which enters directly into the scattering equation, is independent of the density of the material. Since that portion of the foil where the beam passed through was cut out and weighed, local variations in uniformity should not introduce a large error if the beam were uniform. This point was tested with the thinnest foils by rotating the foil one turn and taking readings every 45°. Variations of not more than 2 percent were observed while the average variation was 1 percent.

Experimental Procedure

The current in the solenoid was set and kept at a constant value while the voltage of the electron beam was increased until a maximum current came through into the scattering chambers as indicated by the galvanometer G'. (See Fig. 1). R_2 was kept constant at 10^4 ohms and R_1 adjusted until G read zero deflection. A change of resistance in R_1 of 0.1 ohm would give a deflection of G of approximately 5 mm. Since R_2 was 10^4 ohms, changes in ρ of 1 part in 10^6 of the main beam could be detected. When a balance of G was obtained, the drop in potential across R_2 was the same as that across R_1 and the apparent value of scattering within the given angles was then given by,

$$\rho = \frac{R_1}{R_1 + R_2}.$$

To this value of ρ several corrections must be applied.

1. A correction for the value of ρ when no foil was present. It varied with the height of the ring h, the kind of foil used as a stopping potential and the potential of the primary beam. This "zero correction" was checked at various times. A typical selection of values is given in the table below for a foil with an equivalent stopping potential of $-27{,}000$ volts.

Table I.

V	θ_1	θ_2	ρ (correction)
68.9 kv	95°10′	172°5′	0.00022
96.9	95°10′	172°5′	0.00026
129.0	95°10′	172°5′	0.00028
145.0	95°10′	172°5′	0.00030

This "zero correction" is to be subtracted from the apparent value of ρ.

2. A correction for the wire of which the grid was constructed. It amounted to 0.8 percent for the foil covered grids and 1.6 percent for the fine mesh wire grid. This correction is to be added.

3. A correction for the stopping power of the foil grids for elastically scattered electrons. This was obtained from Fig. 3 and amounted at most to only a few percent. This is to be added.

4. A correction for the reflection out of chamber B and for the absorption by the foil grid of electrons reflected from the walls of B. Two experimental methods could be used to determine the magnitude of these two effects. (1) The dimensions of the scattering chamber could be increased and an extrapolation to an infinitely large one made; or, (2) the chamber could be lined

with different metals of known reflection coefficients and an extrapolation to zero reflection made. The latter method was chosen as the more practical. Consequently, the reflection coefficients of aluminum and brass were determined as well as the angular distribution of these reflected electrons. The ratio of the coefficients for aluminum and brass is $0.13/0.29=0.45$. A typical example showing the effect of lining the chamber B with brass and aluminum is given below:

Metal	V	θ_1	θ_2	V_s	ρ
Al	96.9 kv	108°	173°	−27 kv	0.001260
Brass	96.9 kv	108°	173°	−27 kv	0.001253

The effects increased slightly for lower voltages and decreased for higher voltages. In most cases the correction was negligible.

When the foil grid was used it was connected electrically to chamber A. This was necessary since B was to collect only those electrons scattered elastically while A was to collect all others. Secondaries emitted from the foil or other parts of A subtracted in one place but added in another so that the net result was nil.

Results

Secondary electrons.

It is of great importance to eliminate the effect of secondary electrons if nuclear scattering is to be studied. When stopping potentials are applied to the electrons coming from a thin metal foil which is being bombarded with a homogeneous beam of high velocity electrons, it is found that the electrons so emitted have a wide distribution of energies. A large number have energies below 100 volts, but an appreciable number, compared with the electrons which have been scattered elastically, have much higher energies. It is necessary to determine how high a stopping potential must be applied to stop all secondary electrons and still not stop those scattered elastically.

Secondary electrons have been defined by other investigators in various ways. Becher[10] and Stehberger,[11] working at energies below 12,000 volts defined as secondary electrons all those with energies below 36 volts. Wagner[12] defined all electrons coming from the material bombarded as secondary. In this paper a different definition based upon the process of collision of two electrons will be adopted. It is well known that as a purely mechanical process, when two electrons collide, one of them being initially at rest, they part at an angle of 90° to one another. We shall distinguish them after collision by defining the one with the greater energy as the primary and the one with the lesser energy as the secondary.

It will be apparent from the above considerations that for a sufficiently thin foil, many secondary electrons formed in the center of the foil will have

[10] A. Becher, Ann. d. Physik **78**, 288 (1925).
[11] K. H. Stehberger, Ann. d. Physik **86**, 825 (1928).
[12] P. B. Wagner, Phys. Rev. **35**, 98 (1930).

sufficient energy to emerge. If stopping potentials equal to one-half the energy of the initial beam are applied it is certain that all secondaries are stopped and that the remaining electrons are those which have been scattered by nuclei alone.

The effect of applying successively higher stopping potentials to the electrons emitted by thin foils of aluminum bombarded with 128 kv electrons is shown in Fig. 5. The ordinate gives the ratio of the number of electrons penetrating the stopping potential (given by the corresponding abscissa) to the total number of primary electrons incident on the scatterer. The angles between which the scattered particles were collected in each case were 95° and 172°. The values of ρ given in Fig. 5 refer only to curve (*a*).

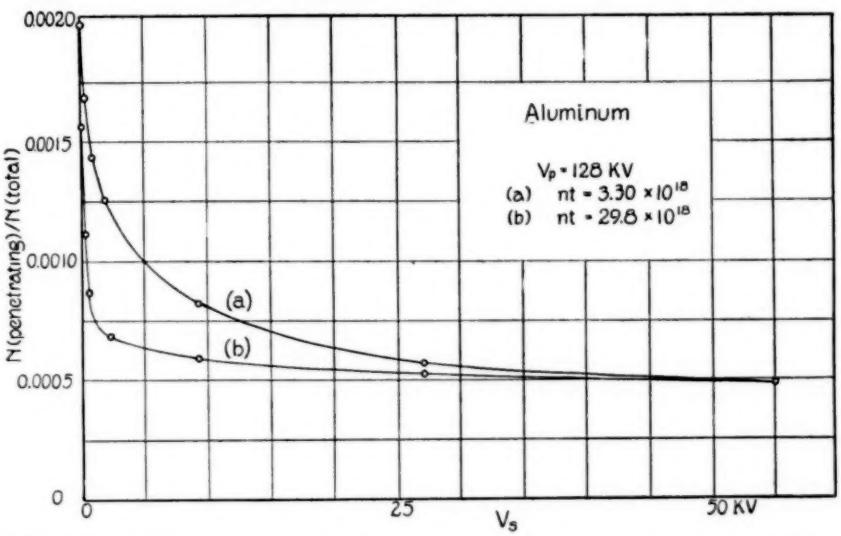

Fig. 5. Shows (1) that an appreciable number of secondary electrons are present from a thin foil at very high energies, (2) that secondary electrons are more important for a thinner foil. Curve (*b*) fitted to (*a*) at 55 kv.

The relative importance of secondary electrons for thin foils is greater than for thicker foils. This is shown in curve (*b*) where the foil was eight times the thickness of that used in obtaining curve (*a*). (*b*) is fitted to (*a*) at 55 kv. This difference of relative importance of secondary electrons may be explained by the greater probability of a secondary electron emerging from the thinner foil. In each case the probability of the nuclearly scattered primary electron emerging is practically 1.

It might be thought that the electrons stopped between 25 and 55 kv were those which had been scattered by the nuclei but which had gradually lost sufficient energy to other electrons in the foil so that they were stopped by a potential less than half their original value. If this were so one would expect the curve for the thicker foil to nearly coincide with the one for the thinner foil. It therefore appears that there are a few secondary electrons at very high energies, although they form an appreciable percentage of the total number collected.

It is interesting to note that Schonland used 150 volts stopping potential and assumed that all secondary electrons were eliminated.

Single scattering.

Experimentally if ρ increases linearly with nt single scattering is the predominating factor. The results of these tests are shown in Fig. 6. Wentzel[13] has

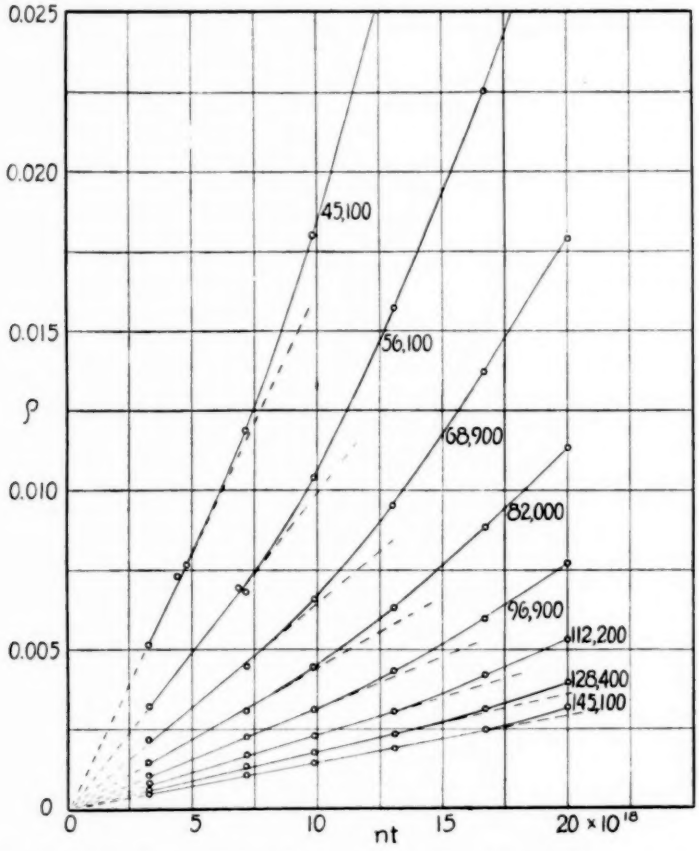

Fig. 6. Tests of single scattering—ρa nt. Angles: $\theta_1 = 95°\ 10'$, $\theta_2 = 172°\ 5'$.

obtained a criterion based on classical reasoning which must be satisfied for single scattering to be the predominating factor. It may be stated as follows: If

$$4\omega_{\min} = 8 \cot^{-1} \frac{2V}{Ze} \left(\frac{2}{\pi nt}\right)^{1/2},$$

then for single scattering,

$$\frac{\theta}{4\omega_{\min}} = 3 \text{ or } 4.$$

If we apply Wentzel's criterion to the point where the curves depart from linearity in Fig. 10 we obtain the values given in Table II.

[13] G. Wentzel, Ann. d. Physik **69**, 333 (1922).

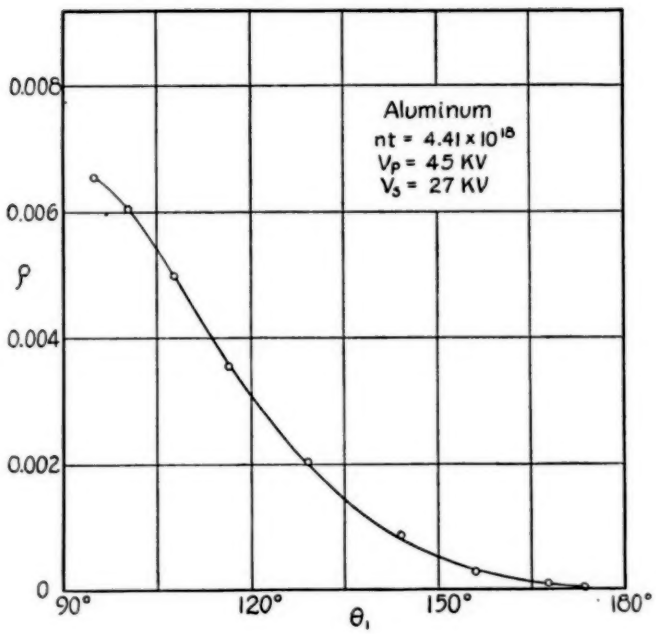

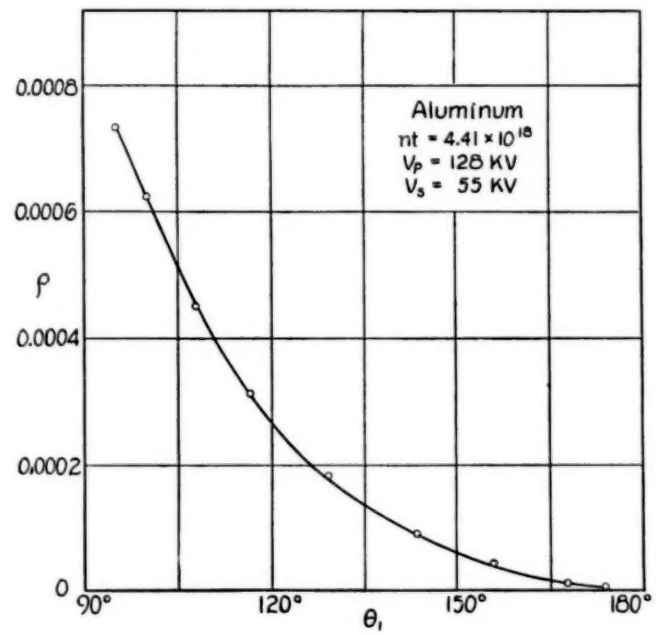

Figs. 7 and 8. More accurate test of single scattering by thin foils. Hump in Fig. 7 disappears for $V_p > 90$ kv for a foil of this thickness as shown in Fig. 8.

TABLE II. *Aluminum.*

	$\theta_1=95°10'$	$\theta_2=172°5'$	
nt	V	$4\omega_{min}$	$\theta_1/4\omega_{min}$
6.0×10^{18}	45.0	28°56′	3.3
7.4	56.0	25°52′	3.7
8.3	68.9	22°40′	4.2
9.4	82.0	20° 0′	4.7
11.3	96.9	18°40′	5.0
13.2	112.5	17°20′	5.5
15.5	129.0	16°24′	5.8
17.6	145.0	15°36′	6.1

The factor $\theta/4\omega_{min}$ is not a constant but increases with the voltage. The value reported by Schonland is $\theta/4\omega_{min}=3.0$, which is for both 60 and 80 kv. Judging from the results given here this value is much too low.

A more accurate criterion for single scattering from a foil can be obtained experimentally from the shape of the curve showing the variation of ρ with angle. Near 90° a scattered electron emerging from the foil must go a greater distance through the metal than one coming out at larger angles, and the probability of a second collision is increased. This will have the effect of decreasing the slope of the curve near 90°. These plurally scattered electrons will be partially thrown into larger angles and will give the hump shown in Fig. 7, which is for 45,000 volts with a stopping potential of 27,000. Fig. 8, for the same foil ($nt=4.41\times10^{18}$) but a primary voltage of 128,000 and a stopping potential of 55,000, shows how the hump has completely disappeared. The shape of the curve for this particular thickness of aluminum foil remains unchanged from 90 to 145 kv. A necessary and sufficient condition for single scattering at angles from 90° to 180° when a foil is bombarded normally is that the curve connecting ρ with θ shall not change its shape when the primary potential is increased.

TABLE III. *Aluminum.*

$V_s=-27{,}000$ kv, $\theta_1=95°10'$, $\theta_2=172°5'$							
kv	56.1	68.9	82.0	96.9	112.2	128.4	145.1
$\frac{\rho}{nt}$	9.47	6.35	4.38	3.05	2.34	1.63	1.35×10^{-22}
	9.65	6.41	4.31	3.14	2.29		
	9.69	6.38	4.43	3.09	2.31	1.71	1.41
	8.70	6.31	4.17	2.97	2.31	1.72	
	8.92	6.12	4.38	3.10	2.28	1.73	1.35
av.	9.29	6.31	4.33	3.07	2.31	1.70	1.37×10^{-22}

An indication of the accuracy obtainable, using foils of such thickness in each case that single scattering was predominate, is shown in the following table for five different foils. The value ρ/nt should be constant for constant voltages, angles and atomic number. The stopping potential, V_s, in each case was 27,000 volts.

Dependence of scattering on energy of primary beam.

The variation of the amount of scattering for aluminum between the angles of 95°10′ and 172°5′ as a function of the energy of the beam is shown in Fig. 9. Plotted in the same figure are the relations k/V^2 and the relative values computed from Mott's equation, each being fitted to the experimental value at 56 kv.

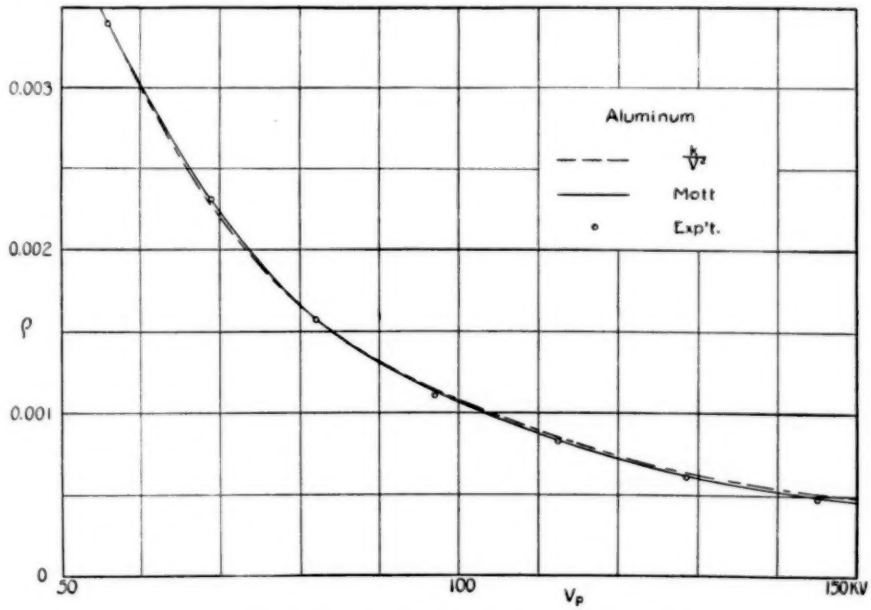

Fig. 9. Dependence of ρ upon energy of primary beam with appropriate stopping potentials in each case.

TABLE IV. *Aluminum.*

$nt=3.68\times10^{18}$		$\theta_1=95°10'$		$\theta_2=172°5'$	
β	V	Relative values of ρ			
		Exp	Mott	Darwin	k/V^2
0.436	56.1 kv	0.00340	0.00340	0.00340	0.00340
0.474	68.9	0.00231	0.00229	0.00241	0.00226
0.511	82.0	0.00157	0.00157	0.00178	0.00160
0.543	96.9	0.00110	0.00114	0.00134	0.00115
0.574	112.2	0.00082	0.00084	0.00104	0.00085
0.603	128.4	0.00061	0.00064	0.00088	0.00065
0.630	145.1	0.000485	0.000495	0.00077	0.000505
β	V	Absolute values of ρ			
		Exp	Mott	Darwin	Rutherford ($\alpha 1/V^2$)
0.436	56.1 kv	0.00340	0.00257	0.00460	0.00264
0.474	68.9	0.00231	0.00174	0.00326	0.00176
0.511	82.0	0.00157	0.00118	0.00242	0.00124
0.543	96.9	0.00110	0.00086	0.00182	0.00089
0.574	112.2	0.00082	0.00063	0.00141	0.00066
0.603	128.4	0.00061	0.00049	0.00119	0.00051
0.630	145.1	0.000485	0.000375	0.00104	0.00039

A comparison of the relative as well as the absolute values of ρ is given in Table IV. The following points should be noted: (1) The dependence on energy of beam given by Mott's equation and by the empirical relation k/V^2 agrees well with experiment, while the equation based on relativity correction of the classical theory does not agree. (2) Absolute values of scattering within the angles given do not agree with any of the theories. Rutherford's equation cannot be written proportional to $1/V^2$ above 30 to 40 kv. Mott's result is the one we shall consider most seriously. Comparing with the experimental values we obtain,

$$\text{Exp} = 1.32 \text{ Mott}$$

which represents the facts quite closely for aluminum. It will be shown later that Mott's equation also gives the correct dependence on θ. The above relation, then, is valid in the case of aluminum within the ranges, $V = 56{,}000$ to 145,000 volts and $\theta = 95°$ to 173°.

Dependence of scattering on Z.

In Table V the factor $\rho/ntZ^2f(\theta/2)$ is compared for Al, Ag and Au at $\theta_1 = 95°10'$ and $\theta_2 = 172°5'$ for $\beta = 0.603$ and $\beta = 0.630$. All the theories require that this factor should be a constant for all elements but it actually increases. Schonland also reports a value too high for gold and attributes it to an abnormal emission of secondary electrons. This explanation is hardly tenable for the results reported here because of the stopping potentials used. It may be pointed out here that Mott's equation applies best to the lighter elements and neglecting further terms in the expansion (see Eq. (2)) is scarcely justifiable in the cases of silver and gold.

TABLE V.

	$\beta = 0.603$			$\beta = 0.630$		
	Al	Ag	Au	Al	Ag	Au
Mott	1.52	1.77	2.41×10^{-24}	1.24	1.38	1.95×10^{-24}
Ruth.	1.18	1.65	2.50	0.94	1.19	1.77

In view of the fact that plural scattering contributed something to the value of ρ for the thinnest silver and gold foils (800A and 1200A respectively) it would be expected that the value would be high. Wentzel's criterion for both these elements gives $4\omega_{\min} = 5.3$ at 128,000 volts. We should then expect mostly single scattering and the large values obtained for these elements must indicate that ρ increases faster than Z^2.

Dependence of scattering on angle.

C. E. Eddy[14] has studied the angular distribution of β-rays scattered by thin foils from 0° to 50° but under conditions where plural scattering was very prominent. Kemplerer[15] working with voltages between 10 kv and 40 kv

[14] C. E. Eddy, Proc. Camb. Phil. Soc. **25**, 50 (1929).
[15] Klemplerer, Ann. d. Physik **3**, 849 (1929).

found an angular dependence between 10° and 120° not given by any existing theory. The accuracy of this latter work, however, was probably insufficient to warrant conclusions. Certain definite angles have been used by other observers, but a consistent effort to obtain an accurate dependence on angle has not been made.

The dependence of scattering on angle found experimentally is well illustrated in Fig. 10 which is for aluminum. θ_1 is plotted as abscissa so that any ordinate gives the value of the ratio of the number of electrons collected between θ_1 and θ_2 to the total number of electrons incident on the foil. θ_2

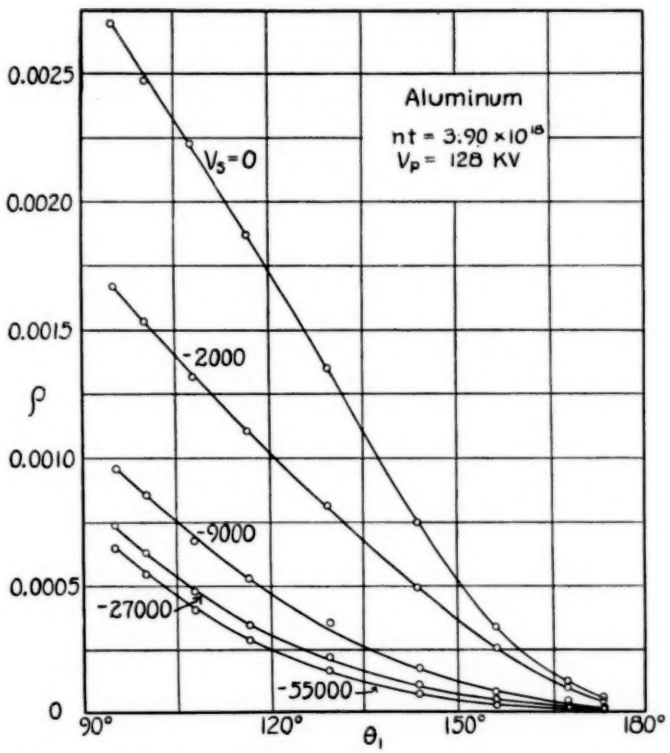

Fig. 10. Dependence of ρ upon angle. Shows effect of applying successively higher stopping potentials both on absolute magnitude and shape of curve.

varies from 172° when $\theta_1 = 95°$, to 178° when $\theta_1 = 173°$. The primary voltage for each curve is 128,000. The four curves plotted are for the stopping potentials given. In Fig. 11 plotted with values for $V_s = -55{,}000$ volts and fitted at 95°10′ is given the variation with θ from both Mott's and Rutherford's equations. All curves which have been obtained from 97 to 145 kv are very similar in shape to the one given in Fig. 11 if the proper stopping potential is applied. At voltages below 97 kv, the hump shown in Fig. 7 begins to appear for the thinnest foil available, and no comparison with theory based on the assumption of single scattering can be made. For sufficiently high voltages either the equation of Mott or Rutherford gives a dependence on θ between 95° and 173° which agrees well with experiment.

Similar curves have been obtained for gold and silver. The angular dependence for these two metals agrees well with Rutherford's $\cot^2 \theta/2$ relation but the agreement is not as good with Mott's equation. This deviation is probably due to the fact that, as mentioned before, neglecting further terms in the expansion is not permissible for the heavy elements.

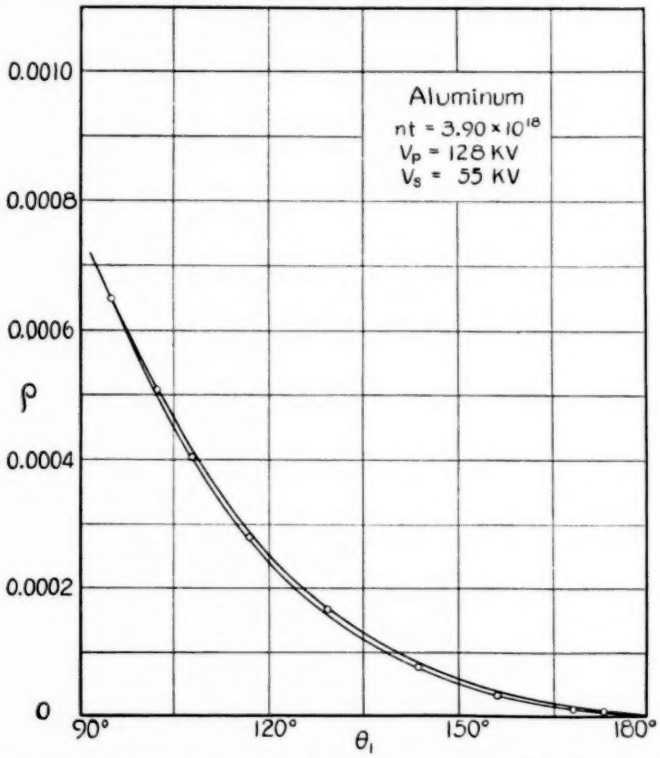

Fig. 11. Lowest curve of Fig. 10 compared with the angular distribution given by Mott and Rutherford. Theoretical curves fitted at 95°.

Angular distribution of secondary electrons.

To find the dependence on angle of the secondary electrons emitted between two energies, we need only to take the difference in ordinates of two curves for two different stopping potentials. Fig. 12 shows the result for aluminum taken from Fig. 10. It was found that the points agree very well with the curve $k'(\sin^2 \theta_1 - \sin^2 \theta_2)$. Since the second term in the parenthesis is small compared with the first this may be written as $k' \sin^2 \theta_1$. If this is differentiated with respect to θ and divided by $\sin \theta$ the result is $2k \cos \theta$, which represents the intensity of the secondary electrons at the angle θ. The following conclusions may then be drawn: The electrons that come from a thin foil when bombarded with high velocity electrons may be divided into two definite and distinct groups:

1. Those that are scattered without an appreciable loss of energy and have an intensity distribution given by either Rurtherford's $\operatorname{cosec}^4 \theta/2$ law, or Mott's equation.

2. Those that come off with low velocities and have an intensity distribution given by cos θ. It is interesting to note that the cosine distribution is also obtained for the emission of electrons from solid surfaces.

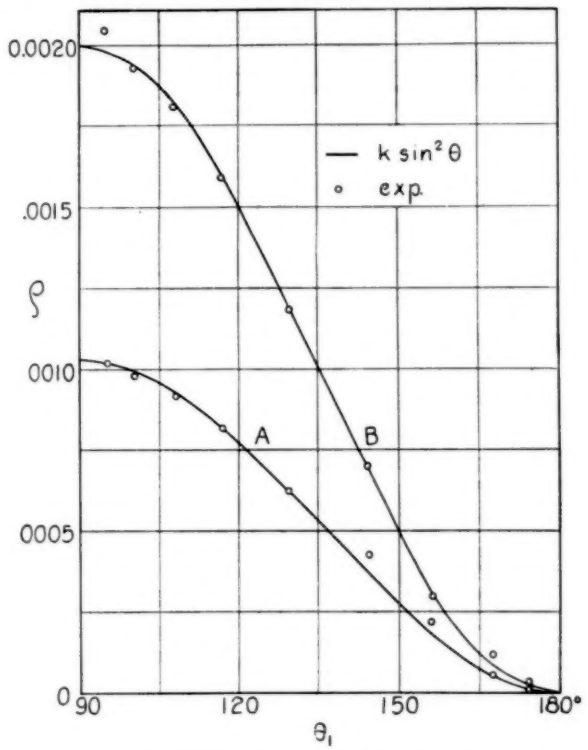

Fig. 12. Angular distribution of secondary electrons from a thin foil taken from Fig. 10. Curve A,0 to 55 kv, curve B,2 to 55 kv.

Effects Due to Radiation

When an electron is accelerated energy is lost due to radiation. The continuous x-ray spectrum is due to the hyperbolic orbits of the electron around the nuclei of the atoms composing the x-ray target. Some electrons will lose all their energy through radiation and these will give the short wave-length limit or the maximum frequency of the radiation emitted according to the relation of Duane and Hunt, $Ve = h\nu_{max}$. Kramers[16] has computed the amount of energy lost by an electron deflected through an angle θ upon the assumption that the orbit is not appreciably disturbed. He finds the expression,

$$R = \frac{4}{3}(\tfrac{1}{2}mv^2)\frac{\beta^3}{Z}\tan^5\frac{\theta}{2}\left[(\pi+\theta)\left(1+\tfrac{1}{2}\operatorname{cosec}^2\frac{\theta}{2}\right)+3\cot\frac{\theta}{2}\right].$$

For a 50,000 volt electron deflected through 90° by an aluminum nucleus, the relative amount of energy lost is ten percent according to the above relation.

Mott[17] has considered the effect of radiation forces on the angular distribu-

[16] H. A. Kramers, Phil. Mag. **46,** 826 (1923).

[17] N. F. Mott, Proc. Camb. Phil. Soc. **27,** II, 255 (1931).

tion of nuclearly scattered electrons. Although an exact solution is not obtained, he concludes that the correction to be applied to the scattering equation is an addition of not more than a few percent. However, until a more accurate calculation is made, especially to determine the dependence on angle, no definite conclusions can be drawn.

Qualitative tests may be made experimentally as follows:

1. For large angles it might be expected that many electrons have lost a large portion of their energy and that an appreciable number would be stopped by $-55{,}000$ volts if the original energy were 110,000. If this were true the curve showing the variation of ρ with θ would come close to the axis $\rho = 0$ at large angles. No such effect is noticed.

2. Since light atoms 2, according to Kramer's equation cause a greater loss of energy than heavier atoms, we should expect a differently shaped curve connecting ρ and θ for aluminum and gold. Both elements follow the same law experimentally.

3. The relative loss of energy according to Kramers is proportional to β^3. We should expect, then, that for two widely different potentials with one-half the primary voltage used as a stopping potential in each case, we should get departures from scattering equations that are based on purely elastic scattering. No such departures are found.

What can be said, then, about the electrons that generate the continuous x-ray spectrum? There seem to be at least two possible explanations. Either, (1) The number losing one-half their energy or more is inappreciable compared with a given fraction of the main beam collected between 140° and 180°, or, (2) Momentum relations are such as to distribute over various angles those electrons losing energy.

Discussion of Errors

It is thought that the main error entering into the measurement of ρ experimentally came from an inaccurate knowledge of the "zero correction" when the foil was in place. The foil distributed the electrons going through in a different way than was the case when the "zero correction" was taken with the foil present. It is estimated that this error was not more than 1 or 2 percent; first, because of the small "zero correction" when the foil was absent, (about 0.0002 of the main beam), and second, because with a very thin foil, where the "zero correction" was comparable with the true value of ρ, the main beam was not scattered appreciably.

An analysis showed that the error due to the finite size of the beam and its slight divergence was negligible.

To make certain that no appreciable impurities of large atomic number were present in the aluminum foil used, some very pure aluminum from Siegbahn's laboratory was tested. The values of ρ/nt agreed to within 1 percent of those obtained with the foils regularly used.

The value of nt could be determined to 1 percent and the error in measuring the angle on the factor $\cot^2 \theta_1/2$ was of the same magnitude.

It may, therefore, be concluded that the experimental error in the absolute

value of ρ for aluminum cannot be greater than 3 or 4 percent. For gold and silver the error may be slightly larger since only three and not five different foils were used for each in determining the final average values of ρ/nt.

Conclusions

Comparison with theory.

The experimental results when compared with existing theories may be summarized as follows:

1. Dependence on energy of primary beam: Either Mott's equation or the empirical relation k/V^2 gives good agreement within the range 56 to 145 kv.

2. Dependence on atomic number: According to Mott's equation, ρ increases faster than Z^2. This is found experimentally but the increase is not sufficient to give good agreement. All other equations give ρ proportional to Z^2.

3. Dependence on angle: Either Rutherford's or Mott's equation gives good agreement.

4. Absolute values of ρ: Within the ranges $\theta = 95°$ to $173°$, and $V = 56$ to 145 kv, absolute values of scattering by aluminum are given by, Exp. $= 1.32$ Mott.

The classical relativistic result of Darwin as applied by Crowther and Schonland does not agree with the experimental values reported here, either in absolute magnitude or in its dependence on θ and β.

The difference in absolute magnitude between theory and experiment is the most outstanding discrepancy. The effect of a nuclear magnetic moment has been computed by Massey[18] and was found to be negligible. Also, it appears both from an experimental point of view and from Mott's theoretical investigation that radiative forces cannot account for the difference. The explanation must be looked for elsewhere. It might be expected that since the discrepancy becomes less for lighter elements, some information might be obtained by using hydrogen, helium and beryllium. It is planned to extend this work to the case of gases in the near future.

Comparison with other observers.

The absolute values of ρ for aluminum obtained in this paper are from one-half to two-thirds those obtained by Schonland. The results on silver and gold given here are from 0.7 to 0.8 of his values. It is quite apparent that the difference is mainly due to secondary electrons. A comparison with the work of Chadwick and Mercier can hardly be made since they used much smaller angles and an extrapolation is not permissable at this stage of experimental knowledge.

The writer wishes to take this opportunity to express his appreciation to Professor E. C. Watson who suggested the problem and who has continuously been interested in the work. His sincere thanks are also due Dr. R. A. Millikan for the personal interest he has shown.

[18] H. S. W. Massey, Proc. Roy. Soc. **A127,** 666 (1930).

THE CAPTURE AND LOSS OF ELECTRONS BY HELIUM IONS IN HELIUM

By Philip Rudnick
University of Chicago

(Received August 26, 1931)

Abstract

Mean free paths for capture (L_1) and loss (L_0) of electrons by helium ions in helium have been measured by a method whose chief novelty is the use of an ion source which gives quite strictly homogeneous velocities. In the range of velocities 0.6×10^8 cm/sec. to 1.0×10^8 cm/sec. L_0, reduced to 760 mm, is found to decrease from 21.5×10^{-4} cm to 8.6×10^{-4} cm and L_1 is practically constant at 1.2×10^{-4} cm. These results are compared to similar measurements by other observers, particularly with regard to the manner of dependence on velocity. The relation of the results to available information on ionization and energy loss is discussed.

INVESTIGATION of hydrogen canal rays has shown that there is a definite probability, varying with the velocity of the rays and with the nature of the gas through which they pass, that any proton in the beam may capture an electron[1,2,3,4,5,6] without appreciable loss of velocity.[2] The rapidly moving neutral atom thus formed may again lose an electron. If the beam traverses field-free space an equilibrium is established in which the numbers of charged and uncharged particles are in direct proportion to the probabilities of the changes which produce them. When fast alpha-particles penetrate matter similar interchanges occur between doubly and singly charged states.[7,8,9] At lower velocities the equilibrium shifts; the doubly charged ions disappear and neutral helium atoms appear. The present experiments are in this lower velocity range. They report probabilities for the interchanges between neutral and singly charged helium atoms in helium.

A simple quantitative theory of this phenomenon has been given by Wien[1] and more recently discussed by Rüchardt.[10] If a beam is initially composed of a fraction F_0 of neutral atoms and the remaining portion $(1-F_0)$ of ions, the fraction F of all the atoms which will be neutral at any subsequent point x in the path is given by

[1] W. Wien, Sitz. d. K. P. Akad. d. Wiss., July 1911, p. 773.
[2] J. Koenigsberger u. J. Kutschewski, Ann. d. Physik **37,** 161 (1912).
[3] A. Rüttenauer, Zeits. f. Physik **4,** 267 (1921).
[4] E. Rüchardt, Ann. d. Physik **71,** 377 (1923).
[5] H. Bartels, Ann. d. Physik **6,** 957 (1930).
[6] F. Goldmann, Ann. d. Physik **10,** 460 (1931).
[7] E. Rutherford, Phil. Mag. **47,** 277 (1924).
[8] G. H. Henderson, Proc. Roy. Soc. **A109,** 157 (1925).
[9] J. C. Jacobsen, Phil. Mag. **10,** 401 (1930).
[10] R. Rüchardt, Handbuch der Physik XXIV, p. 90.

$$F = F_\infty + (F_0 - F_\infty)e^{-(1/L_0+1/L_1)x} \tag{1}$$

where dx/L_1 and dx/L_0 are the respective probabilities for capture and loss of an electron by a particle in the distance dx and F_∞ is the equilibrium value approached by F, determined by

$$F_\infty = L_0/(L_0 + L_1) \tag{2}$$

L_1 and L_0 have the interpretation of mean free paths and are inversely proportional to the pressure. If the beam, originally neutral, traverses a path distance x along which a transverse electric field continuously removes all positive ions as they form, before there is time for them to return to the neutral state, the intensity decreases according to a simple absorption law depending only on L_0:

$$I = I_0 e^{-x/L_0}. \tag{3}$$

Preliminary Experiments

Some early experiments were performed with the apparatus shown in Fig. 1, of the type used by Rüchardt and earlier workers. Helium canal rays from a discharge tube were deviated through an angle of about five degrees

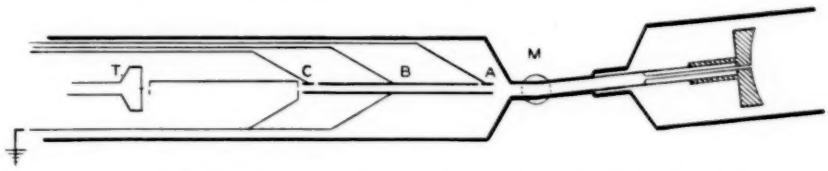

Fig. 1. Preliminary apparatus. M, magnetic field. A, B, C, deflecting condensers. T, thermocouple.

by the magnetic field M, from which ions of relatively homogeneous velocity proceeded to the thermocouple T, passing between the condenser plates A, B, and C. By applying deflecting potentials to these condenser plates one could remove all positive ions existing in the beam at one or both of the points A and C, or continuously over the path ABC. The relative reduction of intensity at the thermocouple was observed when a deflecting field was applied at A only, at C only, at C after A had previously been applied, and finally along B and C after A had previously been applied. Any two of these four measurements could be used to deduce values for the two independent parameters in Eqs. (1) and (3), that is to say F_∞ and $(1/L_0+1/L_1)$, or equivalently L_0 and L_1. This could be accomplished in many different ways varying in precision and convenience; in practice F_∞ and L_0 were most reliably and directly determined. In any event there remained two independent measurements with which to check the validity of the exponential relation (1), without recourse to determination of the variation of L_0 and L_1 with pressure, which is of course another important check.

The results were unsatisfactory in two respects. First, observations were not reproducible from day to day; fluctuations of from ten to fifteen percent in values of F_∞ and L_0 could not be eliminated, though attention was given

to careful electrical control of the discharge and to removal of traces of water and mercury vapors by repeated flaming of the tube. The second difficulty was a consistent indication, in each set of observations, of a departure from the behavior implied in Eq. (1) in the sense that F approached its ultimate value F_∞ more rapidly on the early part of the path, between M and A, Fig. 1, than later, between A and C. In other words, $(1/L_0+1/L_1)$ appeared to decrease along the path.

Since the resolution of velocities employed here was necessarily imperfect because of intensity limitations, it seemed that the remaining inhomogeneity was the most probable cause of the difficulties, and a strictly homogeneous source of ions was accordingly sought. Experiments with such a source are described in the following sections; the results there obtained were satisfactorily reproducible, and not significantly different from averages of the values obtained above. The second question, of deviations from the exponential law (1) is not definitely answered because the new apparatus was not adapted to a direct measurement of $(1/L_0+1/L_1)$.

Final Apparatus

The tube in which final measurements were made employed a source of homogeneous ions similar to that used by Batho and Dempster[11] in a study of the Doeppler effect, with which they obtained very sharp displaced lines, indicating homogeneity in velocity. Fig. 2 shows the arrangement. A low

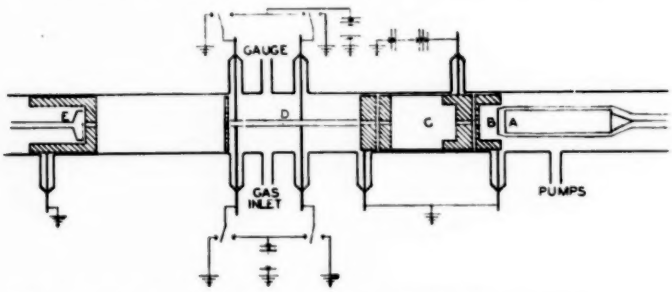

Fig. 2. Diagram of apparatus. A, anode. B, hot cathode. C, accelerating electrode. D, deflecting condensers. E, thermocouple.

voltage arc is operated between the hot cathode B, at ground potential, and the anode A, a hollow cylinder with open ends. Ions thus produced are drawn through the intervening diaphragm into electrode C, which is charged to a high negative potential. Within C many of the ions lose their charge; only these neutral atoms can proceed beyond the retarding field which exists between C and the succeeding grounded diaphragm. Thus a completely neutral beam enters the observation space, in which deflecting condensers D and thermocouple E follow the earlier arrangement except that the condenser A of Fig. 1 is omitted here.

[11] H. F. Batho and A. J. Dempster, to be published shortly in the Astrophysical Journal. Abstract, Phys. Rev. **37**, 100 (1931).

The filament and anode at one end, and the thermocouple at the other, were carried on ground joints, permitting of convenient removal for visual alignment of parts within the tube. The entire path length from filament to thermocouple was 28 cm. The two condensers were 7.5 cm and 1 cm long, their plates about 3 mm apart. These plates were made of nickel gauze in such fashion as to minimize the possibility of specular reflection of ions to the thermocouple. All diaphragm openings were circular, of 2 mm diameter, except the one immediately in front of the filament, which was a half-millimeter larger.

The arrangement of the tube was such that the thermocouple was not exposed to direct radiation from any hot surface, the filament being located off the axis of the tube, and the anode hollow. Those parts which are cross-hatched in Fig. 2 were of solid aluminum of substantial thickness, and probably contributed materially to the adequate protection of the thermocouple from filament radiation. This consideration was important, since in operation the filament end of the tube became decidedly hot to the touch, while the thermocouple was sensitive to temperature changes of the order of 0.001°C. With the arrangement shown, any disturbance caused by the filament was less than that arising from variations in room temperature, and so gradual as to be unnoticed. The shield immediately surrounding the thermocouple protected it in large degree from short period fluctuations in room temperature.

The thermocouple itself was a single junction of a fine platinum wire and an extruded bismuth wire of diameter 0.01 inch. These two were spot-welded to a small piece of platinum foil of area about 1 mm^2 which served as a target for the impinging rays. The two outer ends were joined to the supporting wires with other strips of platinum foil. This couple was connected directly to a galvanometer of resistance 16 ohms and sensitivity 168 megohms.

Helium was purified by two passages through charcoal at liquid air temperature, the second time at low pressure immediately before use. Gas was streamed through the apparatus during all experiments, entering and leaving through liquid air traps. Pressures were measured with a McLeod gauge, also separated from the tube by a liquid air trap.

Storage batteries maintained the hot cathode arc and supplied potentials to the deflecting condensers. A steady accelerating potential was supplied to *C*, Fig. 2, by a high tension transformer with half-wave rectification, and a condenser in parallel. This potential was measured with an electrostatic voltmeter which had been calibrated against a micrometer sphere gap.

Measurements and Results

Determinations of F_∞ and L_0 were made at pressures between 0.007 mm and 0.070 mm of mercury, and with accelerating potentials between 7.5 kv and 21 kv. The lower limit of pressure was set by the decreasing number of ions formed in the arc. L_0 was determined from Eq. (3) by observing the intensity at the thermocouple with all condensers grounded and again with deflecting potentials applied to both the long and short condensers.

$1/L_0$ was proportional to the pressure at all pressures over 0.015 mm within an experimental uncertainty of about ten percent. At the lowest pressures $1/L_0$ appeared to be 30 to 40 percent higher than was to be expected from the linear relation at higher pressures. No definite explanation is offered for this result.The values at the lowest pressures were omitted from the averages, which are given in Table I, column 4, reduced to 760 mm pressure. The long condenser was considered to extend right up to the electrode C, Fig. 2, where the beam contained only neutral particles. Actually it failed to do so by about 15 mm. The error thus introduced is easily computed and was found to be negligible at all except the highest pressures, where the appropriate small corrections were applied to the data.

TABLE I.

1 Accelerating potential in kv	2 Velocity in cm per sec.	3 F_∞	4 L_0	5 L_1	6 $1/L_0$	7 $2/(L_0+L_1)$
21	1.00×10^{8}	0.87	8.6×10^{-4}	1.3×10^{-1}	1160	2000
15	.84	.90	10.5	1.2	950	1700
11	.72	.93	14.0	1.1	710	1300
7.5	.60	.95	21.5	1.1	460	880
5	.49		40		250	

The mean free paths are expressed in centimeters, reduced to 760 mm pressure, but uncorrected for temperature. The kinetic theory mean free path in helium at 760 mm and 300°A is 1.9×10^{-5} cm.

For the arrangement of potentials shown in Fig. 2 the beam approached equilibrium from an initial neutral state, for which $F_0=1$. It was also possible to allow a beam to come to equilibrium from an initial state consisting entirely of ions, for which $F_0=0$, by grounding electrode C and applying a high positive potential to all parts shown to the right of C in Fig. 2. F was measured, both for $F_0=1$ and for $F_0=0$, by observing the intensity at the thermocouple with the condensers grounded, and again with a deflecting potential applied to the short condenser only. The two values of F so obtained agreed within an experimental uncertainty of from one to two percent for pressures above 0.020 mm and were then considered to give the equilibrium value F_∞. At the highest pressures F showed small decreases attributable to the finite length of the short condenser. The following figures are the averages obtained for F_∞ at pressures between 0.020 mm and 0.030 mm: 0.86, 0.89, 0.90, 0.94 for the respective accelerating potentials 21, 15, 11, and 7.5 kv. When L_1 was computed by Eq. (2), taking F_∞ from above and L_0 from Table I, the results were somewhat irregular and too high to explain the differences observed between F and F_∞ at low pressures. It will be noted that very small changes in F_∞ give large variations in the computed value of L_1. It was found that the low pressure observations could be fitted by using the values of F_∞ given in Table I, which are higher than those given above by differences of a few percent, only slightly more than the experimental uncertainty. The figures for L_1 in the table, which follow

from the adjusted values of F_∞, have a relatively large uncertainty, so that the variation with velocity shown in the table is not at all positively established.

The adjustments made in F_∞ are in the same direction as, and less than, the correction for finite length of the short condenser considered by Rüchardt.[10] This correction is applicable when the condenser removes all ions formed between the plates as well as those which enter as ions. This could not be shown to be the case in these experiments. Curves of thermocouple intensity against deflecting potential showed approximate saturation below 500 volts, as was to be expected, but slight dependence of intensity on voltage persisted up to 2000 volts, as far as the observations were carried. Hence it appears that Rüchardt's full correction should not be applied.

The anode voltages in the arc were always less than 100 volts and the occurrence of doubly charged ions in the arc was considered improbable on the basis of experiments such as those of Bleakney.[12] Extrapolation of Rutherford's data for alpha-particles also indicates that doubly charged ions should be few in number at these velocities.

It was found necessary to use a weak magnetic field to protect the thermocouple from secondary electrons which were accelerated away from electrode C when it was negatively charged. Errors from this cause are present in preliminary data already reported.[13]

Observations with Argon

When these same experiments were tried with argon satisfactory intensity was not obtained at any pressure, and none at all above 0.02 mm. This was in marked contrast to helium, where an abundance of ions reached the thermocouple at all pressures up to the arcing point, about 0.2 mm. This suggests much stronger absorption by scattering in argon than in helium. This factor may enter in the results of Kallman and Rosen,[14] who have also observed greater absorption in argon than in helium. These workers ascribe the absorption to neutralization, but reference to a recent paper by Cox[15] will show that scattering is an equally tenable explanation. The absorption mentioned above, however, could not be attributed to neutralization, as neutral atoms and ions affect the thermocouple equally.

Good measurements were not obtained with argon, but the trials roughly indicated values for F_∞ about the same as in helium, and for L_0 one-half to one-fourth of the values for helium.

Discussion of Results

The results in Table I and similar measurements of other observers are plotted logarithmically as a function of velocity in Fig. 3. The free path for capture of an electron varies approximately as v^5 for the alpha-particles

[12] W. Bleakney, Phys. Rev. **36,** 1303 (1930).
[13] P. Rudnick, Phys. Rev. **37,** 1707 (1931), abstract.
[14] H. Kallmann and B. Rosen, Zeits. f. Physik **61,** 61 (1930).
[15] I. W. Cox, Phys. Rev. **34,** 1426 (1929).

(curve A), but shows no certain variation at all with velocity for the slower helium ions studied here (curve E). The measurements of Rüchardt and Goldmann (curves C and C') were made by very different experimental means and should therefore be compared with some caution, but if one accepts the indication that the free path for capture of an electron by a proton in hydrogen has a minimum in the region of 10^8 cm/sec., it is not surprising that the curve for helium should be nearly horizontal in this same region.

The free path for loss of an electron varies approximately as the inverse square of velocity for both hydrogen (curve D) and helium (curve F) at the lower velocities, but increases with velocity for the singly charged alpha-particle (curve B). This contrast probably corresponds at least roughly to the

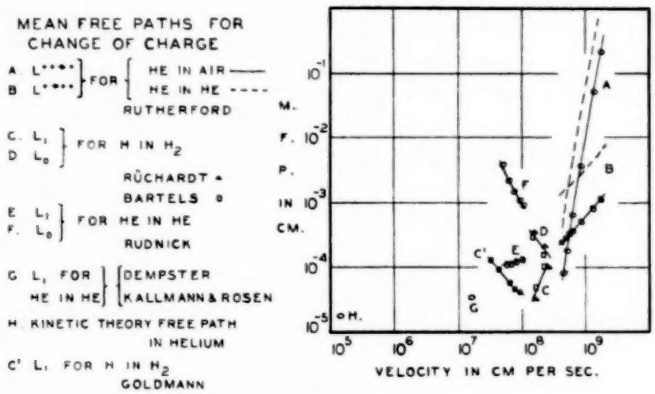

Fig. 3.

occurrence of the maximum of the Bragg ionization curve at intermediate velocities. The broken curve shown for alpha-particles in helium is Rutherford's statement that a few experiments with helium indicated free paths five or six times as great as in air.

Dempster has determined the value 3.5×10^{-5} cm as a mean free path for absorption of 900 volt helium ions in helium.[16] Data for virtually the same experiment given by Kallmann and Rosen[14] permit computation of the free path 3.7×10^{-5} cm for 400 volt ions. An average of these two is plotted in Fig. 3. It will be noted that the point falls below the practically horizontal curve for neutralization of helium ions at higher velocities, as one would expect if the absorption studied at the lower velocities involved scattering as well as neutralization.

If we suppose in these experiments that the fast neutral atoms are in the normal state and hence identical with the molecules of the gas through which they pass, then collisions in which the fast atom ionizes an atom at rest will be just as frequent as collisions in which the fast atom is itself ionized. This means that each particle, in describing its free path as a neutral atom, ionizes only one atom in the gas at rest, although according to kinetic

[16] A. J. Dempster, Phil. Mag. **3**, 115 (1927).

theory about 45 collisions occur over the same path. $1/L_0$ is then the number of ion pairs produced by a neutral atom per centimeter of its path as a neutral. This ionization becomes $1/(L_0+L_1)$ when expressed as the number of ions per centimeter of the path described in both charged and neutral states. If the neutral atoms are not in the normal state[17] they will probably ionize less frequently than they are ionized, and their efficiency of ionization will then be less than $1/L_0$. The increase in $1/L_0$ with velocity, shown in column 6 of Table I, accords with the known increase of ionizing power with velocity for alpha-particles in this range.[18]

From the table the ionizing power of the neutral atom is 1160 ions per cm for the velocity 10^8 cm/sec. In contrast to this, an electron of the same velocity has an energy of only 3 volts and hence no ionizing power whatever in helium. Even at its maximum the ionizing efficiency of electrons,[19] achieved at a velocity of 6 or 8 times 10^8 cm/sec., is only about equal to the value mentioned above for the slower atoms.

For each capture of an electron, a positive ion is formed in the gas; each electron lost also remains in the gas. Accordingly, each particle produces a pair of ions in the distance (L_0+L_1), or $1/(L_0+L_1)$ ion pairs per cm by capture and loss of electrons. Combining this with the ionization by neutral atoms considered above gives $2/(L_0+L_1)$ for the ionization per particle per cm in the composite beam attributable to the neutral atoms and to the alternations of charge. Ionization in excess of this would presumably be produced only by the positive ions. Numerical values are given in column 7 of Table I. The value for $v=10^8$ cm/sec., when multiplied by 24.6, the ionization potential of helium, indicates energy dissipation due to ionization of at least 5×10^4 equivalent volts per cm.

Recent range-velocity data[20] for slow alpha-particles, combined with the value 0.179 for the relative stopping power of helium,[21] show that helium particles of velocity 10^8 cm/sec. lose their energy in helium at a rate of about 1.6×10^5 volts per cm. Thus the minimum ionization $2/(L_0+L_1)$ deduced above represents about one-third of the total energy dissipated by the particles.

The remaining two-thirds of the energy could be spent in either or both of two ways: first, in additional ionization by the positive ions along their short paths, which however, still involve about seven collisions according to kinetic theory, compared to about 45 for the neutral free path; second, in elastic or inelastic collisions not involving ionization. The first of these alternatives is suggested by the conclusion reached by Gurney[22] that alpha-particles in helium expend almost all of their energy in ionization. This result seems clearly established for the average behavior at least below $v=10^9$

[17] M. L. E. Oliphant, Proc. Roy. Soc. **A124,** 228 (1929).
[18] G. H. Henderson, Phil. Mag. **42,** 538 (1921).
[19] P. T. Smith, Phys. Rev. **36,** 1293 (1930).
[20] P. M. S. Blackett and F. C. Champion, Proc. Roy. Soc. **A130,** 380 (1931).
[21] R. W. Gurney, Proc. Roy. Soc. **A107,** 340 (1925).
[22] R. W. Gurney, Proc. Roy. Soc. **A107,** 332 (1925).

cm/sec. A direct estimate of ionizing power at $v = 10^8$ cm/sec. from Henderson's curve[18] and the relative value 1.3 for ionization in helium[22] also supports the first hypothesis, as it indicates roughly the formation of 9000 ions per cm, requiring an energy of 2.2×10^5 volts per cm, more than the total dissipation 1.6×10^5 volts per cm estimated above. It thus appears probable that the helium particles studied here produce ionization several times the minimum estimate $2/(L_0+L_1)$, and that the ionization in excess of this minimum must be attributed to the positive ions. This conclusion has the somewhat surprising corollary that the positive helium ion has an ionizing power in helium about 28 times that of the neutral helium atom at the velocity 10^8 cm/sec.

It is a pleasure to acknowledge the many essential suggestions and constantly helpful advice and criticism which Professor A. J. Dempster has given in the course of this work.

IONIZATION OF CAESIUM VAPOR BY LIGHT*

By F. W. Cooke
University of Illinois

(Received August 12, 1931)

Abstract

The photo-ionization of caesium vapor as a function of the wave-length of the light has been measured at low pressure. The curve has a maximum at the principal series limit, decreases to a minimum at 2800A, and rises again at shorter wave-lengths. The pressure was too low for the ionization by line absorption to be observed. The absolute value of the atomic ionization coefficient at the series limit was found to be 6×10^{-19}, in fair agreement with Mohler's value, which is 2.3×10^{-19}.

The Problem

When the monatomic vapor of an alkali metal is irradiated by monochromatic light of sufficiently high frequency, the atoms may absorb some of the light and thereby become ionized. If the frequency ν of the light is higher than the convergence frequency ν_0 of the principal series of the element, then the ejected electron leaves the atom with a velocity v given by the equation

$$h(\nu - \nu_0) = \tfrac{1}{2}mv^2,$$

where h is Planck's constant, and m is the mass of the electron.

Consider a beam of monochromatic light incident on a given volume of the vapor. Let J_ν be energy flux density in ergs per cm² per sec.; A the cross-section area of vapor column taken normal to the light path; x the length of absorbing column of vapor; and N the number of atoms per cc of the vapor. Then the number of quanta absorbed per sec. is

$$n = \frac{KNAxJ_\nu}{h\nu}$$

and the "atomic absorption coefficient" is $K = n \cdot 1/NAx \cdot h\nu/J_\nu$ quanta absorbed per atom per quantum per cm² of incident energy. If I is the saturation ionization current and e the electron charge, the number of positive ions produced per sec. is I/e, which is the number of quanta absorbed per sec., assuming that the absorption of one quantum produces one positive ion and one electron. Hence the "atomic ionization coefficient" is

$$k = \frac{I}{e} \cdot \frac{1}{NAx} \cdot \frac{h\nu}{J_\nu}$$

positive ions per atom per quantum per cm² of incident energy. It may be determined by the measurement of the ionization current produced by the

* Preliminary note, Phys. Rev. **37**, 1707 (1931).

light. On the basis of the simple assumption above, it is identical with the "atomic absorption coefficient" at the frequency ν. The latter coefficient may be measured by the absorption of the vapor directly.

The "atomic ionization coefficient" as a function of the frequency of the light has been studied in recent years for the metals caesium, rubidium, and potassium. Following the detection of the ionization produced by the absorption of ultraviolet light by caesium vapor by Kunz and Williams,[1] Mohler, Foote and Chenault,[2] Little,[3] Mohler and Boeckner,[4] and Lawrence and Edlefsen[5] have determined the shape of the ionization curve on both sides of the principal series limit of caesium. Little used the "direct" method, while the others used the sensitive method of neutralization of the space-charge surrounding a heated filament. Ionization on the long-wave side of the series limit seems to be a definite fact, with maxima in the curve corresponding to the principal series lines $1s$–$5p$ to $1s$–$9p$. Ionization is a maximum at the series limit. The curves of Little and Mohler have a minimum near 2750A with a rise at shorter wave-lengths to 60 and 40 percent, respectively, of the maximum. The curve of Lawrence is monotone on the short-wave side.

Little[3] made the first absolute measurement of the "atomic ionization coefficient," and found the value 2.2×10^{-21} ions per atom per quantum per cm^2 of incident light at 3130A. Mohler and Boeckner[4] obtained the value 1.85×10^{-19} at 3130A, and 2.3×10^{-19} at the limit 3184A, which is one hundred times larger than the value given by Little. However, Mohler and Boeckner[4] measured directly the percentage change in absorption of the 3130A line of mercury between 100°C and 218°C, from which they deduced that the atomic absorption coefficient is about 3×10^{-19} at 3130A.

Ionization by line absorption has been explained by Mohler and Boeckner,[6] also independently by Freudenberg,[7] on the basis of Franck's suggestion[8] of the formation of a molecule ion by the collision of an excited caesium atom with a normal atom. Other hypotheses that have been proposed are shown to be incapable of explaining the observed ionization.

The work reported here was undertaken with three objects in view: (a) To determine by the "direct" method whether ionization at long wave-lengths is real, as found with the space-charge method; and to study it. (b) To settle the discrepancy between the magnitudes of the atomic ionization coefficient as given by Little and by Mohler and Boeckner. (c) To find whether the ionization curve rises again at short wave-lengths; and if so, the reason.

[1] Kunz and Williams, Phys. Rev. **15,** 550 (1920); **22,** 456 (1923).
[2] Mohler, Foote and Chenault, Phys. Rev. **27,** 37 (1926).
[3] Little, Phys. Rev. **30,** 109 (1927); correction **30,** 963 (1927).
[4] Mohler and Boeckner, Bur. Stand. J. Res. **3,** 303 (1929); **5,** 51 (1930).
[5] Lawrence and Edlefsen, Phys. Rev. **34,** 233 (1929).
[6] Mohler and Boeckner, Bur. Stand. J. Res. **5,** 51 (1930).
[7] Freudenberg, Zeits. f. Physik **67,** 417 (1931).
[8] Gudden, "Lichtelektrische Erscheinungen," p. 226 (1928).

Experimental Procedure

In the direct method there are two serious difficulties not inherent in the space-charge method. In the first place there is a large dark current which may be as great as the ionization current of the vapor, or even greater. This dark current is due to the conductivity of the glass tube, to the conductivity of the alkali metal film on the glass, to the thermal ionization of the vapor, and to thermal emission from caesium surfaces. The ionization tube was constructed in such a way as to keep the two surface conductivities and the thermal emission from caesium surfaces at a minimum. Thermal ionization of the vapor can not be avoided, however, in any case.

In the second place, the photoionization of the vapor can easily be masked by surface photoionization, caused by light striking any surface on which there is an alkali metal film. Direct tests for this were made, and it is believed it did not cause serious error.

The continuous radiation from a water-cooled hydrogen discharge tube, in series with a Hilger E2 spectrograph, was used as a source of light. The beams transmitted were about 20A wide at 3000A. The hydrogen tube was similar to the design of Lawrence and Edlefsen,[9] but with the quartz tube silvered on the inside. The discharge was operated at 4.7 amperes. The intensity was proportional to the current.

The ionization tube was made of Pyrex glass with platinum electrodes and plane quartz windows. In preliminary tests with many Pyrex tubes, the Pyrex glass showed a surprising conductivity at low temperatures, with indications of an electrolytic electromotive force. Ordinary soda glass and fused quartz showed no electromotive force or conductivity up to 200°C, and practically none up to 250°C, while Pyrex showed a large electromotive force and conductivity beginning at about 100°C. A somewhat similar behavior of heated Pyrex glass has been recently reported by Mitchell,[10] who found that treatment with hydroflouric acid was most effective in restoring the low conductivity, and attributed the effect to a surface characteristic of the glass.

On account of this behavior of Pyrex, the collecting electrode connected to the electrometer was insulated from the body of the ionization tube by a section of quartz tubing five cm long. In other respects the arrangement of electrodes and internal and external guard cylinders of platinum was similar to that of Little.

A long side tube extended through the wall of the main furnace and contained the caesium, which was vaporized by a separate furnace, as in the work of Mohler and Boeckner. In order to reduce the surface conductivity due to a caesium film, the experiments were made with a large temperature difference between the ionization tube and the caesium reservoir, at least 100°C at all times. The empty tube became conducting near 220°C, hence the main furnace was kept at a temperature near 180°C. The caesium reservoir

[9] Lawrence and Edlefsen, Rev. Sci. Inst. **1**, 45 (1930).
[10] Mitchell, Phil. Mag. **11**, 748 (1931).

was heated to about 60°C in the experiments. At higher temperatures the dark current became relatively too large.

The ion current was measured by the rate of drift of a quadrant electrometer. A drift of one mm per minute was produced by a current of 2.51×10^{-15} amp. During all the measurements the insulation of the ionization tube was excellent, as indicated by a negligible leak of the electrometer when it was charged sufficiently to produce a large deflection.

The energy of the ionizing light entering the tube was determined by means of a potassium photoelectric cell in quartz, the cell being calibrated throughout the spectrum with a mercury arc and thermopile, the latter being calibrated from a Hefner lamp. The measurements were corrected for absorption and reflection by the quartz windows of the tube.

The cross-section area of the beam of light for each of four wave-lengths was measured at two places near the ends of the collecting electrode and the mean value plotted against wave-length. An area from this curve multiplied by the length of the collecting electrode (9 cm) gave the volume of illuminated vapor for any desired wave-length.

The number of atoms per cubic centimeter of the vapor was calculated from the vapor pressure, which was found from Rowe's equation[11] based on Kroner's data at 250°–350°C:

$$\log_{10} p = 7.1650 - \frac{3966}{T},$$

where p is the pressure in mm of mercury corresponding to the absolute temperature T.

Results

The data for one set of measurements are given in Table I. Another set gave somewhat larger values for the atomic ionization coefficient, with 7.6×10^{-19} at the series limit. The curve in Fig. 1 is drawn for the mean of both sets.

(a) At higher caesium pressures the dark current became excessive, so that the photoionization current, due to the small energy in the beam of light, could not be found with sufficient accuracy. In accord with the work of Mohler and Boeckner only slight ionization was found for wave-lengths greater than the series limit, since the direct method restricts the observations to pressures too low for the effect of line absorption found by others with the more sensitive space-charge method to be detected, even though a continuous source was used.

(b) The mean absolute value at the series limit of the atomic ionization coefficient, 6×10^{-19}, with an uncertainty of the same order of magnitude, agrees fairly well with the determination of Mohler and Boeckner, which is 2.3×10^{-19} at the series limit, and is in complete disagreement with the value of Little, which is 100 times smaller than that of Mohler and Boeckner.

[11] Rowe, Phil. Mag. **3**, 534 (1927).

In Little's experiment, the internal earthed guard ring was very close to the "collecting" electrode, with good opportunity for a caesium film to settle in this region, since no appendix was used as a caesium reservoir. It seems possible in view of the present work, that the surface conductivity in this region resulted in partially earthing the collecting electrode itself. This would be the equivalent of a second shunt resistance on the electrometer,

TABLE I.

Wave-length Å	Caesium Temper-ature °C	I/e ions per sec. $\times 10^4$	N atoms per cc $\times 10^{11}$	A area of beam cm²	$J_\nu/h\nu$ quanta per cm² per sec. $\times 10^{11}$	k ions per atom per quantum per cm² $\times 10^{-19}$	mean k $\times 10^{-19}$
3263	55	3.3	3.45	0.96	2.70	0.42	0.22
	58	zero	—	—	—	zero	
3232	57	10.3	4.12	0.95	2.84	1.06	1.34
	54	13.9	3.19		2.84	1.86	
	58	11.1	4.47		2.84	1.06	
3184	55	28.4	3.45		2.87	3.36	4.92
	55	50.0	3.45		2.87	5.92	
	55	46.0	3.45		2.87	5.46	
3174	55	28.0	3.45		2.94	3.26	3.64
	57	39.6	4.12		2.94	3.84	
	54.5	31.6	3.32	0.95	2.94	3.80	
3154	55	19.8	3.45	0.94	2.97	2.28	2.28
3090	53	21.8	2.97	0.94	3.17	2.76	2.76
3006	53	22.8	2.97	0.93	3.44	2.70	2.46
	56	24.2	3.80	0.93	3.44	2.22	
2900	56	27.6	3.80	0.91	3.65	2.44	2.22
	58	26.6	4.47	0.91	3.65	2.00	
2804	55	23.2	3.45	0.90	3.80	2.18	2.18
2707	55	19.0	3.45	0.89	3.88	1.78	1.78
2597	57	29.6	4.12	0.88	3.80	2.38	2.38
2498	57	37.2	4.12	0.86	3.72	3.14	2.64
	56	23.4	3.80	0.86	3.72	2.14	
2396	58	30.6	4.47	0.85	3.40	2.62	2.62
2302	56	28.6	3.80	0.84	2.93	2.90	2.80
	58	26.8	4.47	0.84	2.93	2.70	
2225	55	17.6	3.45	0.83	2.40	2.94	2.94
	54	16.2	3.19	0.83	2.40	2.94	

and if it were 100 times less than the shunt resistance intentionally used (and measured), then only one percent of the ionization current would be measured by the electrometer.

(c) In the region of continuous absorption there is a rise of the ionization curve at short wave-lengths, in agreement with the results of Mohler and Boeckner, but not in agreement with the curve of Lawrence and Edelfsen. The curve has a minimum at 2800A and rises at 2200A to 60 percent of the maximum at the series limit. The shape of the curve remains an unsettled question, especially so, in the light of the conflicting results of Mohler and Lawrence, who both used the more sensitive space-charge method.

To test this point further, absorption photographs of the caesium vapor were made at various temperatures, with an absorbing vapor column of 14

inches. Twelve or more lines of the principal series were very clearly shown at the higher temperatures. Comparison of microphotometer records of photographs at room temperature and at 265°C lead to an absorption curve

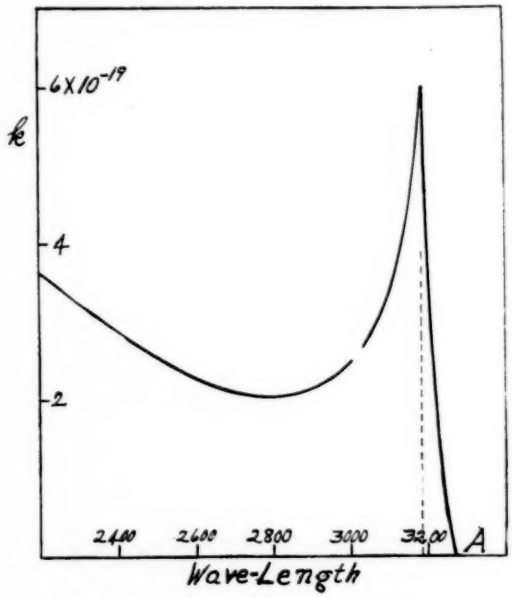

Fig. 1. The atomic ionization coefficient k.

decreasing from the limit and becoming asymptotic to the wave-length axis near 2700A. These experiments should, however, be continued.

ACKNOWLEDGMENTS

This investigation was suggested by Professor J. Kunz and carried out under his direction, and the writer is greatly indebted to him for his continued interest and advice throughout the progress of the investigation. Thanks are due to Professor C. T. Knipp for assistance with the experiments on the conductivity of the Pyrex glass tubes. The writer wishes also to express his thanks to Professor F. W. Loomis, Head of the Department of Physics, for valuable suggestions and for his interest in the work, and to Professor Loomis and Professor A. P. Carman for providing the equipment and for the use of the facilities of the laboratory.

SOME ELECTRICAL PROPERTIES OF SPECTROSCOPICALLY PURE ZINC CRYSTALS

By A. G. Hoyem
Physical Laboratory, State University of Iowa

(Received August 11, 1931

Abstract

With single crystal specimens of *spectroscopically pure* zinc (99.9999 percent zinc), the Thomson coefficient at 49.5°C has been measured as a function of orientation. A very accurate confirmation of the Voigt-Thomson symmetry relation is obtained, the principal values of the Thomson coefficient being: $\sigma_\perp = 0.86 \times 10^{-6}$ cal./coul./deg., and $\sigma_\parallel = 0.34 \times 10^{-6}$ cal./coul./deg. The thermal e.m.f. of these same specimens against copper has been determined as a function of orientation throughout the temperature range −180° to 200°C. From these data, the values of the Peltier coefficient, the Thomson coefficient, and the difference in principal Thomson coefficients have been computed as functions of temperature by means of the relations given by the Kelvin thermodynamical theory of thermoelectricity. The values of the Peltier coefficient of $Zn_\perp$ against $Zn_\parallel$ thus obtained are: $\pi = 658$ microvolts at 49.5°C and $\pi = 1080$ micro-volts at 125°C. For the difference in the principal Thomson coefficients, the values are: $\sigma_\perp - \sigma_\parallel = 0.58 \times 10^{-6}$ cal./coul./deg. at 49.5°C and $\sigma_\perp - \sigma_\parallel = 1.20 \times 10^{-6}$ cal./coul./deg. at 125°C. The predictions of the Kelvin theory regarding $\sigma_\perp - \sigma_\parallel$ are thus found to be in agreement with the direct determinations by Ware and the writer. The Voigt-Thomson law is found to hold also in the case of thermoelectric power and the other thermoelectric properties to which it should apply. The dependence of resistivity on temperature has been investigated for the temperature range −170° to 25°C. The average value of the temperature coefficient of resistivity obtained is: $\alpha = 4.058 \times 10^{-3}$. For comparison purposes, a direct determination of the Thomson coefficients of single cyrstal specimens of *Kahlbaum's best* zinc at 49.5°C has also been made, as well as a study of the dependence of their resistivities on temperature. For this less pure zinc, the principal values of the Thomson coefficient are: $\sigma_\perp = 0.91 \times 10^{-6}$ cal./coul./deg. and $\sigma_\parallel = 0.38 \times 10^{-6}$ cal./coul./deg. For the temperature coefficient of resistivity, the average value is: $\alpha = 4.009 \times 10^{-3}$. A variation in the values of α for specimens of the same grade of zinc is observed which is considerably greater than can be attributed to experimental error.

Introduction

THAT the presence of even slight amounts of impurity may have a very pronounced influence on some of the properties of metals is well known. Consequently, in trying to ascertain the properties truly characteristic of a metallic element, it is obviously of great importance that the specimens studied be as free from foreign substances as possible. If at the same time simplicity and uniformity characterize the spatial arrangement of the atoms throughout the specimen, such as is the case in single crystals, it is evident that the characteristics obtained ought to be even more closely associated with the true properties of the element itself. Several investigations dealing with the electrical properties of zinc single crystals have been reported, none, however, for zinc of exceedingly high purity. Linder,[1] Bridgman,[2] and

[1] E. G. Linder, Phys. Rev. **26**, 486 (1925), **29**, 554 (1927).

[2] P. W. Bridgman, Nat. Acad. Sci. Proc. **11**, 608 (1925); Proc. Amer. Acad. Sci. **61**, 101 (1926).

Grüneisen and Goens[3] have measured the thermal e.m.f. of zinc against copper, and from the thermoelectric power thus obtained have computed by means of the customary thermodynamical relations the Peltier coefficients of the zinc crystals (against copper) and the difference in the Thomson coefficients of the two principal orientations as functions of temperature. Specific resistance and the temperature coefficient of resistivity have been measured by Grüneisen and Goens,[4] Bridgman,[2] and Ware.[5] Direct determinations of the Thomson coefficient have been made by Ware[5] and by Veleger.[6] None of these investigators give the exact analysis of the zinc used except to state that it was Kahlbaum's, Kahlbaum's best, or Merck's brand of zinc. Hence it is reasonable to assume that the specimens varied considerably in purity and that all contained not less than 0.01 percent impurity, the percentage of impurity usually present in chemically pure zinc. The zinc used in the present investigation was obtained through the courtesy of the New Jersey Zinc Company and is known as *spectroscopically pure* zinc. Its analysis is given as 99.9999 percent pure.[7] On single crystal specimens made from this S. P. zinc, a direct determination was made of the Thomson coefficient, together with measurements of thermal e.m.f. against copper, of specific resistance,[8] and of the temperature coefficient of resistivity. From the thermal e.m.f. data, the Peltier coefficient against copper and the difference in the principal Thomson coefficients, $(\sigma_\perp - \sigma_\parallel)$, were computed as functions of temperature. Thus, in view of the fact that the thermal e.m.f. and the Thomson coefficient measurements were obtained for the same crystal specimens, it is possible to make a better comparison between the predictions of thermodynamical theory and the results of direct measurement than would have been possible in using only the results of previous investigators for comparison purposes. In addition, in order that the comparison between the results for the S. P. zinc and less pure grades of zinc might be more trustworthy, the Thomson coefficient, specific resistance,[8] and temperature coefficient of resistivity were also determined for a set of single crystal specimens made from Kahlbaum's best zinc.

Apparatus and Experimental Procedure

1. Production of the single crystals

The Czochralski-Gomperz method, described in considerable detail in a recent paper by the writer and E.P.T. Tyndall,[9] was used with a few slight modifications in growing the single crystal specimens. Due to the fact that the quantity of zinc available was comparatively small, approximately 250

[3] E. Grüneisen and E. Goens, Zeits. f. Physik **37** 278, (1926).

[4] E. Grüneisen and E. Goens, Zeits. f. Physik **26,** 250 (1924).

[5] L. A. Ware, Phys. Rev. **35,** 989 (1930).

[6] H. Veleger, Ann. d. Physik **9,** 366 (1931).

[7] The writer is very grateful to the New Jersey Zinc Company for providing him with a quantity of this exceedingly pure material. For a description of its properties and the method of production, see H. M. Cyr, Tran. Amer. Electrochem. Soc. **52,** 349 (1927).

[8] E. P. T. Tyndall and A. G. Hoyem, Phys. Rev. **37,** 101 (1931).

[9] A. G. Hoyem and E. P. T. Tyndall, Phys. Rev. **33,** 81 (1929).

grams, and the fact that the greater the purity of the metal the more readily it oxidizes when it is in the molten state, it was very necessary to minimize the two chief sources of waste, namely, loss of specimens due to imperfections caused by occasional unsteadiness of the crystal growing apparatus, and loss of material due to oxidation. To overcome the former difficulty, a new drawing mechanism was constructed, the square brass rod and the slides used in the former apparatus being replaced by a hexagonal brass rod which was guided by two sets of three ball-bearings. Oxidation was eliminated by having the entire growth process take place inside of a Pyrex glass tube, 5 cm in diameter and 25 cm tall, which contained a mixture of hydrogen and nitrogen. In order to avoid the possiblities of contamination, the crucible, as well as the tools used for handling the zinc, were also made of Pyrex.

The crystals were all grown in the "region of successful growth" designated in the earlier paper.[9,10] These S. P. crystals are extremely ductile and as a consequence are very difficult to handle without bending. Though the near zero degree orientations are the most brittle, they are not nearly as much so as the corresponding orientations of crystals made from Kahlbaum or other grades of zinc. Twenty-six crystals in all were grown ranging from fifteen to twenty centimeters in length and having a mean diameter of from two to three millimeters. Prior to the growing of these crystals, numerous K zinc crystals were grown under practically the same conditions with the double purpose of establishing the technique of crystal growth in the new apparatus and to provide material for the comparison between the S. P. zinc and a grade of zinc more nearly like that used by previous investigators.

2. The Thomson coefficient

The Thomson coefficient was measured by means of the Nettleton[11] method described by Ware[5] with further slight modifications.[12] In brief, the essential features of the method are as follows: The two ends of a single crystal specimen of zinc are maintained at different, but constant, temperatures. The Thomson effect, which is positive for zinc, will then cause an e.m.f. to be set up within the crystal, directed from the colder to the hotter portion. If an electric current is now set up in the crystal so that it flows down the temperature gradient, there will be a generation of heat in the crystal, a portion of which will be caused by the resistance of the crystal, the remainder being caused by the fact that the current is flowing in opposition to the Thomson

[10] Some recent work by Mr. H. K. Schilling performed in this laboratory seems to indicate that this region is successful growth may be considerably extended provided exceeding care be taken to minimize vibration and temperature fluctuation during the growth process. This raises the question as to whether the apparatus and procedure described here were not sufficiently improved over the first set-up so that crystals might also have been grown outside of the "region of successful growth." The only positive evidence of this is that attempts to grow Kahlbaum crystals of nearly 0° orientation at too high or at too low temperatures were definite failures. Aside from this the growth of crystals was purposely confined to what was believed to be the only suitable conditions.

[11] H. R. Nettleton, Proc. Phys. Soc. Lond. **34,** 77 (1921) ; **29,** 59 (1916).

[12] For diagrams of the apparatus and the electrical circuits involved see the article by Ware, Figs. 1, 2, and 3.

e.m.f. If the same current through the specimen is reversed, the Joulean heat will be of the same magnitude as before, but the Thomson effect will now produce an absorption of heat, hence the temperature of the specimen will be different in the two cases. On reversal, however, the current may be automatically increased to such a value that the temperature of the specimen remains constant. When such a state is reached that the temperature of the specimen does not change when the current is reversed, it has been shown by Nettleton[11] that if certain conditions are met, the Thomson coefficient, σ, will be equal to i_0R/JU calories per coulomb per degree, where i_0 is the above mentioned difference in currents corresponding to no temperature change, R is the resistance of the crystal, J is the mechanical equivalent of heat in joules per calorie, and U is the difference in temperature between the two ends. The two end temperatures used were 99° and 0°, respectively.

The accuracy with which the balancing current, i_0, can be determined hinges essentially on the sensitivity of the device used in detecting temperature changes in the crystal and on the constancy of the end temperatures. In order to increase this accuracy, the following modifications in Ware's procedure were made: The length of the bolometer coils was approximately doubled and better heat insulation provided in the entire bolometer-bridge circuit. The capacity of both the hot and cold reservoirs was increased so as to make it possible to maintain the temperatures at the ends of the crystal very constant throughout longer periods. The constancy of the hot end was further increased by heating the water by means of a different coil than the one which was used in mounting the crystal. This auxiliary coil was wound on the surface of the boiler as far removed from the end of the specimen as possible thus greatly diminishing the variations in temperature caused by occasional fluctuations in the heating current. With these modifications, the uncertainty in the determination of the balancing current, i_0, for most of the crystals was reduced to less than two percent. Two thermocouples, permanently imbedded in the reservoir blocks adjacent to the block-crystal junctions, served in determining the temperatures at the ends of the crystal.

3. Thermal e.m.f.

The thermal e.m.f. of zinc against copper was measured immediately following the determination of the Thomson coefficient of each crystal specimen, that is, while the specimen was still in the Thomson apparatus. A diagram of the circuit is shown in Fig. 1. Determination of the temperature at the ends of the crystal was made by connecting the potentiometer across terminals 1 and 4, and 2 and 3, respectively. These constantan-copper thermocouples are the two couples referred to in the preceding section. Readings across terminals 1 and 3 gave the thermal e.m.f. of the crystal against copper. In obtaning the various temperature differences, the cold end of the Thomson apparatus was maintained at 0°C, while the hot end served as the variable junction. The necessary low temperatures were secured by draining the boiler chamber and then introducing various quantities of liquid air directly into the chamber, the depth of the temperature obtained at the junction naturally depending

on the amount of liquid air introduced and on the extent of the heat insulation. To obtain the high temperatures, use was made of the heating element

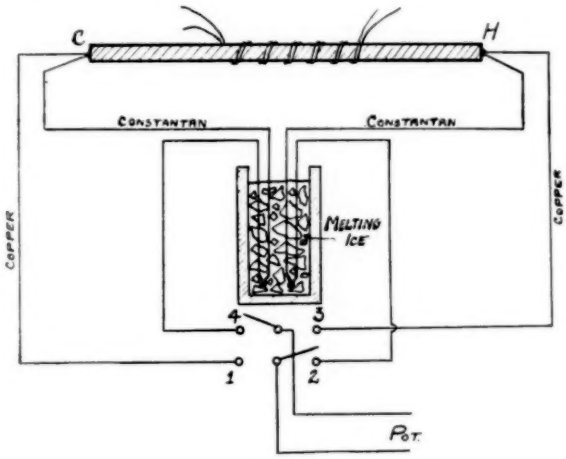

Fig. 1. The thermal e.m.f. circuit.

located in the boiler near the end of the crystal, currents ranging from 0.5 to 1.5 amperes being used. At both the high and the low temperatures, the fluc-

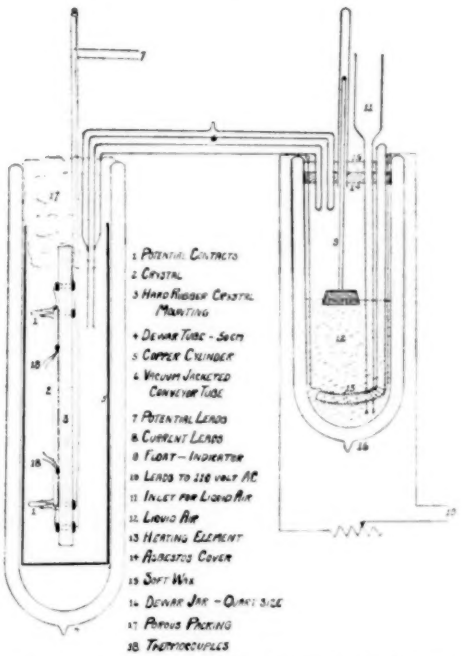

Fig. 2. Cross-sectional view of apparatus used in determining the resistance of the specimens at temperatures ranging from 25° to −170°C.

tuation encountered while the readings of temperature and the thermal e.m.f. were being taken and checked was usually less than half a degree.

4. Temperature coefficient of resistivity

The apparatus used in the determination of the temperature coefficient of resistivity is shown in Fig. 2. It employs the method for the production of low temperatures described by Cioffi and Taylor[13], namely, the evaporation of liquid air by the use of a heating element and the subjection of the specimens under investigation to the stream of cold dry air thus produced, the degree of cold depending on the rate of evaporation and on the insulation used in the transfer of the cold air. In this apparatus cold dry air, obtained by the forced evaporation of the liquid air in the small Dewar container, was transferred by means of the vacuum-jacketed tube into the large Dewar container, the entire apparatus being entirely enclosed in heat insulating material. Two crystal specimens were investigated simultaneously, being placed in parallel grooves on the hard rubber mounting. Chisel-shaped pieces of zinc, held in contact with the specimens by means of springs, served in obtaining the potential drop across any desired portions. These contacts were devised so as to eliminate the possibility of effects which might be due to contamination by soldered connections or due to irregularities in the crystal structure caused by cutting. The current leads were attached to the ends of the specimens. To insure greater constancy and uniformity of temperature throughout the region containing the specimens, the specimens and the mounting were placed inside of a copper cylinder fitting closely in the large Dewar container. Two thermocouples placed about ten centimeters apart between the two specimens furnished the means of determining the exact temperature as well as to show the absence of any appreciable vertical temperature gradient. The temperature coefficient was computed by using the relationship:

$$\alpha = \frac{1 - p}{t_2 p - t_1}$$

where p is the ratio of R_1 to R_2, R_1 and R_2 being the resistances of the specimen at the temperatures t_1 and t_2, respectively. The resistance measurements were made by the usual potentiometer method, the current used in the crystals being 0.5 ampere.

This low temperature apparatus proved very satisfactory particularly in regard to the constancy with which the temperature could be maintained and the fact that a temperature as low as $-170°$C could be obtained without excessive consumption of liquid air. At this temperature the consumption was approximately three liters per hour, but less, of course, at higher temperatures.

Results

1. Thomson coefficient

The experimental results obtained in the direct determination of the Thomson coefficient are represented graphically in Fig. 3. The values obtained for the S.P. crystals are represented by circles, the values for the K crystals being denoted by dots. Both sets of data are for a mean temperature of 49.5°C.

[13] P. P. Cioffi and L. S. Taylor, Opt. Soc. Amer. J. **6**, 906 (1922).

In agreement with Ware's findings, both sets of data indicate that the Voigt-Thomson symmetry relationship for the Thomson coefficient holds at this temperature, the linearity being particularly definite in the case of the S.P. zinc. It is only fair to state that the greater regularity in the results for the S.P. zinc is largely due to the greater care taken in this case and that with the possible exception of the two points for the K zinc at $\cos^2\theta=0$ and at $\cos^2\theta=0.74$, the deviations are no larger than the probable experimental error.

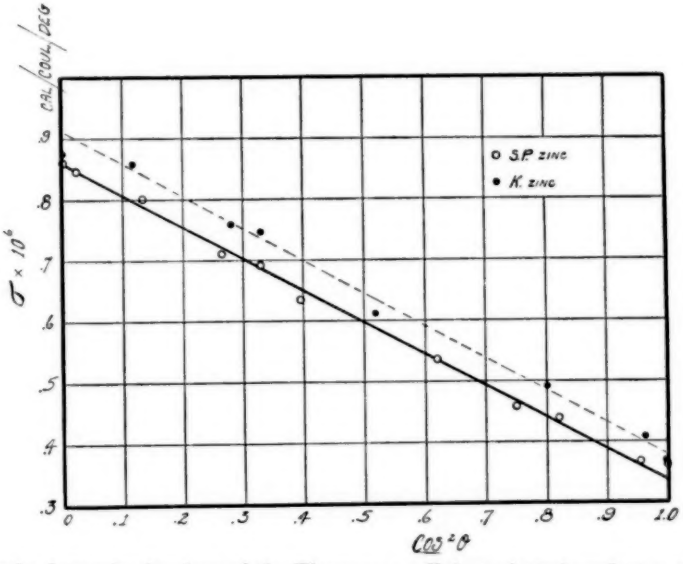

Fig. 3. Directly determined values of the Thomson coefficient plotted against $\cos^2\theta$. The S.P. values are represented by ○————○, and the K zinc values by ●- - - - -●.

The values for $\sigma_\perp$ and $\sigma_\parallel$ for the S.P. zinc, expressed in micro-calories per coulomb per degree, are 0.86 and 0.34, respectively, while for the K zinc the values are 0.91 and 0.38, respectively, in fairly good agreement with Ware's values of 0.98 and 0.38 respectively, for the same grade of zinc. Comparing the results for the S.P. crystals with the writer's K crystals it is evident that the effect of impurity is to cause a practically constant increase in the Thomson coefficient for all orientations, the ratio, $\sigma_\perp/\sigma_\parallel$, and the difference, $\sigma_\perp-\sigma_\parallel$, being almost identical for the two sets of crystals. The effect of impurity on specific resistance is apparently of the same type.[8]

2. Thermal e.m.f.

The observed values of the thermal e.m.f. of zinc against copper are represented graphically in Fig. 4, the e.m.f. being considered positive when it is directed from the hot to the cold junction through the zinc. The four different notations used in plotting these values were used merely for the sake of clarity to aid in associating the various points with the curves to which they belong. The numbers alongside the curves indicate the crystal orientations. Representing these curves by empirical equations of the form: $E=at^3+bt^2+ct$,

where a, b, and c are constants which are characteristic of the individual curves, and differentiating these equations with respect to t, equations giving the value of the thermoelectric power, $e(=dE/dt)$, are obtained. Fig. 5 shows the values of the thermoelectric power, obtained in this manner, plotted against the square of the cosine of the angle of orientation. The ordinate

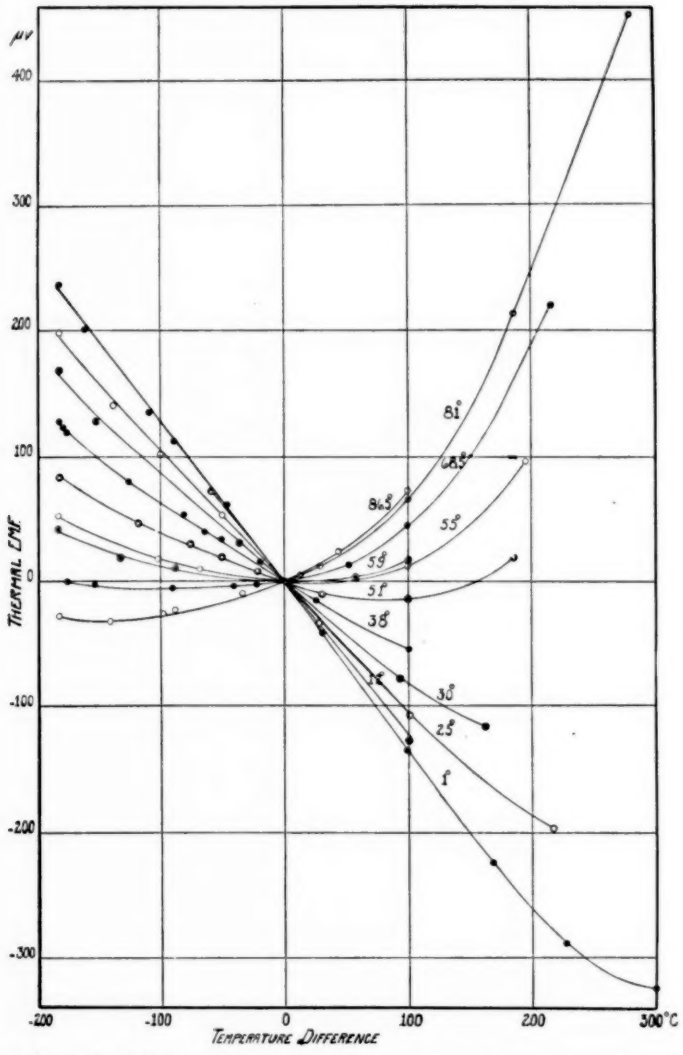

Fig. 4. Thermal e.m.f. of S.P. zinc against copper represented as a function of temperature difference. The crystal orientations are indicated on the curves.

scale indicated applies to the curve for the temperature of $-180°$. To avoid confusion, the origin for the values corresponding to a temperature of $-150°$ is shifted upward one whole unit, the origin for those corresponding to $-100°$ being shifted upward two whole units, etc. That the Voigt-Thomson symmetry relation holds for this zinc throughout the range of temperature investigated seems quite evident. The slight scattering of points for the tempera-

ture of 180° is believed to be due to the fact that the probable error in the determination of e is greatest here, since this region is for some of the crystals very near the upper limit for the thermal e.m.f. measurements and is also a region for which e changes quite rapidly.

The thermoelectric properties of single crystals may be obtained without reference to any other metal by expressing the characteristic values for the one principal orientation ($\theta = 90°$), against those for the other principal orientation ($\theta = 0°$). These values for thermal e.m.f. were obtained by using

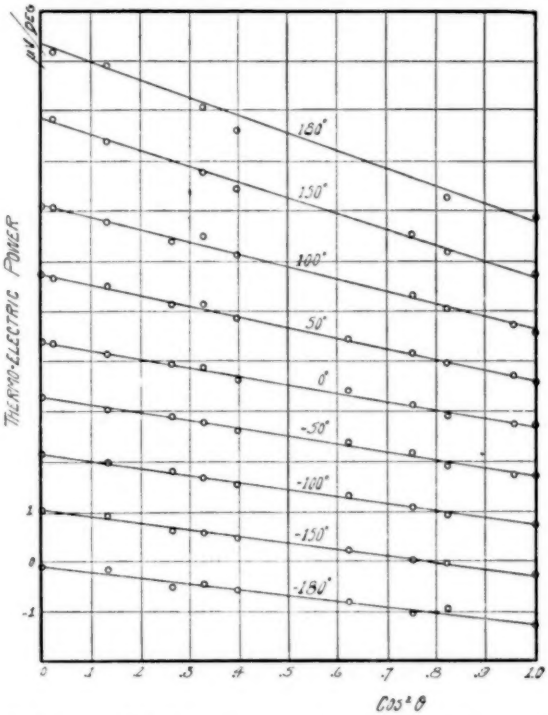

Fig. 5. Thermoelectric power at various temperatures represented as a function of $\cos^2\theta$.

the empirical equations for E and plotting values of E against $\cos^2\theta$ in the same manner as e is represented in Fig. 5. Definite straight line relations were obtained from which the values of $E_\perp$ and $E_\parallel$ were observed and their difference plotted against the corresponding temperature. The results are represented in Fig. 6 by the circles and the solid, heavy curve. The results obtained by Linder[1] and by Grüneisen and Goens[3] are also shown, being represented by the double circles and the dots, respectively. In order to make this comparison, the writer's results had to be reduced by the use of the law of intermediate temperatures, whereby

$$E(t, -253°) = E(0°, -253°) + E(t, 0°).$$

The value of $E(0°, -253°) = 483.6\mu v$, taken from the work of Grüneisen and Goens, was used in carrying out the reduction. It is to be noted that the writer's results are in closest agreement with those of Grüneisen and Goens.

By noting the values of $e_\perp$ and $e_\parallel$, in Fig. 5, and plotting their difference against temperature, the variation of thermoelectric power for $Zn_\perp$ against $Zn_\parallel$ is obtained. This is represented in Fig. 7.

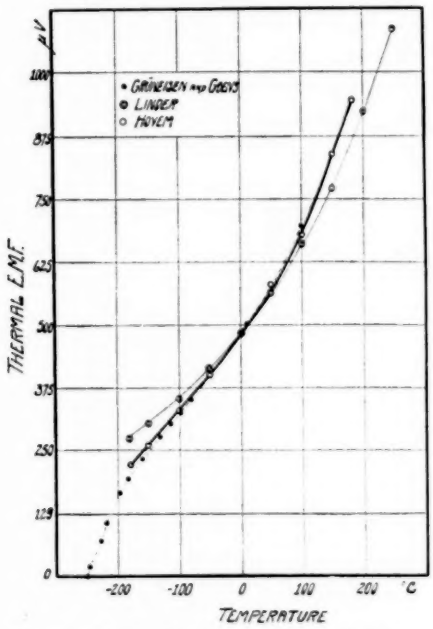

Fig. 6. Thermal e.m.f. of $Zn_\perp$ against $Zn_\parallel$.

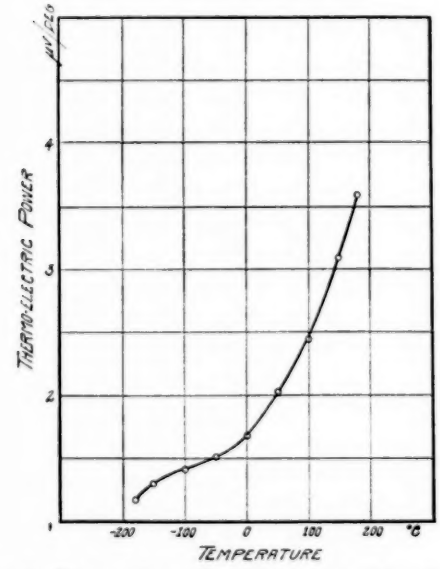

Fig. 7. Thermoelectric power of $Zn_\perp$ against $Zn_\parallel$.

The Peltier coefficient, π, for $Zn_\perp$ against $Zn_\parallel$ and the difference in the principal Thomson coefficients, $\sigma_\perp - \sigma_\parallel$, are, according to the Kelvin thermodynamical theory, given by Te and $T(de/dt)$, respectively, where T is the

absolute temperature and e is the thermoelectric power for $Zn_{\perp}$ against $Zn_{\parallel}$. The Peltier coefficient, π, obtained in this manner, is represented in Fig. 8 as a function of temperature. Similar results obtained by Linder[1] and by

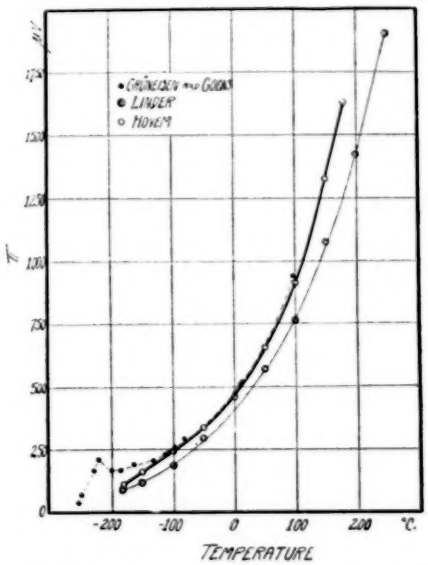

Fig. 8. The Peltier coefficient of $Zn_{\perp}$ against $Zn_{\parallel}$.

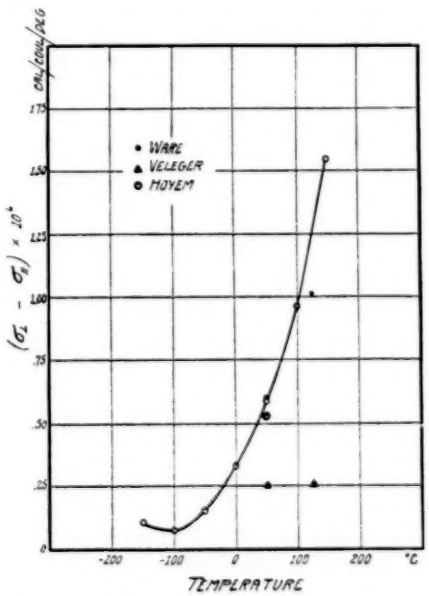

Fig. 9. The difference in the principal Thomson coefficients represented as a function of temperature.

Grüneisen and Goens[3] have been included on the graph for comparison. The values obtained by the writer throughout the greater part of the range are seen to be in very close agreement with those obtained by Grüneisen and

Goens. The writer's measurements did not extend below the temperature of liquid air, consequently all that can be said about the slight maximum in the Peltier coefficient at low temperatures obtained by these earlier investigators is that there is no definite indication of such an increase in the present results.

In Fig. 9 the difference in the principal Thomson coefficients,[14] $\sigma_\perp - \sigma_\parallel = (T/J)(de/dt)$, is represented also as a function of temperature. The value of de/dt used in the above computations was obtained by differentiation of a series of second degree equations which represented overlapping sections of the thermoelectric power versus temperature curve shown in Fig. 7. These equations were of the form: $e = at^2 + bt + c$, where a, b, and c were constants characteristic of the various sections of the curve. This method for determing de/dt was chosen primarily because of its simplicity and because of its superiority to the graphical method of measuring the slopes of tangents drawn to the curve. The graph indicates that for temperatures above -100°C there should be a very definite increase in the difference in Thomson coefficients with temperature. On this graph are also indicated the values of $\sigma_\perp - \sigma_\parallel$ taken from the direct determinations of Ware,[5] Veleger,[6] and the writer. The writer's values for the S.P. zinc and for the K zinc are represented by the one double circle at $t = 49$°C, the two values being practically identical. The results of Ware and Veleger are represented by dots and by triangles, respectively. Very good agreement is seen to exist between the predictions of the thermodynamical theory, as exemplified by the curve in the figure, and the directly determined results of Ware and the writer. Veleger's results, on the other hand, show considerable disagreement both as to magnitude and as to variation with temperature. In view of the fact that all other "indirectly determined" values of the difference in the principal Thomson coefficients, such as those by Linder,[1] Bridgman,[2] and Grüneisen and Goens,[3] are in much better agreement with the writer's results than with those of Veleger, it seems very improbable that the discrepancy in the latter's results can denote any failure on the part of the thermodynamical theory.[15] It should be borne in mind here that the writer's "indirectly determined" values, given by the curve in the figure, were obtained from the same set of S.P. specimens as were used in the direct determination for the S.P. zinc.

It is possible also to obtain from the thermal e.m.f. curves (Fig. 4) the Thomson coefficient of any specimen as a function of temperature, the procedure being as follows: Differentiating the empirical equations for E twice with respect to t and multiplying by the absolute temperature, T, one obtains $T(d^2E/dt^2) = \sigma_{ZN} - \sigma_{CU}$. By adding the Thomson coefficient of copper at the given temperature, the coefficient for the zinc specimen results. This has been done for crystals representing the extreme orientations, using a 1° crystal to get $\sigma_\parallel$ and two crystals, 81° and 86.5°, for $\sigma_\perp$. The 81° crystal was used since the thermal e.m.f. curve for the highest orientation (86.5°) did not extend above 100°C. From 0° to 100°C the range common to both, the crystals yield

[14] Expressed in calories per coulomb per degree, the units previously used for the Thomson coefficient.

[15] See for instance Table 6 in Veleger's article.

practically identical values. The results of this computation are shown in Fig. 10. The values of the Thomson coefficient for copper at various temperatures were taken from the work of Berg[16] and Borelius and Gunneson,[17] a mean value being adopted. Since the writer, of course, used a different specimen of copper, the results shown in Fig. 10 cannot be expected to represent absolute values. The variation with temperature, to obtain which the computations were especially made, is considered somewhat more reliable. In this connection it is to be noted that this variation of σ with temperature is very different from that recently obtained by Veleger, but in good agreement with Ware's results, as may be seen in the figure.

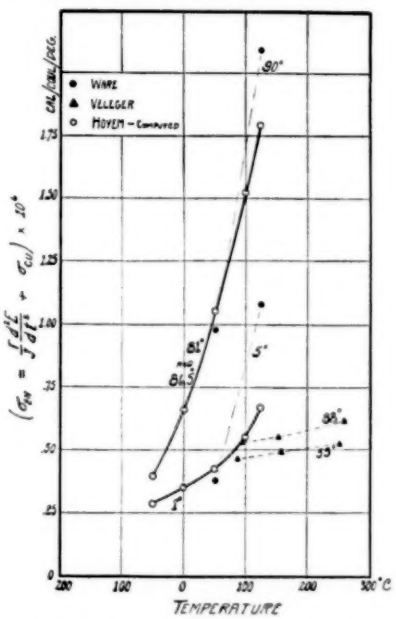

Fig. 10. The Thomson coefficients of the specimens having orientations 86.5°, 81°, and 1°, represented as functions of temperature. Veleger's directly determined values are indicated by ▲------ ▲-, Ware's by ●-------●.

If in Fig. 10 the difference in the ordinates of the two curves corresponding to a given temperature be noted, the difference should obviously be very nearly equal to $\sigma_\perp - \sigma_\parallel$. Values so obtained are found to be in very good agreement with the $\sigma_\perp - \sigma_\parallel$ values given in Fig. 9. It should be mentioned here that while the first method of computing $\sigma_\perp - \sigma_\parallel$ makes use only of first derivatives of empirical equations, the second uses second derivatives. The agreement between the two methods thus serves as a double check on the reduction of the results. It need hardly be said that the values obtained by the first method are more reliable, depending as they do on data for all the crystals, whereas data for only two crystals are used in the second method. The second method can obviously be extended to include all the crystals, but it is not considered worthwhile to do so.

[16] O. Berg, Ann. d. Physik **32**, 477 (1910).

[17] G. Borelius and F. Gunneson, Ann. d. Physik **65**, 520 (1921).

3. Temperature coefficient of resistivity

The observed values of the temperature coefficient of resistivity are listed in Table I. These results were obtained by plotting the resistance of the

TABLE I.

S.P. crystals		K crystals	
θ	α	θ	α
1	4.043×10^{-3}	26.5	3.994×10^{-3}
12	4.086	34	3.960
16	4.039	40	3.986
22.5	4.019	44	4.019
25	4.049	66	3.963
28.5	4.059	90	4.069
30	4.042	90	4.069
33	4.043		
37	4.064		
39	4.046		
42	4.051		
44	4.004		
52	4.072		
53	4.049		
55	4.051		
59	4.067		
61.5	4.080		
65	4.055		
68.5	4.071		
71	4.058		
81	4.086		
81	4.096		
86.5	4.081		
Average value	4.058×10^{-3}		4.009×10^{-3}

various specimens against temperature on millimeter cross-section paper, the dimensions of the graph being approximately one by one and a half meters. On this immense scale nine-tenths of the points fall within one millimeter of the lines as drawn, the remaining points having deviations which would lead to errors in α not to exceed three-tenths of one percent. Hence the relationship between resistance and temperature throughout the entire ranged used, ($-170°$ to 25°C), is considered to be accurately linear. With this degree of accuracy it is evident that the difference in the values of α for the individual crystals must be thought of as real. The distinct difference which exists between the average value of α for the K specimens and the average value for the S.P. specimens, α in general being higher for the S.P. group, is in accord with what would be expected in view of the higher purity of the S.P. zinc. It might be argued that the variation of α within a group (such as the S.P.) should also be used as an indication of difference in purity, with the idea that either contamination occurred during the growth of the crystals or that some purifying process took place, the residue of zinc in the crucible getting more impure with time. In either case there should be a correlation between the order of growing a crystal and its value of α. No such correlation exists. Moreover it may be pointed out that if α is taken as an indicator of relative purity within a group, there should be a corresponding well-marked effect in the specific resistance. This, however, is not true. In spite of the over-lapping of

the α-values in the two groups, S.P. and K crystals, the resistivities of the S.P. crystals are almost without exception lower than those of the K crystals, comparing, of course, corresponding orientations. It may be further remarked that other properties, such as the Thomson effect, the unusual mechanical properties of the very pure zinc crystals, etc., should also give some clue to any possible purity difference of individual crystals in the same group. No such effects are found. Hence the difference in α amongst crystals made from the same grade of zinc must be attributed to some other factor than purity. There is an indication that α may increase with orientation, but the presence of several anomalous cases, high values for low orientations and vice versa, makes it difficult to consider α as purely a function of orientation. This variation of α amongst specimens made from the same grade of zinc is therefore a rather open question.

Ware in his determination obtained an average value of 0.00425 for the temperature coefficient in the temperature range, 20° to 110°C. In this connection, the writer wishes to point out that prior to the measurements of the temperature coefficient of resistivity just mentioned, an oil bath arrangement similar to that described by Ware was employed using a temperature range, 20° to 110°C. The average value of α obtained with that apparatus for K specimens was in very close agreement with Ware's results. It was, however, observed that with the writer's set-up, the resistance-temperature relationship was not linear in all cases, the departure from linearity being greater the longer the specimens had been immersed in the oil bath and always of such a type as to make the curves concave upward. This apparent increase in the resistance of the specimens, when the readings are taken starting with low temperatures, tends to give α a high value. An investigation proved that the zinc was being dissolved in the oil, the increased resistance of the specimens being exactly accounted for by the loss in weight. The effect was first noted with the same grade of oil that was used by Ware and the dissolution was more pronounced the longer the oil had been in use. At this time the oil was heated in a tin container with the heating element and its asbestos board form directly immersed in the oil. Removing the heating element from contact with the oil, using a Pyrex container, and a different grade of oil did not eliminate the effect. Since there is no indication of any departure from linearity in the upper range of the low temperature determinations and in view of the effect of the oil bath, it seems very unlikely that there is any departure of the resistance-temperature curves from linearity in the temperature range 20° to 100°C. Hence only the values obtained from the low temperature determinations have been listed in the table and in all probability these will apply to the higher temperature range as well.

The writer wishes to express his sincere thanks to the members of the staff of the Physics department of the State University of Iowa for their assistance and suggestions throughout the course of this investigation. The writer wishes in particular to express his appreciation to Dr. E. P. T. Tyndall for suggesting and directing this problem and for the encouragement and the many helpful criticisms he has so generously given.

THE INTERNAL MOLECULAR POTENTIAL BETWEEN THE SUBSTITUENT GROUPS IN A BENZENE RING AS DERIVED FROM THE HEATS OF COMBUSTION*

By H. A. Stuart[1]

(Received August 6, 1931)

Abstract

It is shown that differences in the observed heats of combustion of isomeric benzene derivatives can be interpreted as the internal molecular potential existing between their substituent groups. A like interpretation can be given for the differences between the values observed for the heats of combustion of certain nonisomeric benzene derivatives and those calculated by the rule of additivity. This internal potential, to which the attractive and repulsive forces between the groups are due, results from the electrostatic potential of the group moments (dipole effect), the polarization of the substituents and of the ring (induction effect), the dispersion effect, and from steric hindrance. We have, therefore, a new and direct method of measuring the internal potential, which determines both the internal motion of groups within an organic molecule and its most stable configuration. The values thus measured are in good agreement with values theoretically evaluated from the above intermolecular (van der Waals) forces. From the data derived by this method we conclude in the case of o-xylene that valence angles of 120° between the C–CH_3 bond and the aromatic C–C bonds are extremely stable, for the energy required to distort these angles through 10° is greater than 2 K cal/mole. We find, also, very restricted rotation for the butane molecule, from which it follows that saturated aliphatic hydrocarbons in the gaseous state tend to form zigzag chains. Such restricted rotation is found for the ether molecule as well.

Introduction

ONE of the most interesting structure problems at present is the question as to the rotation of groups around a bond and to their most stable orientation within an organic molecule. This rotational motion of course is governed by the forces acting between the different groups, that is, by the internal molecular potential between them. It is necessary, therefore, to study by means of theory the nature and distance of action of these forces, and to develop experimental methods for determining the mutual influence and the potential energy of the neighboring groups.

As to the nature and classification of these forces we will make the following assumptions, which agree nicely with our empirical knowledge. The forces leading to a chemical bond between two atoms are given principally by the interchange binding forces and can be calculated only by the methods of quantum mechanics. The forces between two neighboring atoms, not too close together, are the van der Waals forces. These intermolecular forces can be

* Contribution from the Chemical Laboratory of the University of California.

[1] Universität Königsberg, at present International Research Fellow University of California, Berkeley, California.

treated by classical and wave mechanics methods. If two atoms not connected by a chemical bond approach each other too closely, there are produced strong repulsive forces, which have not yet been treated theoretically, and which we will classify generally as caused by steric hindrance. We shall use this scheme in interpreting the results derived in this paper from the heat of combustion as it is all we have at present. It may be pointed out, however, that most of our conclusions are independent of the nature of the assumed forces. The sphere of action is determined by the surface at which we have equilibrium between repulsive and attractive forces, i.e. a minimum of potential energy.

Of the different methods which permit us to study the rotation within, and the most stable configuration of a molecule, we may mention measurements and discussions of electric moments,[2] investigations of the Kerr effect,[3] x-ray[4] and electron beam[5] interferences. The interference methods yield direct information concerning the distance between the atoms in a molecule. By the use of all these methods we may determine whether repulsive or attractive forces act between these atoms. But none of these methods gives us the internal potential energy between the atoms and atom groups, by which the internal motion of groups and the configuration of the molecule are determined.

It is therefore justifiable and useful to look for other methods, which may allow us to measure directly the internal potential and settle these questions of structure.

Such a method is given by the discussion of the heats of combustion, especially of isomeric compounds. It will be shown here that the differences in the energies of the molecules can be easily interpreted as the differences in the internal potential of the substituent groups, which is due to the attractive and repulsive forces acting between them.

As is well known, simple addition of the different bond energies concerned yields a value, correct to within a few percent, for the heat of formation of an organic molecule. This value is approximate because the value of any bond energy may depend in some measure upon the nature of the other bonds acting on the same atom[6] since such bonds often influence each other. If we take isomeric compounds such as isomeric benzene derivatives, however, where the same bonds act on the corresponding atoms, we expect constant heats of formation and therefore also constant heats of combustion so long as there is no marked difference in the internal potential energy between the sub-

[2] See for instance H. Sack, Erg. d. exakt. Naturw. **8,** 307 (1929) and H. A. Stuart, Phys. Zeits. **31,** 80 (1930); L. Meyer, Zeits. f. physik. Chem. **B, 8,** 27 (1930).

[3] H. A. Stuart, Zeits. f. Physik **63,** 533 (1930) and H. A. Stuart, Erg. d. exakt. Naturw. **10** (1931) in press.

[4] P. Debye, Phys. Zeits. **30,** 84, 524 (1929); **31,** 142 (1930). L. Bevilogna, ibid. **32,** 265 (1931).

[5] H. Mark and R. Wierl, Zeits. f. Physik **60,** 741 (1930); R. Wierl, Phys. Zeits. **31,** 366, 1028 (1930) and Leipziger Vorträge 1930, (1930).

[6] So we generally find differences in the aromatic and aliphatic bond energies, see H. Grimm and H. Wolff, Handbuch d. Physik **24,** 526 (1926).

stituents. We further expect that, on substituting in a benzene ring several groups, one after the other, the energy which is necessary for the successive groups will be independent of the presence of other substituents, so long as the internal potential between the substituents may be neglected. In this case the heat of combustion of the compound ought to be equal to the heat of combustion of benzene plus the amounts of energy characteristic of each substituent. The deviations from this additivity rule ought to increase with the potential energy between the substituents.

We shall first show that these ideas are in agreement with experimental data, and that deviations of the observed heats of combustion from the additivity rule can be interpreted quantitatively as potential energies between the substituent groups.

Experimental Data

In Table I, column 3, are summarized the observed heats of combustion of benzene and some simple derivatives in K cal/mole. As we have to compare the heats of combustion of the free molecules, or the heats of combustion for the gas at room temperature, we have to add to these observed values the heats of vaporization and in the case of solids also the heat of fusion, which are tabulated in columns 4 and 5. For our purpose it is sufficient to use the

Table I. *Thermal data and amounts of energy characteristic of each substituent for various benzene derivatives.*

Substance	Formula	H. Comb[7] obs. K cal/mole	H. Fusion K cal/mole	H. Vap. K cal/mole	H. Comb gas obs. K cal/mole	Q_{subst}
Benzene	C_6H_6	783.4		7.4	790.8	
Toluene	$C_6H_5 \cdot CH_3$	936		8	944	+153.2
Phenol	$C_6H_5 \cdot OH$	732	2.8	9	743.8	−47.0
Benzoic Acid	$C_6H_5 \cdot COOH$	771.2	(5)	(10.5)	786.7	−4.1
Aniline	$C_6H_5 \cdot NH_2$	812		9	821	+30.2
Nitrobenzene	$C_6H_5 \cdot NO_2$	739		10	749	−41.8
Fluorobenzene	$C_6H_5 \cdot F$	747.2		7.6	754.8	−36.0

[7] All data of heats of combustion are taken from the Intern. Crit. Tables, which are based on the critical compilation by M. S. Kharasch, Bureau of Standards, J. of Research, *2*, 359 (1929).

heats of fusion and of vaporization for the melting and the boiling point respectively. Where the heats of vaporization are not known, they are calculated by means of the Trouton rule, heat of vaporization $= 20 \times T_{abs}$ cal/mole. The heats of fusion, when not measured, are interpolated and extrapolated. All values for the heat of fusion and heat of vaporization, which are not known by direct measurements, are put in parantheses in this and the following tables. The values corrected for the gaseous state are tabulated in column 6 and in the last column we find the differences between the heats of combustion of benzene and the different derivatives, that is the energy Q_{subst} characteristic of the substitution for the different groups.

In order to show how far the energy necessary to substitute a certain group is independent of the presence of other substituents, we give, in Table II, the observed heats of combustion of some p-derivatives which are cor-

rected to the gaseous state. In column 4 we find the heats of combustion calculated by adding the Q_{subst} values (Table I, last column) to the heat of combustion of the benzene. The energy differences ΔU between the observed and calculated values are given in column 5. The plus sign shows that the observed value is greater than the calculated one. In the next column, 6, are tabulated the electric moments of the substituents together with their direction. A minus sign means that the group is negative with respect to the carbon atom of the ring. We recognize that the energy differences ΔU or the deviations of the additivity rule are increasing with the electric moment of the

TABLE II. *Comparison of observed and calculated heats of combustion of various p-derivatives.*

Substance	Substituents	H. Comb.[8] (gas obs.) K cal/mole	H. Comb. (calc.) K cal/mole	Energy difference ΔU K cal/mole	Elec. moments $\mu \times 10^{18}$
p-Xylene	CH_3; CH_3	1097.7	1097.2	+0.5	+0.4; +0.4
p-Nitrotoluene	NO_2; CH_3	903	902.2	+0.8	−3.8; +0.4
p-Fluoronitrobenzene	NO_2; F	714	713	+1.0	−3.8; −1.3
p-Nitrophenols	NO_2; OH	701[9]	702	−1.0	−3.8; +1.6
p-Nitrobenzoic Acids	NO_2; COOH	747.8	744.9	+2.9	−3.8; (2.7 and 1.6)[10]
p-Nitranilines	NO_2; NH_2	777[9]	779.2	−2.2	−3.8; (+1.5)
p-Dinitrobenzenes	NO_2; NO_2	712.5	707.2	+5.3	−3.8; −3.8

[8] The observed data for the liquid state and the heats of fusion and vaporization are tabulated in Table III.

[9] Heat of Comb. observed = 686; H. Fusion (5.5); H. Vap. (9.5) gives for H. Comb. for the gas 701; K cal; for p-nitraniline the values are 761; 5; (11), respectively, which gives 777 K cal for the gas.

[10] The moment of the COOH group consists of three bond moments: $\mu_{c=o} = 2.3.10^{-18}$; $\mu_{o-H} = 1.6.10^{-18}$ and $\mu_{c-o} = 0.7.10^{-18}$.

substituents, i.e., with the electrostatic potential of the groups. The differences for the first four compounds are within the limits of experimental error. We further find a negative deviation where the electric moments have different signs and therefore attract each other. This is to be expected since a negative difference must be interpreted as attraction.

In Table III are shown as a further example of the connection between the deviation from the additivity rule and the internal potential of the groups the heats of combustion of some isomeric di- and tri-substituted benzene derivatives. We always find that these energy differences ΔU given in the last column increase in the order para, meta and ortho positions. That is to be expected, since the potential between the groups, which is for these compounds, excepting for p- and m-nitraniline always repulsive, increases in the same direction. Besides the electrostatic potential and the polarization of the benzene ring we have in the case of the o-compounds always steric hindrance, that means strong repulsion.

CALCULATION OF THE INTERNAL MOLECULAR POTENTIAL BETWEEN THE SUBSTITUENT GROUPS

The question arises now, how far can these deviations from the additivity rule be interpreted as the internal potential of the substituents and how far

TABLE III. *Observed and calculated heats of combustion of some di- and tri-substituted benzene derivatives.*

Substance	Heat Comb. observed K cal/mole			H. Fusion K cal/mole			H. Vap. K cal/mole			H. Comb. gas K cal/mole observed			calc.	Energy Differences ΔU K cal/mole		
	p	m	o	p	m	o	p	m	o	p	m	o		p	m	o
Fluoronitrobenzene	703_s	706	707	(21)				9.5		714.5	715.5	716.5	713	+1.5	+2.5	+ 3.5
Nitrotoluene	889_s	893	897	(3)				(10)		902	903	907	902.2	−0.2	+0.8	+ 4.8
Nitrobenzoic Acid	728_s	729_s	735_s	8.8	4.6	6.7		(11)		747.8	744.6	752.7	744.9	+2.9	−0.3	+ 7.8
Dinitrobenzene	695_s	697_s	703.2_s	6.5	4.2	5.3	(11)	(11.5)	(11.5)	712.5	712.7	720	707.2	+5.3	+5.5	+12.8
Xylene	1089.1	1089.6	1092[11]				8.6	8.6	8.7	1097.7	1098.2	1100.7	1097.2	+0.5	+1.0	+ 3.5
	sym. 1, 3, 5	asym. 1, 2, 4		sym.	asym.		sym.		asym.	sym.	asym.			sym.	asym.	
Trinitrobenzene	664	674		(5.5)	3		(13)		(13)	682.5	690		665.4	+17.1	+24.6	

[11] Instead of 1093 K cal as given in the Int. Crit. Tables, we use 1092 K cal, as Richards and Barry, J. Amer. Chem. Soc. **37,** 993 (1915) find for the difference between p- and o- xylene 2.6 K cal.

can they be explained by the well-known forces acting between different molecules, i.e., the van der Waals forces.

There are three effects which contribute to the potential of molecules or in our case to the potential of the substituent groups. First of all the electrostatic potential of the permanent electric moments associated with the substituent groups, the dipole effect, secondly the induction effect (Debye effect) caused by the polarization of the molecule by the electric field of the moments of the substituents.[12] In this connection we must consider not only the mutual polarization of the substituents but also the polarization of the benzene ring, which contributes large amounts to the potential energy. The third effect is the so called dispersion effect, which has been introduced by London[13] into the theory of molecular forces. This effect consists in the mutual perturbation of the rapid internal motion of the electrons and always gives attraction.[14]

The energy of the dispersion effect can be approximately calculated, ac cording to London, by the following relation.

$$E_{\text{disp.}} = -\frac{3}{4}\frac{h\nu_0 \cdot \gamma^2}{r^6}$$

γ is the polarizability, that is the electric moment, induced by the unit of electric intensity, r the distance of the groups; for $h\nu_0$ the ionization potential may be used. This effect is in meta- and para-position always negligible (50 to 100 cal/mole), in ortho-position greater, for instance for two NO_2 groups 1500 cal/mole. But as we usually have steric hinderance in ortho-position, i.e., strong repulsion, the dispersion effect will be overcompensated.

The dipole effect may be neglected for para- and meta-positions, excepting in the case of two NO_2 groups. The electrostatic potential of two dipoles whose vectors lie in a plane can be calculated by means of the following expression

$$E_{\text{dipole}} = -\frac{\mu_1 \cdot \mu_2}{r^3}[2 \cos \alpha_1 \cos \alpha_2 - \sin \alpha_1 \sin \alpha_2].$$

α_1 and α_2 are the angles between the direction of the electric moments 1 and 2 and the line connecting both dipoles.

The energy contribution of the induction effect is given by the formula

$$E_{\text{ind.}} = -\tfrac{1}{2}\gamma F^2.$$

F is the electric intensity of the dipole moments. This energy may be neglected as far as the mutual induction of the substituents is concerned, excepting for a very strong group moment, such as the moment of NO_2 with $\mu = 3.8 \times 10^{-18}$. Considering the polarization of the benzene ring we find that

[12] In this case the groups and molecules behave as systems with static charge distribution, dipoles, quadrupoles and so on, which polarize each other.

[13] F. London, Zeits. f. Physik **63,** 245 (1930); Zeits. f. physik. Chem. **B, 11,** 222 (1930).

[14] The van der Waals forces of the noble gases and of nonpolar molecules can be explained only by this effect.

this effect involves very large energies. If we substitute, for instance, one NO_2 group in the benzene ring the field of the group moment will polarize the rest of the molecule, first of all the six aromatic C–C bonds, 1, 2, 3 . . . 6, see Fig. 1. The energy of this polarization effect for the bonds 1 and 6 amounts to 3650 cal for each bond. For the 2 and 5 bonds we find 250 cal and for the 3 and 4 bonds 50 cal each. The total energy is therefore 7900 cal/mole.[15]

If we substitute two or more groups, we have to calculate the resulting field of all group moments acting on the different C–C bonds. It turns out that the energy contributed from the induction by one group depends on the presence of the other ones and that the total energy of the induction effect is not the sum of the energies characteristic of the single groups, whereas the potentials of the dipole and the dispersion effect are always additive and independent of the benzene ring. As long as the groups have electric moments

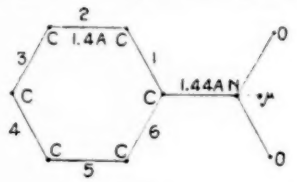

Fig. 1.

with the same direction with respect to the ring, the fields of the single moments weaken each other in most cases so that we get less energy for the induction effect. This corresponds to an increase in the total potential energy or in the heat of combustion.

In Table IV are given some of these calculated energies which arise from the polarization of the ring. In column 1 we find the number and nature of the substituents and in column 2 the energies of the induction effect. Column 3 shows the deviations from the energies we should find if each substituent would polarize the ring independently. These deviations, as mentioned above,

TABLE IV. *Calculated energies which arise from a polarization of the ring.*

Substituent	Induction effect calc. K cal/mole	Deviation from additivity K cal/mole
1 NO_2	−7.9	
2×NO_2 p	−12.7	+3.1
m	−11.3	+4.5
o	−15.9	+0.7
3×NO_2 sym.	−10.9	+12.8
asym.	−15.1	+8.6
1 F	−1.5	
1 F and 1 NO_2 p	−8.2	+1.2
m	−7.5	+1.9
o	−8.5	+0.9
1 NH_2	−1.9	
1 NH_2 and 1 NO_2 p	−10.6	−0.8
1 CH_3	0	
1 CH_3 and 1 NO_2 p	−7.9	0

[15] The fact that all aromatic bond energies are larger than the aliphatic ones may be to some extent due to this induction effect.

in so far as they are positive, increase the total potential and this corresponds to repulsion or higher heat of combustion.

In the calculations the following distances and assumptions are used. The distances of the atoms are known from x-ray diffraction data, which give us for C–C_{ar} 1.4, for C–C_{al} 1.5, and for C–N 1.44A; the distance C–F is about 1.6A. The electric moment of the NO_2 group is localized at a point 0.4A behind the N-atom. The distance between this moment and the C-atom of the ring is therefore 1.84A and the distance between the moment of the C – F bond and the C atom is 1.4A.[16] The refraction R of the six aromatic C–C bonds is equal to the molecular refraction of benzene minus the refraction of the six C–H bonds, i.e., $26.18-6\times1.7=16$. The polarizability, $\gamma=3R/4\pi N$, of one C–C bond amounts therefore to $10.6.10^{-25}$. The C–C bonds are treated as polarizable spheres located in the middle of the bond.

After we have determined in this way the energy amounts caused by the induction of the C–C bonds, we can calculate the total internal potential of the substituent groups for some simple derivatives. In Table V, columns 2

TABLE V.

Substance[17]	Dipole effect cal K—— mole	Disp. effect cal K—— mole	Induct. of subst. cal K—— mole	Induct. of ring cal K—— mole	Total int. potential calc. cal K—— mole	Energy diff. ΔU obs. cal K—— mole	Potential of steric hindrance cal K—— mole
p-dinitrobenzene	+1.6	0	0	+3.1	+4.7	+5.3	0
m- "	+1.8	0	0	+4.5	+6.3	+5.5	0
o- "	+7.7	−1.9	−1.0	+0.7	+5.5	+12.8	+7.3
1, 3, 5, trinitrobenzene	+5.3	0	0	+12.8	+18.1	+17.1	0
1, 2, 4 "	+10.8	−1.9	−1.0	+8.6	+16.5	+24.6 (20.8)	+8.1
p-fluoronitrobenzene	+0.5	0	0	+1.2	+1.7	+1.5	0
m- "	+0.8	0	0	+1.9	+2.7	+2.5	0
o- "	+3.2	−1.7	−0.2	+0.9	+3.2	+3.5	+0.3
p-nitrotoluene	−0.1	0	0	0	−0.1	−0.2	0
m- "	−0.1	0	0	0	−0.1	+0.8	0
o- "	−0.8	−1.6	−0.4	0	−2.8	+4.8	+7.6
p-nitraniline	−0.6	0	0	−0.8	−1.4	−2.2	0
p-xylene	0	0	0	0	0	+0.5	0
m- "	0	0	0	0	0	+1.0	0
o- "	0	−1.0	0	0	−1.0	+3.5	+4.5

[17] The values for m- and o-nitraniline, the nitrobenzoic acids, and the nitrophenols are not given, as we do not know enough about the situation, the orientation, and the amount of the moments associated with these groups, which are not in the plane of the ring.

to 5, are given the energy amounts of the dipole and dispersion effects as well as of both induction effects. In column 6 and 7 we find the sum, i.e., the total potential energy together with the observed energy differences ΔU taken from Table III, last column.

[16] The distances N–O and O–O are 1.13 and 2.09A respectively. Using the fact that for the N=O bond the center of the positive charges is located at 1/4th of the distance N=O near the oxygen atom, we can localize the moment of the NO_2 group (see L. Meyer, Zeits. f. physik. Chem. **B, 8,** 27 (1930)).

[18] For these calculations the following data are used. The polarizabilities are for NO_2 32.2×10^{-25}, for CH_3 24.9×10^{-25} and for F about 7×10^{-25}, the ionization potentials are for Cl 13 volts, for F 16.9, for NO_2 estimated to 13 volts and for CH_3 estimated to 10 volts.

There is an excellent agreement between the observed and calculated values, excepting for the ortho- compounds where we have steric hindrance. The agreement is surprisingly good considering the simplifying assumptions, which are the dipole moments are localized at a point and that the polarizable C–C bonds are substituted by polarizable spheres in the middle of the bonds. In the case of p-nitraniline we find in agreement with the observation an attractive potential and for p- and m-xylene within the limits of experimental error no internal potential at all. We are therefore justified in interpretating an observed energy difference ΔU as the internal potential between the substituent groups.

In the case of the ortho-compounds and of 1, 2, 4 trinitrobenzene the observed energy differences are always much greater than anticipated. The calculation of the electrostatic potential is in these cases somewhat uncertain because the distances of the group moments are comparable with the real dimensions of the dipoles. However we can best explain these deviations as caused principally by steric hindrance, which produces strong repulsive forces. These potentials of steric hindrance or these deviations are tabulated in the last column of Table V. We expect an increase in these deviations with an increase in the diameter of the substituent groups, as is observed. Fluoronitrobenzene has the smallest repulsion potential 0.3 K cal, o-xylene 4.5 K cal, nitrotoluene 7.6 K cal, dinitrobenzene 7.3 K cal and 1, 2, 4 trinitrobenzene 8.1 K cal. The two last compounds have, as is to be expected within the limits of experimental error, the same repulsive potential.

The total internal potential of o-xylene, which is given by the energy difference of the para- or meta- and ortho-compound, as there is no internal potential in p- and m-position, amounts to about 3 K cal.[19] In order to find the internal potential for the higher CH_3 derivatives we have tabulated in Table VI the heat of combustion for each of these compounds together with

TABLE VI.

Substance	H. Comb. obs. cal K—— mole	H. Fusion cal K—— mole	H. Vap. cal K—— mole	H. Comb. gas obs.	K cal/mole calc.	Internal potential cal K—— mole
1,2,4 Trimethylbenzene (Pseudocumene)	1241.7		9	1250.7	1250.4	+0.3
1,2,4,5 Tetramethylbenzene (Durol)$_s$	1393.6	(5)	9.5	1408.1	1403.6	+4.5
Pentamethylbenzene$_s$	1554	(4)	(10)	1568.0	1556.8	+11.2
Hexamethylbenzene$_s$	1711.9	(6)	10.5	1728.4	1710.0	+18.4

the values calculated according to the additivity rule. The last column gives us the energy difference ΔU or the internal potential. We recognize that these energies are increasing with the number of the substituents as is to be expected. We see furthermore that these potentials are within the limits of

[19] This value depends only on the relative accuracy of the measurements of the heats of combustion of the three xylenes and is therefore more reliable than the difference of 3.5 K cal between the observed and calculated heat of combustion of o-xylene.

error, 6×3, 4×3, and 2×3 K cal, for hexamethylbenzene, pentamethylbenzene and tetramethylbenzene respectively.[20] Because the CH_3 groups have no induction effect where the energy is not additive, and because the p- and m-compounds have no marked internal potential, the total internal potential for hexamethylbenzene is six times as large as the single potentials between two neighboring CH_3 groups. Thus we find that two neighboring groups in hexamethylbenzene have practically the same repulsive potential as in o-xylene. This result is not obvious. Using it we can draw some conclusions regarding the stability of the valence angles between the C–CH_3 and the C–C bonds.

Conclusions

It is known from Lonsdale's x-ray[21] investigations of the crystal structure of $C_6(CH_3)_6$ that the carbon atoms of the CH_3 groups are situated in the plane of the ring, in spite of the repulsive forces (this already shows the stability of the valence angles). We have therefore valence angles of 120° between C–CH_3 bonds and the aromatic C–C bonds. In the case of o-xylene both groups may yield to the repulsive forces but remain in the plane of the ring so that we get a deviation of these valence angles. The angles will not be

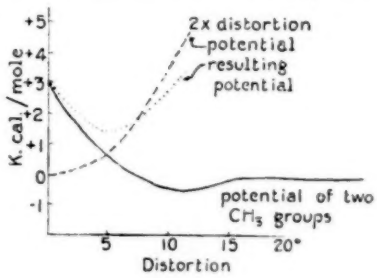

Fig. 2.

distorted more than 10° each, as this change is already sufficient to increase the distance between the carbon atoms of the two CH_3 groups from 2.9 to 3.4A where we certainly have equilibrium or even attraction of the two groups.

As we find for the o-position in xylene the same potential energy of 3 K cal as for the ideal 120° position in hexamethylbenzene, the decrease of the repulsive potential caused by the increasing C–C distance in case of o-xylene must be compensated by the energy, which is necessary to distort both valence angles. Such a compensation is only possible if the energy which is necessary to bend the angles so far that the two CH_3 groups are in the equilibrium position, is greater than the energy difference between the ideal 120° position, and this equilibrium position.[22]

[20] The values for hexa-and pentamethylbenzene are very reliable as here experimental errors do not effect the value for the internal potential energy very much. This is not true for trimethylbenzene where the observed heat of combustion is certainly too small.

[21] K. Lonsdale, Proc. Roy. Soc. (London), **A123,** 494 (1929).

[22] If the distortion potential for this equilibrium angle is equal or smaller than 4.5 K cal, the resulting potential, see Fig. 2, has a minimum and therefore the total potential for o-xylene would be less than 1/6 of the potential of hexamethylbenzene, therefore the distortion energy must be greater than about 2 K cal for each angle.

This energy difference is about 4 K cal since the minimum potential due to the dispersion attraction is about 1 K cal, and the energy required to distort the valence angles between a C–CH_3 and C–C bonds in a benzene ring through 10° is therefore greater than 2 K cal. Thus we see how stable the valence angles are. It may be mentioned that this result is in agreement with values which the author[23] has calculated for the stability of the valence angles of some molecules such as HCN, C_2H_2, CO_2, CS_2, where the fundamental frequencies are known. The distortion energies for these molecules vary between 700 and 4000 cal/mole for a deviation of 10°.

From the heats of combustion for the xylenes we found that two CH_3 groups have a repulsion potential of about 3 K cal/mole. On the other hand the very exact measurements of the heats of combustion of the nine isomeric heptanes established by the Bureau of Standards give nearly constant energies. There are some small deviations which might indicate a slight attraction between two CH_3 groups bound to the same carbon atom, but not a re-

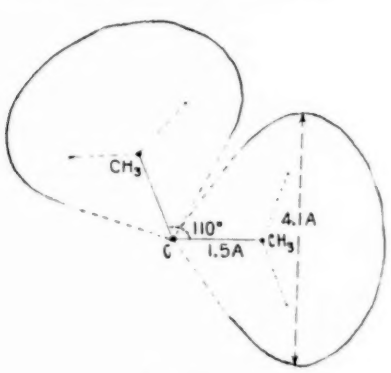

Fig 3a.

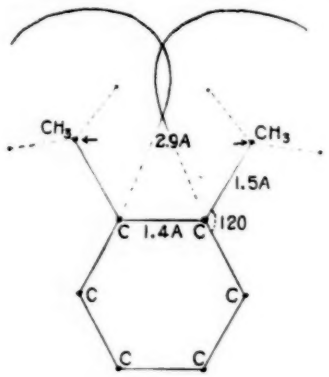

Fig. 3b.

pulsion,[24] although the carbon atoms are only 2.5A distant. From this result we recognize very distinctly that the potential of two CH_3 groups depends, as is to be expected, not only on their distance, but also on their orientation. Therefore the diameter of the sphere of action of a CH_3 group is not the same in all directions. The shape will be very irregular, but will have approximately rotational symmetry around the direction of the C–CH_3 bond. The following form of the sphere of action, see Fig. 3a and b, may explain that we have no marked repulsion for two CH_3 groups bound on the same carbon atom, but a strong one in o-xylene. The greatest diameter perpendicular to the direction of the fourth valence may be taken from Lonsdale's data for the crystal structure of hexamethylbenzene. She finds for the closest distance, to which two CH_3 groups in different molecules can approach each

[23] H. A. Stuart, Phys. Zeits. **32** (1931) in press.

[24] As an alternative to the assumption of zero repulsion, we should have to assume that any possible changes in the internal potentials of adjacent CH_3 groups are just compensated by bond energy changes resulting from the replacement of C-H by C-C bonds. That such compensation exists in all nine isomers with their different configurations is, of course, highly improbable.

other, 4.1A.[25] The greatest radius of the group taken from the C-atom as the center will probably be in the direction of the C–H bonds. We see that for o-xylene the spheres of action overlap each other.

Finally we will discuss the most stable positions of saturated hydrocarbons and of the ether molecule, using the fact that two CH_3 groups in o-xylene have a repulsive potential of about 3 K cal. In the butane molecule where the valence angles are 110° (tetrahedron angle of the quadrivalent carbon atom), we have rotation of the last CH_3 group around the C–C bond. In position II the distance of the two carbon atoms is only 2.6A, so we must have a greater repulsive potential than that in o-xylene, where the dis-

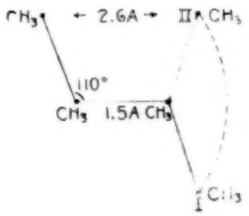

Fig. 4.

tance is 2.9A, or more, and the potential amounts to 3 K cal. As this energy is much greater than the energy of the temperature motion, KT about 600 cal at room temperature, it follows that position II is impossible.[26] In position I (180°) we certainly have no repulsion, perhaps a little attraction, so we probably have at room temperature torsional vibrations with great amplitudes around position I. We may therefore expect for the saturated hydrocarbons also in the gaseous state a tendency towards zigzag chains, as they are observed in liquids and crystals. Nevertheless it is possible that we will find for long chains something like a closed form which, of course, is oriented very far from a planar configuration, especially if the chain has large dipoles on its ends.

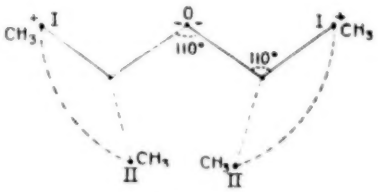

Fig. 5.

Let us consider now the ether molecule, see Fig. 5. We assume as usual 110° for the valence angle of the oxygen atom. We recognize then that position II is absolutely impossible as we have here an enormous steric hindrance, the distance of the carbon atoms of the CH_3 groups being only 1.7A. If at the same time we turn both CH_3 groups through 90°, the distance is still 3.2

[25] This diameter is very reasonable, as with a smaller one, about 3.4A, we could not understand the repulsion in o-xylene

[26] A rotation through 90° to 120° from position II will be sufficient to avoid the repulsive forces as the distance is 3.0A for 60° and 3.5A for 120°.

to 3.3 and becomes, at about 110°, 3.5A, where the repulsion disappears. A configuration with one group in II, the other in I, also seems to be impossible as we have then a repulsive potential similar to that in butane (distance C–C 2.5A). On the other hand, position I is, on account of the dipole attraction, energy approximately equal to $\frac{1}{2}KT$, the most stable one, so that we have in the ether molecule rotation vibrations of about 70° around position I. This is in excellent agreement with results derived by the author from discussions of electric moments in homologous series[27] and from observations of the Kerr constant[28] of the ether molecule, which show directly that position I is the most stable one.

If we had more and, what is of even greater importance, more exact data for the heats of combustion of other isomeric compounds, such as the CH_3 and Cl derivatives of methane, ethane, ethylene, benzene, etc., we should be able to draw very precise conclusions regarding the internal potential of the substituent groups as a function of the distance and the orientation and also as to the mutual influence of the bond energies. This paper may be considered as a first attempt to employ heats of combustion in answering questions as to the free rotation and the stable configuration of groups in an organic molecule.

In conclusion the author wishes to express his thanks to Professor Lewis for his hospitality, and to Professor Pauling, and the other members of the University of California with whom he has had the privilege of discussing this problem.

[27] H. A. Stuart, Phys. Zeits. **31,** 81 (1930).
[28] H. A. Stuart, Zeits. f. Physik **63,** 533 (1930).

FURTHER APPLICATION OF HUANG'S GENERAL EQUATIONS OF ENERGY AND ENTROPY OF GASES: THE GENERAL ADIABATIC EQUATION OF GASES

By Tzu Ching Huang
Department of Chemistry, National Tsing Hua University, Peiping, China

(Received August 14, 1931)

Abstract

From Huang's general equation of entropy there is deduced a general adiabatic equation,

$$\int \psi(v)dv - \int \frac{\partial F}{\partial T} dv + \int c_{va} \frac{dT}{T} = \text{const},$$

for any gas of the type, $p = T\Psi(v) - \Phi(v) - F(v, T)$. The result is tested satisfactorily with perfect gas as gases obeying van der Waal and Beattie-Bridgeman's equations of state.

THE present short paper aims to deduce a general adiabatic equation of gases belonging to the type,

$$p = T\Psi(v) - \Phi(v) - F(v, T), \tag{1}$$

in which p is the pressure, T the temperature of the gas, $\Psi(v)$ and $\Phi(v)$ are functions of volume, and $F(v, T)$ the function of volume and temperature.

Recently, the author[1] showed that for any gas in the form of Eq. (1), its entropy s is

$$s = \int \Psi(v)dv - \int \frac{\partial F}{\partial T} dv + \int c_{va} \frac{dT}{T} + k \tag{2}$$

in which c_{va} = heat capacity of the gas at constant volume and at infinite dilution. Since the necessary condition for any gas to be in adiabatic state is s = const, we have immediately,

$$\int \Psi(v)dv - \int \frac{\partial F}{\partial T} dv + \int c_{va} \frac{dT}{T} = \text{const}, \tag{3}$$

as the general adiabatic equation of gases. The following applications show the validity and usefulness of this equation.

(1) Perfect gas:

$$p = \frac{RT}{v}.$$

Referring to Eq. (1) and applying Eq. (3), we get

$$Tv^{R/c_v} = \text{const}.$$

[1] Huang, Phys. Rev. **37**, 1171 (1931).

(2) van der Waal's equation of state:

$$p = \frac{RT}{v - b} - \frac{a}{v^2}.$$

Eqs. (1) and (3) give

$$T(v - b)^{R/c_v}.$$

The above results are well known in classical thermodynamics.

(3) Beattie-Bridgeman's equation of state:[2]

$$p = \frac{RT}{v^2}\left[v + B_0\left(1 - \frac{b}{v}\right)\right] - \frac{A_0}{v^2}\left(1 - \frac{a}{v}\right) - \frac{cR}{v^3T^2}\left[v + B_0\left(1 - \frac{b}{v}\right)\right].$$

Eqs. (1) and (3) give

$$R \ln v - \frac{R}{v}\left(B_0 + \frac{2c}{T^3}\right) + \frac{RB_0}{v^2}\left(\frac{b}{2} - \frac{c}{T^3}\right) + \frac{2bcRB_0}{3v^3T^3} + \int c_{v\alpha}\frac{dT}{T} = \text{const.}$$

[2] Beattie and Bridgeman, Proc. Am. Art. Sci. **63,** 231 (1928).

LETTERS TO THE EDITOR

Prompt publication of brief reports of important discoveries in physics may be secured by addressing them to this department. Closing dates for this department are, for the first issue of the month, the twenty-eighth of the preceding month; for the second issue, the thirteenth of the month. The Board of Editors does not hold itself responsible for the opinions expressed by the correspondents.

Intensity of Raman Lines in Estimating the Concentration of the Components Present in Benzene-Toluene Mixtures

Every substance gives its characteristic Raman spectrum in which the frequency shifts of the modified lines can be attributed to the presence of particular groups and linkages in the molecule, and the intensity of the lines under given conditions can be related to the molecular density.[1] Dadieu and Kohlrausch[2] have obtained Raman spectra of binary mixtures in which the characteristic lines of the two components appear without change of frequency, except in a few cases where a slight shift occurs due to the high dipole moment of the molecule. It seemed, therefore, probable that for ordinary liquid mixtures a fair estimate of the concentration of the components present could be made from measurements of the relative intensity of the Raman lines.

Photographs were taken of Raman spectra of benzene-toluene mixtures of varying concentration using a Hg arc as source of excitation as described by R. W. Wood. Experimental conditions were maintained, as nearly as possible, the same for each series of spectra photographed.

The first spectra obtained indicated that a difference of 25 percent in concentration of either component was easily perceptible. Photometric measurements with a Moll densitometer showed a marked change in the contour as well as in the height of the intensity curves of the Raman lines. Some of the results for 25 percent change in concentration are listed in Table I which gives the relative height of the intensity curve for three of the characteristic benzene and toluene lines excited by their respective Hg lines.

TABLE I. *Relative intensity [Ht. in mm].*

Hg Line	4046	4358	4358
	T	*B*	*T*
Raman line	2917	1178	1207
B % *T*			
100– 0	7.1	36.3	2.2
75– 25	18.2	25.6	12.3
50– 50	26.5	22.0	17.8
25– 75	31.0	18.9	23.4
0–100	35.7	12.6	27.2

Five percent variations in concentration could be less readily discerned from the Raman plates; however, intensity curves showed, without doubt, that decided differences existed, as can be seen in part from the measurements given in Table II.

TABLE II. *Relative intensity [Ht. in mm].*

Hg line	4358	4358	4347
	T	*B*	*B*
Raman line	781	884	991
B % *T*			
100– 0	3.2	9.8	19.0
95– 5	7.0	9.0	14.0
90–10	7.3	7.6	11.0
85–15	7.8	6.6	8.5

At present no attempt has been made to determine less than 5 percent change in concentration. Longer exposures as well as change in other conditions may yield more quantitative results, especially when one of the components is present at low concentration.

The experiments indicate, that with proper control of conditions, concentrations of a given mixture, to within at least 5 percent, can be estimated from a study of the relative intensity of the Raman lines.

ELIZABETH A. CRIGLER
Chemistry Laboratory,
Johns Hopkins University,
September 10, 1931.

[1] Daure, P., Comptes Rendus **186,** 1833 (1928); Venkateswaran, S. Ind. J. Phys. **3,** 105 (1928).

[2] Dadieu, A. and Kohlrausch, K. W. F., Phys. Zeits. **31,** 514 (1930).

X-ray Diffraction Patterns of Mixtures[1]

In the March 15 Physical Review, Mr. Roy W. Drier reported that in a number of instances which had come to his attention the x-ray diffraction pattern of mixtures did not correspond to a composite pattern of the components, but on the contrary some lines of the components were absent and new lines appeared. Somewhat earlier,[2] he had reported elsewhere the detection of extremely small amounts of silver (as low as 0.003%) in samples of copper. A comment by Mr. Cyril S. Smith[3] on this earlier paper has already been published to the effect that the silver lines might very well be due to the molybdenum K-beta radiation diffracted by the copper lattice. In private correspondence, we had called Mr. Drier's attention to this interpretation, but it was not entirely convincing to him since his experiments had indicated that spectroscopically silver-free copper did not give the so-called silver lines.

These two papers of Mr. Drier's bring up so clearly the question of the interpretation of the diffraction patterns of mixtures obtained with the General Electric apparatus and his inferences are so surprising that we feel them worthy of comment.

With regard to the presence of silver in copper, we found it quite possible, using sodium chloride as a sample, to demonstrate the presence of molybdenum K-beta radiation under experimental conditions similar to Mr. Drier's. Furthermore, contrary to his experience, we found we could obtain these lines with a sample of copper which was spectroscopically silver-free. On the other hand, we found that palladium, which has an atomic number differing only by one from that of silver but has different lattice dimensions, could not be detected in mechanical mixtures with copper unless present in amounts of the order of 1 to 2 percent. We may add that a copper specimen[4] containing 0.03 percent silver, which gave the apparent silver lines when irradiated with molybdenum, failed to show any silver lines when exposed to copper radiation. We believe, therefore, with Mr. Smith that the effect Mr. Drier observed was due to the inhomogeneity of the radiation employed and that no trustworthy evidence for the presence or absence of silver could be adduced from his experiments.

Our experimental results likewise differ from Mr. Drier's in the study of other mixtures such as those of barium sulfate-titanium dioxide. The barium sulfate pattern itself contains so many lines as to render the titanium dioxide pattern difficult to isolate, and there is the further factor that titanium dioxide may exist in three crystalline forms. In a considerable number of experiments, however, we have found no instance of a diffraction pattern from a mixture of these materials which could not be explained as a composite of the patterns of the components. We repeated Mr. Drier's experiments with copper-zinc mixtures, which he instanced as a particularly good case, and again failed to reproduce his results. The diffraction patterns contained all the strong lines of copper and of zinc and we detected no lines attributable to alpha-brass. If, as Mr. Drier reported, as many as eight lines of alpha-brass could be detected, the strongest of these (111 and 100) must have been of appreciable intensity, but we failed to develop even them.

It is difficult for us to offer an explanation of Mr. Drier's experimental findings, but we think that the question of the homogeneity of the radiation has not been carefully considered and also the possibility of a shift in the position of lines by diffraction from the edges of opaque samples. In any case, it seems to us that the explanation for these surprising effects should first be sought in a very careful examination of the technique rather than in speculations as to the formation of new phases.

A. W. KENNEY
HENRY AUGHEY

Wilmington, Delaware,
September 10, 1931.

[1] Communication No. 80 from the Experimental Station of E. I. duPont de Nemours & Co., Inc., Wilmington, Delaware.

[2] Drier, Ind. Eng. Chem. **23**, 404–5 (1931).

[3] C. S. Smith, Ind. Eng. Chem. **23**, 969–70 (1931).

[4] We wish to acknowledge the assistance of the American Brass Company, who gave us a number of samples of copper containing varying amounts of silver which had been accurately determined.

A New Method of Producing Negative Ions

In some recent experiments on the bombardment of metal surfaces with positive ions, negative ions formed at the surface by the positive ion impacts were observed. The apparatus used was an adaptation of the Dempster type mass spectrograph in which the negative particles formed could be analysed. Platinum targets were used in most cases and the impacting ions were of lithium (chiefly Li_7^+) produced by a spodumene source on a hot filament. The positive ions were accelerated through 500 volts to the target where any negative particles formed would be driven back to the first slit of the mass spectrograph with the same velocity as the impinging positives. Identification of the negative particles was made from the calibration of the spectrograph with known positive ions. All experiments were made in a good vacuum of the order of 10^{-6} mm of mercury.

In this way negative ions of $OH^-=17$ and $Cl^-=35$ were found to result from the bombardment with positive lithium ions. Secondary electrons were also observed together with two ions which were probably H_1^- and H_2^-; the latter two ions were not easily analysed due to the width of the slits and the small values of the magnetic field at which they were observed. For platinum targets which had not been outgassed the negative OH ion was strong and steady over a period of several hours; its intensity was of the same order of magnitude as the electron emission. The H_1 and H_2 ions accompanied the OH ion, H_1 being several times as intense as H_2. The Cl ion was not resolved into its components and was not always observed; its presence was more noticeable when the target was coated with spodumene showing that it probably arose from some chance contamination of the target. Strong outgassing of the platinum target did not affect the electron emission but caused the negative ions to disappear.

This method of forming negative ions while of interest in itself may also be of importance in interpreting related experiments. It is possible that in studies of ionization and secondary electrons produced by positive ions this type of emission may contribute to the effects observed. The general presence of water vapor in most metals and compounds will probably give rise to negative ions as well as electrons while the negative chlorine ion indicates that other substances may form other ions under the influence of positive ion bombardment.

Negative ions have been observed previously by J. J. Thomson[1] and O. H. Smith[2] as the retrograde rays formed in discharge tubes. These ions, presumably of H_2^- and O_2^-, were formed just in front of the cathode by gas molecules acquiring a negative charge. O. W. Richardson[3] and H. A. Barton[4] have reported a few cases of negative ions formed by direct heating of the salt. Very recently Mueller and Smyth[5] have reported negative hydrogen and hydroxyl ions formed by electron impacts in apparatus containing water vapor. Further work on this type of emission is being carried out and will be reported on later.

JAMES S. THOMPSON

Ryerson Physical Laboratory,
University of Chicago,

Armour Institute of Technology,
Chicago, Ill.,
September 12, 1931.

[1] J. J. Thomson, "Rays of Positive Electricity," pp. 137–138.

[2] O. H. Smith, Phys. Rev. **7**, 625 (1916).

[3] O. W. Richardson, "Emission of Electricity from Hot Bodies."

[4] H. A. Barton, Phys. Rev. **26**, 360 (1925).

[5] D. W. Mueller and H. D. Smyth, Program of Schenectady Meeting, American Physical Society, Abstract 11, Aug. 26, 1931.

Variations in the Grating Constant of Calcite Crystals

With the development of the double crystal spectrometer for measuring x-ray wavelengths and the use of the high precision photographic spectrometers now employed, the question of a possible variation in the grating constant of calcite is of considerable importance. Also the chemical purity and density of the crystals should be examined.

In the present experiments optically clear crystals have been secured from four localities, Iceland, Spain, Montana, and Argentina. The crystals were carefully cleaved and the part of the surface used for diffracting the x-rays was almost free from "steps." Small pieces of each crystal were cut from a region very close to the part of the crystal used and a chemical

TABLE I.

Crystal	Silica	Alumina	Ferrous oxide	Manganous oxide	Magnesium oxide	Calcium carbonate
Iceland	absent	absent	0.006%	0.007%	absent	99.98%
Montana	absent	absent	0.005	0.011	absent	99.97
Argentina	absent	absent	0.006	0.010	absent	99.97
Spain	0.004%	absent	0.007	0.006	absent	99.98

analysis of these pieces has been made. The results of these analyses are shown in Table I. Thus chemically there appears to be very little difference between the various samples.

A preliminary determination of the density of each crystal indicated that the density was the same for all crystals within 1 part in 4000. A more precise determination of the densities will be made before a final report of the experiment is given.

The spectrometer was a high precision double crystal spectrometer built by the Société Génevoise. An attempt was made to calibrate the circle with a telescope but no consistent error of as much as 0.5″ was found. This was just about the error of setting the cross hairs in the telescope. A more precise method of testing the circle was as follows: The diffracting angle of the same crystal in the 4th order was determined in three 120° positions of the circle. These agreed to within 0.4″ with an average variation of 0.2″. This average diffracting angle has been used as the absolute value and all other measurements have been made relative to this.

The first crystal of the spectrometer was an Iceland calcite set to diffract the $K\alpha_1$ line of molybdenum over the main axis of the spectrometer. This crystal was made parallel to the spectrometer axis to within 1′ of arc. The surface of the second crystal was mounted on the axis and parallel to it to within 5″ of arc. The correction which must be made in the measured diffraction angle, due to the height of the slits, was determined experimentally in the 4th order. This agreed, however, very closely with the calculated correction. The correction for the thermal expansion of the crystal has been made using Larsson's value[1] ($\alpha = 1.09 \times 10^{-6}$) of the expansion coefficient. The results are for a crystal temperature of 18°C. In calculating the wave-lengths the theoretical value of the index of refraction ($1 - \mu = 1.85 \times 10^{-6}$) has been used and the grating space of the crystal was assumed to be 3.02904A in the first order.

The results given for the 4th order are much more reliable than any others. Eight independent determinations have been made on each crystal in the 4th order and the average variation in each case was about 0.2″. In each of the other orders only two or three determinations have been made and the average

[1] Larsson, Inaugural-Dissertation, Uppsala 1929.

Diffraction angles.

Order	Iceland	Montana	Argentina	Spain
1	6° 42′ 35.4″	6° 42′ 35.6″	6° 42′ 35.5″	6° 42′ 35.3″
2	13° 30′ 44.9″	13° 30′ 45.2″	13° 30′ 45.7″	13° 30′ 45.3″
3	20° 31′ 0.3″	20° 31′ 1.3″	20° 31′ 1.1″	20° 31′ 0.8″
4	27° 51′ 34.0″	27° 51′ 34.6″	27° 51′ 34.7″	27° 51′ 34.4″
5	35° 44′ 28.5″	35° 44′ 30.8″	35° 44′ 29.9″	35° 34′ 29.9″

Wave-lengths.

1	0.707833A	0.707838	0.707837	0.707832
2	0.707827	0.707831	0.707836	0.707832
3	0.707832	0.707841	0.707839	0.707836
4	0.707830	0.707834	0.707835	0.707833
5	0.707827	0.707838	0.707834	0.707834

variation was from 0.2″ to 0.5″. The average wave-length as given by the 4th order is

$$\text{Mo}K\alpha_1 = 0.707833\text{A}$$

Compton[2] has recently reported a precise determination of the diffraction of the $\text{Mo}K\alpha_1$ line in the 4th order using calcite. His value of the diffracting angle is 27° 51′ 32.9″ or a wave-length 0.707824A as calculated above. This is considerably smaller than any of my results, however, Larsson's results[1] agree very closely with the present values obtained with the Iceland crystal.

[2] Compton, Phys. Rev. **37**, 1694 (1931).

The index of refraction of the x-rays in the crystal has been calculated from the 1st and 2nd orders and the 1st and 4th orders. The average values for all crystals are

$$\text{1st and 2nd order } (1-\mu) = 1.90\times10^{-6}$$
$$\text{1st and 4th order } (1-\mu) = 1.86\times10^{-6}.$$

These values are in fair agreement with Larsson's[1] results but differ considerably from the value $(1-\mu) = (2.10 \pm 0.15)\times10^{-6}$ reported by Compton.[2]

J. A. Bearden

Johns Hopkins University,
September 10, 1931.

Thermocouples of Longitudinally and Transversely Magnetized Wires

Recently (Phys. Rev. **38**, 179, (1931)) William H. Ross has performed some experiments designed to give the thermal *emf* between longitudinally and transversely magnetized elements of the same ferromagnetic substance. In these experiments a short length of wire was placed parallel to the magnetic field between the poles of an electromagnet. At each end of this short length the wire was bent at right angles, so that two long segments came out parallel to each other from between the poles of the magnet. These long ends were connected to a galvanometer. The two bends between the magnet poles were kept at different temperatures and when the magnet was excited a thermoelectromotive force was observed.

We may consider that the circuit contains three thermoelectrically distinct metals:—(1) longitudinally magnetized metal, (2) transversely magnetized metal, (3) unmagnetized metal. Assume the junctions of (3) and (2) to be situated at the edges of the magnet poles. These junctions will then be at different temperatures as a result of conduction of heat along the wires, and the resultant *emf* will be partly due to the combination of (2) and (3). The title of the paper by Ross implies the existence of only the elements (1) and (2).

Of course, practically, there is no sharp line of demarcation between the elements (2) and (3), but the results are essentially unchanged in the experiment where a temperature gradient in a nonuniform magnetic field replaces the sharp boundary considered above.

Another point of view would consider the longitudinal thermomagnetic potential differences in the transverse sections of wire. The total *emf* would then involve an integration over a varying magnetic field and a varying temperature gradient.

These considerations are brought forward in order to point out the difficulty of interpreting in a simple way the experiments of Ross. There are conflicting experiments in this field of research and it is highly desirable to keep the various elements clearly segregated in any particular experiment in order to make comparison possible with other results.

C. W. Heaps

Department of Physics,
Rice Institute,
Houston, Texas,
September 7, 1931.

BOOK REVIEWS

Das Jahrhundert der Strahlen. JOSEF ROSENTHAL. Pp. 29, Figs. 18, Georg Thieme Verlag, Leipzig 1930.

In this little book (the substance of a lecture) the author reviews in a popular and concentrated manner the whole field of radiation. He describes the corpuscluar rays: cathode and canal rays, alpha and beta rays, and covers the entire region of what he calls ether-rays. He refers to them as Herz-, heat-, light-, chemical-, Roentgen-, gamma and Hess-rays. These names indicate that the contribution of German scientists to our knowledge in the field of radiation has been particularly emphasized. The tendency of referring as much as possible to German scientists evidently contributed to make the lecture popular and the article is popular in the best sense of the word. Probably it is for the same reason the author refers to the electromagnetic radiation as ether-rays without hinting at any of the modern theories. Sand and water jets are referred to as corpuscular rays and sound waves are discussed in order to prepare the mind for the ether waves. Special emphasis is laid on the practical importance of roentgen rays, particularly in medicine. The book gives a good lesson in how to make scientific discoveries popular to the newcomers who must answer in the affirmative the last question, "Ist es nicht schön das Wunderland der Strahlen?"

K. W. STENSTROM
University of Minnesota

Statistical Mechanics. R. H. FOWLER. Pp. 570. figs. 28, tables 59. University Press, Cambridge, 1929, and the Macmillan Company, New York.

In this monumental volume, R. H. Fowler has assembled all the work done by him and his fellow-workers since, say, 1922 when the first article of Darwin and Fowler appeared. Although of course, he treats very thoroughly the work done elsewhere, still the book reflects very strongly the methods and the interests of what one might call the Cambridge school. The book, which grew out of an essay to which was awarded the Adams Prize, is devoted mainly to the statistical method and its applications. Consequently the book is devoted practically entirely as the subtitle indicates to the theory of the properties of matter in equilibrium. The kinetic method, or as Jeans calls it the method of collisions, in which one has to consider more in detail the elementary interaction processes, and by which one is only able to treat systems not in equilibrium (as in the theory of heatconduction, viscosity, etc.), is only given in the last chapters (Chapters 17 and 19). Fowler does not here discuss the theory of nonequilibrium states; he only considers what restrictions are imposed on the laws of interaction by the theory of equilibrium states. From this point of view the principle of detailed balancing and its consequences are carefully treated. The H-theorem of Boltzmann is proved for collisions with central forces and considered then as a proof of detailed balancing. Though this is of course correct, still in the opinion of the reviewer it does not give full justice to the famous theorem. Because of the cycle-proof of Boltzmann, which Fowler does not mention, we know that the theorem is more general than the principle of detailed balancing. Also its role in the explanation of the laws of thermodynamics is, I think, not sufficiently stressed.

The statistical method is presented from the point of view which characterises the equilibrium state as the average state. The mathematical method of evaluating the summations which occur is that of the generating functions, or partition functions as Fowler calls them. Together with the method of steepest descent for the approximate evaluation of complex integrals, it forms a very powerful tool, which was for the first time applied to problems in statistical mechanics in the well known articles of Darwin and Fowler in the Phil. Mag. These elegant and in the best sense of the term "witty" methods give the book a great unity in the mathematical treatment; and furthermore they have the advantage that in principle one can judge the degree of approximation at every stage of the calculation. Yet the reviewer regrets that the simple approximation method of Gibbs (as Pauli presents it for instance in the Zeits. f.

Physik **41**, 81, (1927)) is not given, and that the usual derivation of the Maxwell-Boltzmann distribution law, etc., as the most probable state is also omitted. I am not quite convinced by Chapter 6, on the connection with classical thermodynamics, that one is allowed to omit the latter; and the consideration of the most probable state would certainly make the mathematics much simpler.

But these criticisms are perhaps quite irrelevant, because the book is not intended to be a textbook for beginners, and the weight obviously lies not so much on the careful discussion of first principles and methods, as on the applications. And here one can only admire the thoroughness with which the great number of subjects have been treated.

The first four chapters give the general method and the more simple applications. Very interesting is the careful discussion connecting the specific heat and the band spectrum data. Though the agreement is in general good, there remain some very surprising discrepancies. Chapter 5 gives the theory of dissociation and sublimation, which links up with the very fine discussion of the Nernst heat theorem and the chemical constants in Chapter 7. Striking are also the next two chapters on the theory of imperfect gases and the chapters on interatomic forces, which was contributed by Lennard-Jones. With the renewed interest at present in the theory of the equation of state, they will become more and more useful. The next chapters bring the theory of thermionics (Chapter 11), of the dielectric and the dia- and paramagnetic constants of gases (Chapter 12) and of the properties of dilute solutions, including the Debye theory of strong electrolytes (Chapter 13). Then follows (Chapter 14, 15, 16) the study of the properties of matter at high temperatures, which formed the original Adams Prize essay. Fowler's work in this field is so well known that there is no need to give the contents of these chapters in more detail. There is further still a chapter on chemical kinetics, and a short account of the theory of fluctuations. The theory of the Brownian motion is only touched upon. The book closes with a Chapter on the new statistics, with applications to the theory of metals.

All this can give only a small idea of the wealth of material, and the completeness with which most of the subjects have been treated. I am certain that for a long time to come Fowler's work will be an indispensable reference book for all those who are interested in the wide field of the kinetic theory of matter.

GEORGE E. UHLENBECK
University of Michigan

La Topographie sans Topographes. F. OLLIVIER. Pp. 301, figs. 158. Revue d'Optique theorique et instrumentale, Paris, 1929. Price, 42 francs.

Surveying by means of the photographic camera on a practical basis had its beginning about 1860 in the work of Colonel Laussedat in France. Considerable attention was given to these methods in various European countries and the major contributions to the subject were made by European engineers.

About 1885 the photographic method was introduced in America by the Canadian government in connection with surveys in the Rocky Mountains and southeastern Alaska. In the latter the U. S. Coast and Geodetic Survey participated in connection with the preliminary reconnaissance for the boundary between Alaska and British Columbia. Aside from this use by the Canadian and United States government in mountain topographic surveys, the photographic method was used comparatively little in North America until the advent of aerial photography since the World War.

This book by Commandant Ollivier of the French army engineers is a treatise on phototopographic surveying. Its three hundred pages embrace an introduction and nine chapters.

Chapter one is devoted to an excellent historical outline of the method from its early development by Colonel Laussedat together with an explanation of the fundamental principles. The second chapter is devoted to a theoretical consideration of methods and instruments for revealing to the eye the topographic relief as a basis for the surveying and mapping. Monocular, binocular, and stereoscopic methods are treated.

The principles underlying the stereoscopic method of phototopographic surveying are developed in chapter three, and the following chapter is devoted to the instruments and apparatus used in the field and in the office work. Special attention is given to the elaborate modern

instruments for mechanically plotting the control points and contours from the original photographs.

In chapters five and six a very full consideration is given to the subject of precision, errors and corrections. Chapters seven and eight are devoted to the methods of reducing the data and plotting the maps. In conclusion, a number of general topics are considered in the final chapter.

This book should be an important addition to the literature of the subject. With the increased use of photography in aerial surveying, it is inevitable that greater attention will be given in the United States to photographic methods and that more books in the English language will appear, in addition to the current periodical literature in the technical press.

O. M. LELAND
University of Minnesota

A Handbook of Physics Measurements, Vol. II. E. S. FERRY in collaboration with O. W. SILVEY, G. W. SHERMAN, JR., D. C. DUNCAN. Pp. xi+277, figs. 143., Third Edition corrected, John Wiley and Sons Inc., 1929. Price, $2.50.

Each of the four chapters in this self contained manual is divided into two parts. The first part includes definitions, descriptions of apparatus and the derivation of the general theory and equations used in the experiments. In the second part each experimental measurement is described in detail as to manipulation and computation.

One suspects that the manual is written for sophomore engineers who are taking calculus, as mathematics including differential equations is used in developing the theory.

The variation of difficulty in the experiments is marked. In all of the chapters except the first on vibratory motion, experiments are found which might well be used for a liberal arts course with a mathematical prerequisite of only high school algebra. All of the first chapter and part of the others contain plenty of experiments that might well be used in an advanced general laboratory with a calculus prerequisite. This dual characteristic is perhaps best illustrated by chapter four on electricity and magnetism where the twenty-four experiments listed might well be those given in a general physics laboratory plus those given in a special course in electrical measurements for electrical engineers.

It appears to be to the disadvantage of the book that the most difficult theory presented is in the first twenty five pages.

Not the least interesting part of this book is the forty two page supplement listing thirty nine projects so designed that the ambitious student may do extra work in the laboratory. The book contains tables of the most used physical constants.

The preface states that experiments are included "which experience has shown to be most available for college and industrial laboratories." One may not agree with the statement but certainly a list of well written and unusual experiments are offered. Any person in charge of a physics laboratory can hardly afford to miss the wealth of suggestions offered in this volume.

C. J. LAPP
State University of Iowa

Vorlesungen über einige Klassen nichtlinearer Integralgleichungen und Integro-differentialgleichungen. L. LICHTENSTEIN, x+164 pp. Springer, Berlin, 1931. Price, RM 16.80.

Although linear equations have played the conspicuous rôle in mathematical physics to date, some mathematicians have thought that important physical concepts may be gained from a study of nonlinear equations. This monograph represents a beginning in this direction.

For nonlinear integral equations *im kleinen* (where the functions are small in absolute value), the method of successive approximations is shown to be applicable. According as the homogeneous equation has not or has eigenfunctions, the regular or the branching case subsists. This theory is extended to systems of nonlinear integral equations. Certain nonlinear integro-differential equations can be reduced to such systems, but even when a reduction is not possible, there are many cases in which the method of successive approximations is capable of justification.

When there is no restriction on the absolute value of the functions, other methods may be

used to solve the integral equation. The problem may be transformed to an extremal problem, which is solved by using the Ritz method in conjunction with a process of selection from the minimal sequence.

In treating all the special cases, the author goes through the same motions time and again, reminding one of the ancient tale in which "another grasshopper went in and brought forth another grain of corn." (Even then, the grasshoppers had made hardly a dent in the corn pile, when the king protested his weariness and ordered the narrator to cease.) It would seem more to the point to make a thorough study of a typical case, rather than to rely on induction to furnish the final theory.

The book contains many references to the literature, and may be of some interest to specialists, even though of a temporary nature.

JAMES H. BARTLETT, JR.
University of Illinois

Annales de L'Institut Henri Poincaré, Vol. I, sections i, ii, and iii, (Under the direction of MM. CH. MAURAIN, E. BOREL, J. PERRIN, AND P. LANGEVIN. Edited by MM. L. BRILLOUIN L. DE BROGLIE, AND M. FRÉCHET). Pp. 308. Les Presses Universitaires de France, Paris.

The purpose of this new journal is the publication of "conferences" given at l'Institut Henri Poincaré by distinguished men of science, the special fields considered being theoretical physics and the calculus of probabilities. The first volume has appeared in three sections.

In section i, the first article is a discussion by Einstein of his unitary field theory. The idea of parallelism at a distance is developed, and it is shown how certain general field equations may be obtained, which reduce in the first approximation to the well-known gravitational and electromagnetic equations. The tentativeness of the theory is emphasized. Darwin next shows how various phenomena may be regarded from the wave point of view. Finally, Fermi gives a clear account of the Dirac radiation theory, but the degree of approximation does not permit of a detailed discussion of dispersive processes. A short treatment of the Compton and Doppler effects concludes the article.

In section ii, De Donder writes on "La gravifique Einsteinienne," using the original general relativity theory, and claims to give a unitary theory of gravitational, electromagnetic, and quantum-mechanical phenomena. The treatment is based on an article of J. M. Whittaker, who attempted to generalize the Dirac wave equation to the case where an external gravitational field is present. This article is more readable than De Donder's version, although it is open to question as to whether the correct generalization has really been found.

There follow articles dealing more with the calculus of probabilities. Paul Levy derives the Gaussian error law for independent errors, showing what the underlying assumptions are. Polya, from certain postulates, finds the possible error functions for this case, obtaining somewhat greater generality. For observations which are interdependent, such as in contagion and heredity, one finds a Gaussian distribution in many cases, but the criterion for such a distribution is as yet unknown. Kostitzin, in the concluding article, tells about the hereditary physics of Volterra. When the hereditary influence is limited to a short interval of time, the equations describing the situation have infinitely many solutions. The author believes that these may have physical reality, saying that we measure by adopting statistical averages and that we invent statistical theories to explain experiment. In the opinion of the reviewer, this point deserves the attention of phyisicists interested in fundamental problems.

In section iii, after explaining the matrix mechanics and the theory of radioactive disintegration, Born speculates about catalysis by adsorption. The width of spectral lines in then calculated by the method of Weiskopf and Wigner. Brillouin points out the difficulties in solving an hyperbolic equation with spherical boundary conditions, and in determining the rate of propagation of solidification in a sphere. He concludes that the present methods are not suited to the study of these problems.

These "Annales" merit a place in the modern physics library, for many interesting topics are treated with unusual clarity.

JAMES H. BARTLETT, JR.
University of Illinois

Radiations from Radioactive Substances. SIR ERNEST RUTHERFORD, DR. JAMES CHADWICK AND DR. C. D. ELLIS. Pp. 588, figs. 140, Cambridge University Press, and The Macmillan Company, New York. Price, $6.50.

Those interested in radioactivity, I am sure feel greatly indebted to Sir Ernest Rutherford for the assistance he rendered through the publication of his earlier volume entitled "Radioactive Substances and their Radiations." Concerning the then rapidly developing subject that volume still stands as a remarkably accurate presentation. Recently there appeared from the Cambridge University Press, a new volume under the joint authorship of Rutherford, Chadwick and Ellis entitled "Radiations from Radioactive Substances." It is inevitable that again those interested in radioactivity will come to feel indebted to Professor Rutherford as well as his coauthors.

As was to be expected under the circumstances, the volume devotes only the first chapter to the radioactive transformations, the character of which is now quite fully established and has been fully treated by various authors. The new volume therefore being devoted primarily to the radioactive radiations, treats more or less consecutively the alpha, beta and gamma-rays. While the three authors have cooperated in the preparation of the volume as a whole, the treatment of the alpha-rays is, according to the preface, primarily due to Professor Rutherford, the subject of scattering of alpha and beta-rays including artificial disintegration to Dr. Chadwick and the treatment of beta and gamma-rays to Dr. Ellis.

Towards the end is a chapter on atomic nuclei followed by a chapter on miscellaneous topics involving questions of technique and standards. The volume has 588 pages and the illustrations and workmanship are on a par with the earlier volume referred to above. As the authors are among the foremost authorities in the field of Radioactivity, the volume is highly authoritative. The volume is virtually nonmathematical but the fullness of the treatment makes it valuable as a reference book as well as a text in radioactivity.

HENRY A. ERIKSON
University of Minnesota

A Survey of Physics for College Students. FREDERICK A. SAUNDERS. Pp. 635+x. Henry Holt and Company, New York, 1930. Price, $3.75.

Professor Saunders has given us an attractive, and very interesting text; his diction is clear and concise, the figures are excellent and in many cases unique.

In mechanics, the practice of placing the chapters on hydrostatics at the beginning of the treatise seems hardly justified, even by the demands of elementary laboratory work. The chapters on 'motion,' and 'force and motion' are more logically developed. The treatment of rotation, while entirely correct and concise seems to have a lack of concreteness which raises the question whether it shall prove teachable to the average beginner in this subject.

Coming to the topics, elasticity and rigidity, one is impelled to wonder: "How long, Oh Lord"!—until a writer of English texts shall have the courage of convictions to make the proper use of these two terms. One can only marvel why, in spite of the fact that Tait so clearly stated, more than a half-century ago: "A substance is said to be *elastic*, when on being left free it recovers wholly . . . or partially, from a deformation," and farther, "sometimes it is more convenient to speak of the property of *resistance to stress*, as when we speak of a body's *Rigidity*" and adds, significantly, "Young's treatment of the subject of Elasticity is one of the few really imperfect portions of his great work,"—the muddled state of presentation persists through the century in this field,—in which the work of Tait, Thomson, Stokes and de St. Venable leaves no want of precision and clarity whatsoever. In this matter Dr. Saunders is strictly conventional.

In the treatment of electricity, magnetism and optics Dr. Saunders has been successful in introducing the conceptions of modern physics along with the essentials of classic science, for the most part. Geometrical optics is so largely based upon light 'rays' that it would seem questionable whether the studied avoidance of this conception, and method of development of the simpler laws of lenses and reflectors is worth the while an elementary text; the loss in clearness and simplicity seems hardly compensated for in the nearer approach to verity in conceptions.

In his treatment of physical optics, especially in the chapter on dispersion and spectra the author has been particularly happy in his blending of the classic with modern physics.

The text as a whole shows evidence of painstaking work and careful editing, although an occasional error has slipped through, for example, the behavior of a diamagnetic substance in a *uniform* magnetic field is not that which is suggested by the illustration of Fig. 19–12, a field which is *not* uniform being required to produce the action characteristic of diamagnetic media.

On the whole, this text constitutes a distinct and worth while contribution in the field of science teaching, and the teachers of physics in the decade just beginning are to be greatly indebted to Dr. Saunders for such a stimulating and generally well-ordered text.

JOHN E. ALMY
University of Nebraska

Applied Geophysics in the Search for Minerals. A. S. EVE AND D. A. KEYES. Pp. 253, figs. 92. Macmillan Company, New York, 1929. Price $3.00.

This little book gives the elementary principles, a description and operation of instruments and some details of field practice of all the methods of geophysical prospecting which have had practical application. Nearly half of the space in the book is given to electrical and electromagnetic methods, and the rest is about evenly divided between magnetic, gravimetric and seismic methods with a very brief discussion of a few other methods and of salt domes.

The treatment of the electrical and electromagnetic methods reflects the author's experience with them and many details of field apparatus and field procedure are given. In all, there are 18 different methods of electrical and electromagnetic prospecting which are described and for most of these the result and effectiveness based on actual field experience are given. The theoretical treatment is elementary, but sufficient to give the working principles of all the methods described.

The treatment of magnetic, gravitational and seismic methods is apparently based much more on published accounts and less on field experience. The theoretical foundations of these methods are clearly presented, although quite brief. A particular example is the very clear development of the elusive curvature quantity measured by the torsion balance. The discussions of field procedure are brief and in some cases slightly erroneous.

The book is the only one in English to which one can turn as an elementary reference on all the applied methods of geophysical prospecting. Because of its emphasis on electrical and electromagnetic methods, it is probably more useful to the geologist or engineer interested in metal deposits, than to those interested in the larger and deeper oil bearing structures for the location of which the seismograph, torsion balance and magnetometer are much more useful.

L. L. NETTLETON
The Gulf Companies

Uber ungëdanpfte elektrische Ultrakurzwellen. K. KOHL. From Vol. 9. Ergebnisse der exakten Naturwissenschaften. Pp. 276–341. Springer, Berlin, 1930.

The various methods of producing very short electrical waves are reviewed briefly. The greater part of the work is devoted to a discussion of the production of waves of lengths between 3.5 and some 100 cm by means of high vacuum tubes, the emphasis being placed on the experimental results and methods rather than on the somewhat unsatisfactory theoretical explanations. The main points of the several theories are, however, pointed out, as are their weaknesses, also. A chapter on the use of the magnetron for short wave production is included. The final chapter deals with the several suggestions which have been made for the practical use of the special properties of ultrashort waves. This chapter contains some hints on reception methods.

Those interested in any one of the many ramifications of the short-wave problem will find this booklet a helpful reference.

F. B. LLEWELLYN
Bell Telephone Laboratories

Artificial Sunlight. M. LUCKIESH, Pp. 254, figs. 65, plates 8, D. Van Nostrand Company, New York, 1930. Price. $3.75.

"Combining radiation for health with light for vision" is the subtitle of this delightfully written book. Its objective is to call attention to the possible usefulness of some new types of electric light bulbs. At first the author makes the point that light is necessary not only for vision but also for maintenance of health. The majority of the population in this country is working indoors and for them the amount of exposure to unfiltered sunshine is very slight. Radiation of wave-lengths between 2800 and 3100A is assumed to be particularly beneficial physiologically. This radiation is stopped by ordinary window glass and also by the glass used in the ordinary type of incandescent electric bulbs. It is present to a relatively great extent in the carbon arcs and the quartz mercury arcs, which are being used by physicians for light treatments. Sunlight, which has been proven to be of particular value for health also contains a portion of rays in this region. The author proposes that a continuous exposure to small intensities of this radiation in hospitals, homes and offices may be of value and he describes how this can be done. A number of tables and charts are given showing the spectral distribution of the radiation energy: in the solar radiation; from a black body and certain incandescent solids at various temperatures; from carbon arcs and some other electric arcs. A short discussion of the whole electromagnetic spectrum is given. Some biological effects are referred to and the erythemal skin reaction is especially considered. The number of foot-candle-minutes necessary to produce an erythema with different light sources is given in tabulated form. Media suitable for transmission and reflection are discussed with suitable data. The permanency of such media is also considered and the extent to which the transmission of these media changes with age is demonstrated by figures. Infrared radiation and its medical use is considered in some of the chapters but ultraviolet radiation constitutes the main subject of the book. A special chapter is devoted to methods available for quantitative measurements of this radiation.

After all the fundamental problems are thoroughly considered the author describes the new "Sunlight" S-1 lamp. This is a combination of a tungsten filament lamp and a mercury arc housed in a bulb made of Corex D glass, which transmits radiation in the ultraviolet region referred to as specially important. This type of burner requires a transformer as it uses much lower voltage than the ordinary types of bulbs do. Finally the possibility of using tungsten filament burners with bulbs made of Corex D and other glasses transmitting far down in the ultraviolet is considered. Such lamps made for 110 volts can be used instead of the ordinary electric bulbs in the home. Special fixtures and reflectors can be made to enhance the efficiency of the installation. Data on measurements are given which show that erythema producing rays are present though of low intensity. These new types of bulbs are now on the market.

The book contains a collection of data which is of great value. It is easy to read and should prove of interest to physicists and physicians as well as to others of college training. When reading the book it is, however, well to remember that the action of radiation on the human system is quite complicated and that our knowledge in this field is as yet very limited. Such a "new era of lighting" as the author proposes may be of very great importance for the health and should be considered seriously. It will, however, take a long time before definite conclusions can be reached. The possibility that some injurious effects may result from too rapid change is not excluded. Will our eyes stand such continuous exposure for a number of years? How about people who are supersensitive to ultraviolet rays? Let us not be too pessimistic. The author's arguments are quite convincing and the book is a very valuable contribution in the field of light and health.

K. W. STENSTROM
University of Minnesota